

e-ISSN 1308-8459

Official Publication of the Turkish Society of Anatomy and Clinical Anatomy

<http://dergipark.org.tr/en/pub/anatomy>

# anatomy

An International Journal of Experimental and Clinical Anatomy

**Volume 16 / Issue 2 / August 2022**

Published three times a year



deomed®

# anatomy

An International Journal of Experimental and Clinical Anatomy

## Official Publication of the Turkish Society of Anatomy and Clinical Anatomy

### Aim and Scope

**Anatomy**, an international journal of experimental and clinical anatomy, is a peer-reviewed journal published three times a year with an objective to publish manuscripts with high scientific quality from all areas of anatomy. The journal offers a forum for anatomical investigations involving gross, histologic, developmental, neurological, radiological and clinical anatomy, and anatomy teaching methods and techniques. The journal is open to original papers covering a link between gross anatomy and areas related with clinical anatomy such as experimental and functional anatomy, neuroanatomy, comparative anatomy, modern imaging techniques, molecular biology, cell biology, embryology, morphological studies of veterinary discipline, and teaching anatomy. The journal is currently indexing and abstracting in TUBITAK ULAKBIM Turkish Medical Index, Proquest, EBSCO Host, Index Copernicus and Google Scholar.

### Publication Ethics

**Anatomy** is committed to upholding the highest standards of publication ethics and observes the principles of Journal's Publication Ethics and Malpractice Statement which is based on the recommendations and guidelines for journal editors developed by the Committee on Publication Ethics (COPE), Council of Science Editors (CSE), World Association of Medical Editors (WAME) and International Committee of Medical Journal Editors (ICMJE). For detailed information please visit the online version of the journal which is available at <https://dergipark.org.tr/pub/anatomy>

### Authorship

All persons designated as authors should have participated sufficiently in the work to take public responsibility for the content of the manuscript. Authorship credit should be based on substantial contributions to (1) conception and design or analysis and interpretation of data, (2) drafting of the manuscript or revising it for important intellectual content and, (3) final approval of the version to be published. The Editor may require the authors to justify assignment of authorship. In the case of collective authorship, the key persons responsible for the article should be identified and others contributing to the work should be recognized with proper acknowledgment.

### Copyright

Copyright © 2022, by the Turkish Society of Anatomy and Clinical Anatomy, TSACA. All rights reserved. No part of this publication may be reproduced, stored or transmitted in any form without permission in writing from the copyright holder beforehand, exceptionally for research purpose, criticism or review. The publisher and the Turkish Society of Anatomy and Clinical Anatomy assume no liability for any material published in the journal. All statements are the responsibility of the authors. Although all advertising material is expected to conform ethical standards, inclusion in this publication does not constitute a guarantee or endorsement of the quality or value of such product or of the claims made of it by its manufacturer. Permission requests should be addressed to the publisher.

### Publisher

Deomed Publishing  
Gür Sok. No:7/B Kadıköy, İstanbul, Türkiye  
Phone: +90 216 414 83 43 (Pbx) / Fax: +90 216 414 83 42  
[www.deomed.com](http://www.deomed.com) / e-mail: [medya@deomed.com](mailto:medya@deomed.com)

### Publication Information

**Anatomy** (e-ISSN 1308-8459) as an open access electronic journal is published by Deomed Publishing, İstanbul, for the Turkish Society of Anatomy and Clinical Anatomy, TSACA. Due the Press Law of Turkish Republic dated as June 26, 2004 and numbered as 5187, this publication is classified as a periodical in English language.

#### Ownership

On behalf of the Turkish Society of Anatomy and Clinical Anatomy, Ahmet Kağan Karabulut, MD, PhD; Konya, Türkiye

#### Editor-in-Chief

Nihal Apaydin, MD  
Department of Anatomy,  
Faculty of Medicine, Ankara University,  
06100, Sıhhiye, Ankara, Türkiye  
Phone: 0090 312 595 82 48  
e-mail: [napaydin@gmail.com](mailto:napaydin@gmail.com); [napaydin@medicine.ankara.edu.tr](mailto:napaydin@medicine.ankara.edu.tr)

#### Administrative Office

Güven Mah. Güvenlik Cad. Onlar Ap. 129/2 Aşağı Ayrancı, Ankara, Türkiye  
Phone: +90 312 447 55 52-53

### Submission of Manuscripts

Manuscripts should be submitted at our manuscript submission and information portal <https://dergipark.org.tr/en/pub/anatomy>

### Categories of Articles

- **Original Articles** describe substantial original research that falls within the scope of the Journal.
- **Teaching Anatomy** section contains regular or all formats of papers which are relevant to comparing teaching models or to introducing novel techniques, including especially the own experiences of the authors.
- **Reviews** section highlights current development in relevant areas of anatomy. The reviews are generally invited; other prospective authors should consult with the Editor-in-Chief.
- **Case Reports** include new, noteworthy or unusual cases which could be of help for basic notions and clinical practice.
- **Technical Note** articles cover technical innovations and developments with a specific technique or procedure or a modification of an existing technique. They should be sectioned like an original research article but not exceed 2000 words.
- **Viewpoint** articles give opinions on controversial topics or future projections, some of these are invited.
- **Historical View** category presents overview articles about historical sections from all areas of anatomy.
- **Terminology Zone** category is a platform for the articles which discuss some terminological controversies or opinions.

The categories above are peer-reviewed. They should include abstract and keywords. There are also categories including Letters to the Editor, Book Reviews, Abstracts, Obituary, News and Announcements which do not require a peer review process.

For detailed instructions concerning the submission of manuscripts, please refer to the Instructions to Authors.

### Advertising and Reprint Requests

Please direct to publisher. e-mail: [medya@deomed.com](mailto:medya@deomed.com)

### Honorary Editor

**Doğan Aksit**, Ankara, Türkiye

### Founding Editors

**Salih Murat Akkın**, Gaziantep, Türkiye

**Hakan Hamdi Çelik**, Ankara, Türkiye

### Former Editors-in-Chief and Advising Editors

**Salih Murat Akkın** (2007–2013)  
Gaziantep, Türkiye

**Gülgün Şengül** (2014–2019)  
Izmir, Türkiye

### Editor-in-Chief

**Nihal Apaydın**, Ankara, Türkiye

### Editors

**Ceren Günenç Beşer**, Ankara, Türkiye

**Zeliha Kurtoğlu Olgunus**, Mersin, Türkiye

**Luis Puelles**, Murcia, Spain

**Gülgün Şengül**, Izmir, Türkiye

**Shane Tubbs**, Birmingham, AL, USA

**Emel Ulupınar**, Eskişehir, Türkiye

### Associate Editors

**Vaclav Baca**, Prague, Czech Republic

**Çağatay Barut**, Istanbul, Türkiye

**Jon Cornwall**, Dunedin, New Zealand

**Ayhan Cömert**, Ankara, Türkiye

**Mirela Eric**, Novi Sad, Serbia

**Georg Feigl**, Graz, Austria

**Quentin Fogg**, Melbourne, Australia

**David Kachlik**, Prague, Czech Republic

**Marko Korschake**, Innsbruck, Austria

**Scott Lozanoff**, Honolulu, HI, USA

**Levent Sarıkçıoğlu**, Antalya, Türkiye

**Cristian Stefan**, Boston, MA, USA

**İlkan Tatar**, Ankara, Türkiye

**Trifon Totlis**, Thessaloniki, Greece

### Executive Board of Turkish Society of Anatomy and Clinical Anatomy

**Piraye Kervancıoğlu** (President)

**Çağatay Barut** (Vice President)

**Nadire Ünver Doğan** (Vice President)

**İlke Ali Gürses** (Secretary General)

**Ceren Günenç Beşer** (Treasurer)

**Esat Adıgüzel** (Member)

**Selçuk Tunalı** (Member)

### Scientific Advisory Board

**Peter H. Abrahams**  
Cambridge, UK

**Halil İbrahim Açar**  
Ankara, Türkiye

**Marian Adamkov**  
Martin, Slovakia

**Esat Adıgüzel**  
Denizli, Türkiye

**Mustafa Aktekin**  
Istanbul, Türkiye

**Abduelmenem Alashkham**  
Edinburgh, UK

**Mahindra Kumar Anand**  
Gujarat, India

**Serap Arbak**  
Istanbul, Türkiye

**Alp Bayramoğlu**  
Istanbul, Türkiye

**Brion Benninger**  
Lebanon, OR, USA

**Susana Biasutto**  
Cordoba, Argentina

**Dragica Bobinac**  
Rijeka, Croatia

**David Bolender**  
Milwaukee, WI, USA

**Eric Brenner**  
Innsbruck, Austria

**Mustafa Büyükmumcu**  
Istanbul, Türkiye

**Richard Halti Cabral**  
Sao Paulo, Brazil

**Safiye Çavdar**  
Istanbul, Türkiye

**Katharina D'Herde**  
Ghent, Belgium

**Fabrice Duparc**  
Rouen, France

**Behice Durgun**  
Adana, Türkiye

**İzzet Duyar**  
Istanbul, Türkiye

**Mete Ertürk**  
Izmir, Türkiye

**Reha Erzurumlu**  
Baltimore, MD, USA

**Ali Fırat Esmir**  
Ankara, Türkiye

**António José Gonçalves Ferreira**  
Lisboa, Portugal

**Christian Fontaine**  
Lille, France

**Figen Gövsay Gökmen**  
Izmir, Türkiye

**Rod Green**  
Bendigo, Australia

**Bruno Grignon**  
Nancy Cedex, France

**Nadir Gülekon**  
Ankara, Türkiye

**Mürvet Hayran**  
Izmir, Türkiye

**David Heylings**  
Norwich, UK

**Lazar JeleV**  
Sofia, Bulgaria

**Samet Kapakin**  
Erzurum, Türkiye

**Ahmet Kağan Karabulut**  
Konya, Türkiye

**S. Tuna Karahan**  
Ankara, Türkiye

**Simel Kendir**  
Ankara, Türkiye

**Piraye Kervancıoğlu**  
Gaziantep, Türkiye

**Hee-Jin Kim**  
Seoul, Korea

**Necdet Kocacıyık**  
Ankara, Türkiye

**Cem Kopuz**  
Samsun, Türkiye

**Mustafa Ayberk Kurt**  
Istanbul, Türkiye

**Marios Loukas**  
Grenada, West Indies

**Veronica Macchi**  
Padua, Italy

**Ali Mirjalili**  
Auckland, New Zealand

**Bernard Moxham**  
Cardiff, Wales, UK

**Konstantinos Natsis**  
Thessaloniki, Greece

**Lia Lucas Neto**  
Lisboa, Portugal

**Helen Nicholson**  
Dunedin, New Zealand

**Davut Özbağ**  
Malatya, Türkiye

**P. Hande Özdinler**  
Chicago, IL, USA

**Adnan Öztürk**  
Istanbul, Türkiye

**Ahmet Hakan Öztürk**  
Mersin, Türkiye

**Friedrich Paulsen**  
Erlangen, Germany

**Wojciech Pawlina**  
Rochester, MN, USA

**Tuncay Veysel Peker**  
Ankara, Türkiye

**Vid Persaud**  
Winnipeg, MB, Canada

**David Porta**  
Louisville, KY, USA

**Jose Ramon Sanudo**  
Madrid, Spain

**Tatsuo Sato**  
Tokyo, Japan

**Mohammadali M. Shoja**  
Birmingham, AL, USA

**Ahmet Sinav**  
Istanbul, Türkiye

**Takis Skandalakis**  
Athens, Greece

**Isabel Stabile**  
Msida, Malta

**Vildan Sümbüloğlu**  
Gaziantep, Türkiye

**(Biostatistics)**

**Muzaffer Seker**  
Konya, Türkiye

**Erdoğan Şendemir**  
Bursa, Türkiye

**İbrahim Tekdemir**  
Ankara, Türkiye

**Hironubu Tokuno**  
Tokyo, Japan

**Mehmet İbrahim Tuğlu**  
Manisa, Türkiye

**Selçuk Tunalı**  
Ankara, Türkiye

**Uğur Türe**  
Istanbul, Türkiye

**Aysun Uz**  
Ankara, Türkiye

**Mehmet Üzel**  
Istanbul, Türkiye

**Ivan Varga**  
Bratislava, Slovakia

**Tuncay Varol**  
Manisa, Türkiye

**Stephanie Woodley**  
Otago, New Zealand

**Bülent Yalçın**  
Ankara, Türkiye

**Gazi Yaşargil**  
Istanbul, Türkiye

**Hiroshi Yorifuji**  
Gunma, Japan

**Anatomy**, an international journal of experimental and clinical anatomy, is the official publication of the Turkish Society of Anatomy and Clinical Anatomy, TSACA. It is a peer-reviewed e-journal that publishes scientific articles in English. For a manuscript to be published in the journal, it should not be published previously in another journal or as full text in congress books and should be found relevant by the editorial board. Also, manuscripts submitted to *Anatomy* must not be under consideration by any other journal. Relevant manuscripts undergo conventional peer review procedure (at least three reviewers). For the publication of accepted manuscripts, author(s) should reveal to the Editor-in-Chief any conflict of interest and transfer the copyright to the Turkish Society of Anatomy and Clinical Anatomy, TSACA.

In the Materials and Methods section of the manuscripts where experimental studies on humans are presented, a statement that informed consent was obtained from each volunteer or patient after explanation of the procedures should be included. This section also should contain a statement that the investigation conforms with the principles outlined in the appropriate version of 1964 Declaration of Helsinki. For studies involving animals, all work must have been conducted according to applicable national and international guidelines. Prior approval must have been obtained for all protocols from the relevant author's institutional or other appropriate ethics committee, and the institution name and permit numbers must be provided at submission.

Anatomical terms used should comply with Terminologia Anatomica by FCAT (1998).

No publication cost is charged for the manuscripts but reprints and color printings are at authors' cost.

#### Preparation of manuscripts

During the preparation of the manuscripts, uniform requirements of the International Committee of Medical Journal Editors, a part of which is stated below, are valid (see ICMJE). Uniform requirements for manuscripts submitted to biomedical journals. Updated content is available at [www.icmje.org](http://www.icmje.org). The manuscript should be typed double-spaced on one side of a 21x29.7 cm (A4) blank sheet of paper. At the top, bottom and right and left sides of the pages a space of 2.5 cm should be left and all the pages should be numbered except for the title page.

Manuscripts should not exceed 15 pages (except for the title page). They must be accompanied by a cover letter signed by corresponding author and the Conflicts of Interest Disclosure Statement and Copyright Transfer Form signed by all authors. The contents of the manuscript (original articles and articles for Teaching Anatomy category) should include: 1- Title Page, 2- Abstract and Keywords, 3- Introduction, 4- Materials and Methods, 5- Results, 6- Discussion (Conclusion and/or Acknowledgement if necessary), 7- References

#### Title page

In all manuscripts the title of the manuscript should be written at the top and the full names and surnames and titles of the authors beneath. These should be followed with the affiliation of the author. Manuscripts with long titles are better accompanied underneath by a short version (maximum 80 characters) to be published as running head. In the title page the correspondence address and telephone, fax and e-mail should be written. At the bottom of this page, if present, funding sources supporting the work should be written with full names of all funding organizations and grant numbers. It should also be indicated in a separate line if the study has already been presented in a congress or likewise scientific meeting. Other information such as name and affiliation are not to be indicated in pages other than the title page.

#### Abstract

Abstract should be written after the title in 100–250 words. In original articles and articles prepared in IMRAD format for Teaching Anatomy category the abstract should be structured under sections Objectives, Methods, Results and Conclusion. Following the abstract at least 3 keywords should be added in alphabetical order separated by semicolons.

#### References

Authors should provide direct references to original research sources. References should be numbered consecutively in square brackets, according to the order in which they are first mentioned in the manuscript. They should follow the standards detailed in the NLM's Citing Medicine, 2nd edition (Citing medicine: the NLM style guide for authors, editors, and publishers [Internet]. 2nd edition. Updated content is available at [www.ncbi.nlm.nih.gov/books/NBK7256](http://www.ncbi.nlm.nih.gov/books/NBK7256)). The names of all contributing authors should be listed, and should be in the order they appear in the original reference. The author is responsible for the accuracy and completeness of references. When necessary, a copy of a referred article can be requested from the author. Journal names should be abbreviated as in *Index Medicus*. Examples of main reference types are shown below:

- **Journal articles:** Author's name(s), article title, journal title (abbreviated), year of publication, volume number, inclusive pages
  - *Standard journal article:* Sargon MF, Celik HH, Aksit MD, Karaagaoglu E. Quantitative analysis of myelinated axons of corpus callosum in the human brain. *Int J Neurosci* 2007;117:749–55.

- *Journal article with indication article published electronically before print:* Sengul G, Fu Y, Yu Y, Paxinos G. Spinal cord projections to the cerebellum in the mouse. *Brain Struct Funct Epub* 2014 Jul 10. DOI 10.1007/s00429-014-0840-7.
- **Books:** Author's name(s), book title, place of publication, publisher, year of publication, total pages (entire book) or inclusive pages (contribution to a book or chapter in a book)
  - *Entire book:*
    - *Standard entire book:* Sengul G, Watson C, Tanaka I, Paxinos G. Atlas of the spinal cord of the rat, mouse, marmoset, rhesus and human. San Diego (CA): Academic Press Elsevier; 2013. 360 p.
    - *Book with organization as author:* Federative Committee of Anatomical Terminology (FCAT). Terminologia anatomica. Stuttgart: Thieme; 1998. 292 p.
    - *Citation to a book on the Internet:* Bergman RA, Afifi AK, Miyauchi R. Illustrated encyclopedia of human anatomic variation. Opus I: muscular system [Internet]. [Revised on March 24, 2015] Available from: <http://www.anatomyatlases.org/AnatomicVariants/AnatomyHPshhtml>
  - *Contribution to a book:*
    - *Standard reference to a contributed chapter:* Potten CS, Wilson JW. Development of epithelial stem cell concepts. In: Lanza R, Gearhart J, Blau H, Melton D, Moore M, Pedersen R, Thomson J, West M, editors. Handbook of stem cell. Vol. 2, Adult and fetal. Amsterdam: Elsevier; 2004. p. 1–11.
    - *Contributed section with editors:* Johnson D, Ellis H, Collins P, editors. Pectoral girdle and upper limb. In: Standring S, editor. Gray's anatomy: the anatomical basis of clinical practice. 29th ed. Edinburgh (Scotland): Elsevier Churchill Livingstone; 2005. p. 799–942.
  - *Chapter in a book:*
    - *Standard chapter in a book:* Doyle JR, Botte MJ. Surgical anatomy of the hand and upper extremity. Philadelphia (PA): Lippincott Williams and Wilkins; 2003. Chapter 10, Hand, Part 1, Palmar hand; p. 532–641.

#### Illustrations and tables

Illustrations and tables should be numbered in different categories in the manuscript and Roman numbers should not be used in numbering. Legends of the illustrations and tables should be added to the end of the manuscript as a separate page. Attention should be paid to the dimensions of the photographs to be proportional with 10x15 cm. Some abbreviations out of standards can be used in related illustrations and tables. In this case, abbreviation used should be explained in the legend. Figures and tables published previously can only be used when necessary for a comparison and only by giving reference after obtaining permission from the author(s) or the publisher (copyright holder).

#### Author Contribution

Each manuscript should contain a statement about the authors' contribution to the Manuscript. Please note that authorship changes are no longer possible after the final acceptance of an article.

List each author by the initials of names and surnames and describe each of their contributions to the manuscript using the following terms:

- Protocol/project development
- Data collection or management
- Data analysis
- Manuscript writing/editing
- Other (please specify briefly using 1 to 5 words)

**For example:** NBA: Project development, data collection; AS: Data collection, manuscript writing; STR: Manuscript writing

**Funding:** information that explains whether and by whom the research was supported.

**Conflicts of interest/Competing interests:** include appropriate disclosures.

**Ethics approval:** include appropriate approvals or waivers. Submitting the official ethics approval by whom the research was approved, including the approval date, number or code is necessary.

If the submission uses cadaveric tissue, please acknowledge the donors in an acknowledgement at the end of the paper.

#### Control list

- Length of the manuscript (max. 15 pages)
- Manuscript format (double space; one space before punctuation marks except for apostrophes)
- Title page (author names and affiliations; running head; correspondence)
- Abstract (100–250 words)
- Keywords (at least three)
- References (relevant to *Index Medicus*)
- Illustrations and tables (numbering; legends)
- Conflicts of Interest Disclosure Statement and Copyright Transfer Form
- Cover letter

All manuscripts must contain the following declaration sections. These should be placed before the reference list at the end of the manuscript.

# The radiological anatomy of clivus for surgical approaches

Tuğba Moralı Güler<sup>1</sup> , Ömer Faruk Ünal<sup>2</sup> , Gökmen Kahiloğulları<sup>3</sup> 

<sup>1</sup>Neurosurgery Unit, Private Medikar Hospital, Karabük, Türkiye

<sup>2</sup>Radiology Unit, Private Medikar Hospital, Karabük, Türkiye

<sup>3</sup>Department of Neurosurgery, Faculty of Medicine, Ankara University, Ankara, Türkiye

## Abstract

**Objectives:** Clivus is the central part of the skull base that extends from the anterior part of the foramen magnum to the posterior clinoid process. Clivus has close relationships with crucial neurovascular structures. The purpose of the study was to evaluate the anatomical relationships at the clival region on computed tomography (CT) images for to provide data to conduct best pathways and safe zones for clival surgeries.

**Methods:** Brain and cervical CT images of 103 patients (48 female, 55 male; mean age: 63) were examined retrospectively. The length of the clivus at the sagittal plane, the width of the inferior and middle parts of the clivus at the midsagittal plane, and the distance between the internal carotid arteries at the sagittal plane in axial sections were measured.

**Results:** The mean length of the clivus at the sagittal plane was  $38.40 \pm 5.82$  mm. The mean width of the inferior and middle parts of the clivus at the midsagittal plane was  $6.67 \pm 1.45$  mm and  $10.32 \pm 1.66$  mm, respectively. In axial sections, the mean distance between the internal carotid arteries was  $22.10 \pm 03.42$  mm in the sagittal plane.

**Conclusion:** Knowing the dimensions of the clivus and the distance between the internal carotid arteries at the sagittal plane is important for a safe and successful clival surgery.

**Keywords:** clivus; computed tomography; skull base

Anatomy 2022;16(2):51–55 ©2022 Turkish Society of Anatomy and Clinical Anatomy (TSACA)

## Introduction

The clivus, which was first named by Johannes Blumenbach, is the central part of the skull base that extends from the anterior part of the foramen magnum to the posterior clinoid process.<sup>[1–3]</sup> It divides the posterior fossa from the nasopharynx and is made up of the posterior region of the body of the sphenoid bone and the basilar segment of the occipital bone.<sup>[4]</sup> The fusion of these bony parts starts in the second month of intrauterine life and completes at the age of 16–20 years.<sup>[5]</sup>

Clivus can be divided into three parts as upper (sellar clivus), middle (sphenoidal clivus), and lower (nasopharyngeal) thirds. The upper and the middle thirds of the clivus are formed by the sphenoid bone, and the lower third is formed by the occipital bone.<sup>[6]</sup>

Clivus is a complex skull base region which has close relationships with crucial neurovascular structures such

as the brainstem, sellar region, and internal carotid arteries.<sup>[3]</sup> In 1992, Samii and Knosp have written a book that reviewed the approaches to the clivus and the name of the book was “Approaches to the clivus: approaches to no man’s land.” Many different approaches to the clival region were defined in the last three decades and particularly with the technological advances in endoscopic surgery, the transnasal transsphenoidal endoscopic approach to the clivus maintains a good exposure for the tumors of this region.<sup>[3]</sup>

Because of the restrictions of the clival region and its complicated relationships, detailed anatomical knowledge plays a critical role in avoiding injury to these vital structures. In this study, the computed tomography (CT) anatomy of the region was analyzed for to provide data to conduct best pathways and safe zones for clival surgeries.

## Materials and Methods

Brain and cervical CT images of the 103 patients (48 females and 55 males) were retrospectively analyzed between January 1, 2022 and December 31, 2022. The mean age of the patients was 63 (range: 1–92) years. The images were randomly selected from Radiology Unit of the Private Medikar Hospital. The CT images were taken with a CT device (General Electric VCT 128 Slice Scanner, Milwaukee, Wisconsin, USA) that had a collimation of 1.25 mm, tube tension of 140 kV, and tube current of 240 mAs (with dosage modulation).

The length of the clivus in the sagittal plane, the width of the inferior and middle parts of the clivus at the midsagittal plane, the distance between the internal carotid arteries at the sagittal plane in axial sections were measured (Figure 1). The wide angle between the line extending across the anterior cranial fossa to the tip of the dorsum sellae, and the line drawn along the posterior margin of the clivus was determined as basal angle and measured on sagittal images (Figure 2).

The Shapiro–Wilk test was used to determine whether continuous variables had a normal distribution or not. The variables were represented as mean and standard deviation if they did not conform to the normal distribution and as median, minimum, and maximum values if they did not conform to the normal distribution. Mann–Whitney U test was employed to compare continuous variables between age and gender groups. Analyses were conducted using SPSS (Version 26.0, IBM Corp., Armonk, NY, USA). The significance level was set at 5%.

## Results

The mean length of the clivus at the sagittal plane was  $38.40 \pm 5.82$  (range: 13–52) mm. The mean width of the inferior part of the clivus at the midsagittal plane was  $6.67 \pm 1.45$  (range: 3–50) mm. The mean width of the middle part of the clivus at the midsagittal plane was  $10.32 \pm 1.66$  (range: 6–14) mm. The mean distance between the internal carotid arteries at the sagittal plane in axial sections was  $22.10 \pm 3.42$  (range: 10–28) mm. The mean basal angle was  $118.08^\circ \pm 9.38^\circ$  (range: 100–150°).

The patients were divided into two age groups being  $\geq 18$  years and  $< 18$  years. The mean distance between the internal carotid artery below the petrous apex and the width of the middle and inferior portions of the clivus, as well as the length of the clivus in the sagittal plane were all higher in the patients elder than 18 years ( $p < 0.001$ ,  $p < 0.001$ ,  $p = 0.006$  and  $p = 0.002$ , respectively). However, there was no difference between the age groups based on

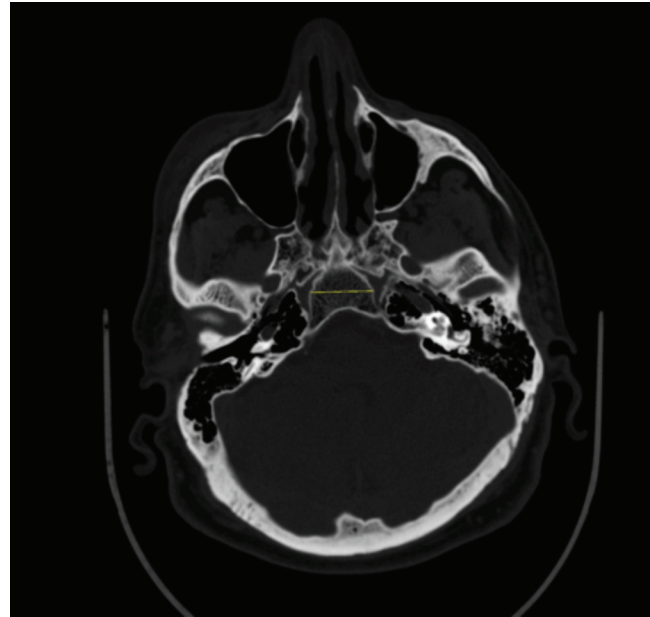


Figure 1. The distance between the internal carotid arteries (yellow line) below the petrous apex in axial views.

the basal angle ( $p = 0.945$ ). The length of clivus at the sagittal plane was found to be higher in males when compared with females ( $p = 0.014$ ), while the other measurements did not differ according to gender ( $p > 0.05$ ) (Table 1) (Figures 3–6).

## Discussion

There are several congenital or acquired pathologies of the clivus, such as developmental anomalies, non-neoplastic and neoplastic lesions, inflammatory processes, and trau-

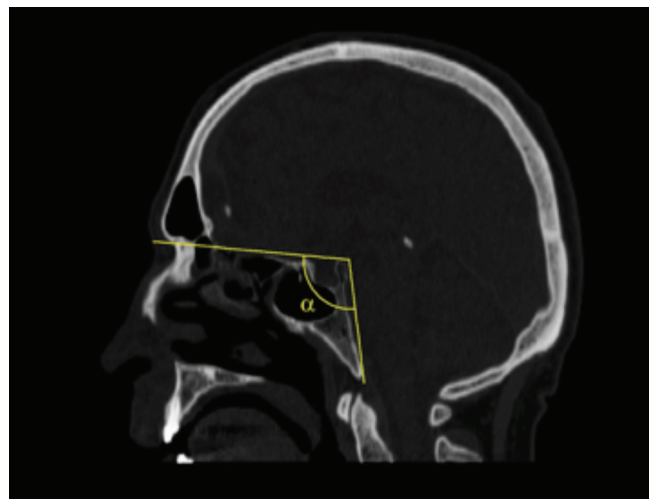
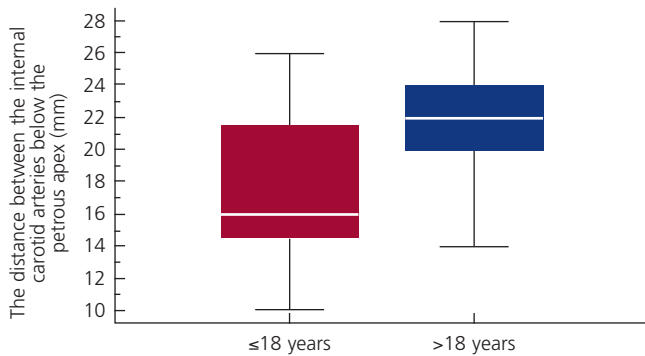


Figure 2. The measurement of the basal angle ( $\alpha$ ).

**Table 1**

Statistically significant differences in the cerebellar volumes and cortical thickness between the depressed and control groups and the percentage differences.

	Age		Gender	
	≤18 years (n=11)	>18 years (n=92)	Female (n=48)	Male (n=55)
The width of the middle part of the clivus (mm)	8 (6–12)	11 (7–14)	10.50 (7–14)	10(6–13)
	p<0.001		p=0.623	
The width of the inferior part of the clivus (mm)	5 (3–7)	7 (4–10)	7 (4–9)	6 (3–10)
	p<0.001		p=0.236	
Length of the clivus in the sagittal plane (mm)	27 (13–45)	39.50 (31–52)	38 (25–48)	40 (13–52)
	p=0.006		p=0.014	
The distance between the internal carotid arteries below the petrous apex (mm)	16 (10–26)	22 (14–28)	22 (14–26)	22 (10–28)
	p=0.002		p=0.141	
The basal angle	117 (111–137)	118 (100–150)	115 (100–150)	118 (103–149)
	p=0.945		p=0.326	



**Figure 3.** Distance between the internal carotid arteries below the petrous apex.

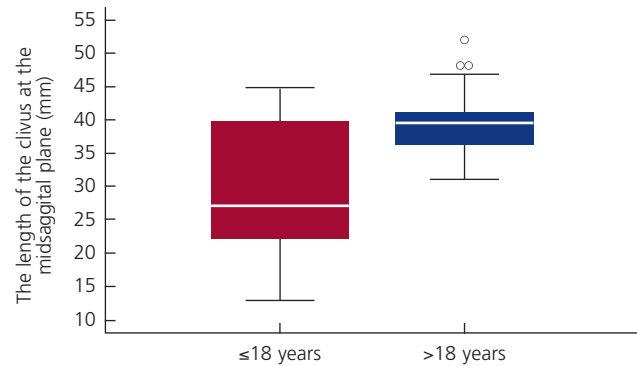


**Figure 4.** The length of the clivus at the midsagittal plane.

matic lesions.<sup>[2–7]</sup> Surgical approaches directed for these pathologies of the clivus include subtemporal approach, suboccipital approach, oropharyngeal approach, and endonasal–endoscopic approach.<sup>[1,3,8]</sup> Traditional transcranial approaches requires excessive brain retraction which

may lead to complications such as brain edema, infarction, and hematoma.<sup>[1]</sup> With the developments in endoscopy, endonasal–endoscopic approaches for the pathologies of the clivus became a good alternative to transcranial methods as it does not require any brain retraction. Endonasal–

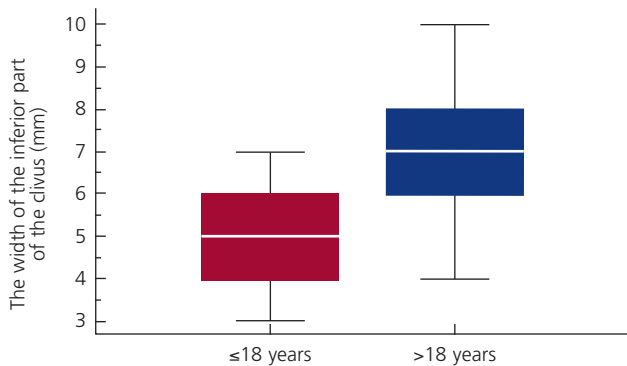


**Figure 5.** The width of the inferior part of the clivus.

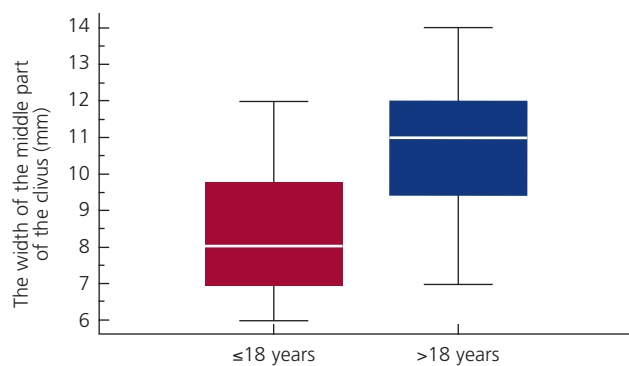


**Figure 6.** The width of the middle part of the clivus.

endoscopic approaches maintain the visualization of the deeper structures, a multi-perspective observation, and also a good exposure to the extradural parts of the lesions.<sup>[1,3]</sup> In this study, some essential morphometric measurements of the clivus were performed to be used during endoscopic surgery of the clivus.

The anatomical relationships of the clival region must be known in details to provide a safe and effective endonasal–endoscopic approach. Cheng et al.<sup>[3]</sup> emphasized the importance of the close relation of the clivus to the optic nerves, the internal carotid arteries, and the sub-petrosal sinuses during transclival surgeries. The cavernous part of the ICA is in close relation to the clivus. It is particularly important to know the mean distance between the internal carotid arteries during transclival surgery to prevent its vascular injury. The results of our study showed that the mean distance between the internal carotid arteries under the level of the petrous apex is  $22.10 \pm 3.42$  mm. The internal carotid arteries inferior to the petrous apex are separated by a distance that is more than twice the distance between the internal carotid arteries superior to the petrous apex, making it an important anatomical landmark.<sup>[3]</sup> Therefore, there is less restriction for the approaches inferior to the petrous apex, and this area is also appropriate for endoscopic surgery.<sup>[3]</sup>

According to Wang et al.,<sup>[9]</sup> the full length of the clivus is 30.6–51.2 mm, with an average length of  $41.7 \pm 2.9$  mm. In our study, it was  $38.40 \pm 5.82$  mm and also the length of clivus at the sagittal plane was shown to be higher in males and in the patient group older than 18 years.

In our study, the mean width of the middle and inferior parts of the clivus was revealed as  $10.32 \pm 1.66$  and  $6.67 \pm 1.45$  respectively. Because of the shape of the clivus, the thickness of the inferior and middle parts of the clivus varies. Knowing these dimensions are particularly important for selection of suitable equipment during the approaches directed to the brain stem.

We suggest that knowing the basal angle is also important for endoscopic approaches. According to Koenigsberg et al.<sup>[10]</sup> the basal angle was  $105^\circ$ – $127^\circ$  for adults and  $104^\circ$ – $124^\circ$  for children with the modified MR imaging technique. In our study, the mean basal angle was found as  $118.08^\circ \pm 9.38^\circ$ . The basal angle was used to be measured using plain radiographs, but with increasing use of MRI and CT, the measurements can now be done with greater accuracy and simplicity.<sup>[10]</sup>

The major limitation of this study was the number of images included to the study. We suggest conducting

further studies done in larger population and in more age groups.

## Conclusion

Clivus surgery has some potential risks such as neurovascular injuries including cranial nerves, internal carotid artery and injury to meninges, or directly injury to the brain. A detailed preoperative evaluation of the patient is necessary to avoid such complications. In particular, reconstructed CT images in addition to enhanced MR images should be examined carefully before surgery. The usage of technologically developed endoscopic techniques maintains good surgical outcomes when compared with traditional transcranial approaches for clival surgery, and the significance of anatomical knowledge still plays a major role in successful and safe surgery.

## Conflict of Interest

The authors declare no conflict of interest.

## Author Contributions

TMG: data collection, data analysis; manuscript writing/editing; OFU: data collection, data analysis; manuscript writing/editing; GK: project development, data analysis, manuscript writing/editing.

## Ethics Approval

Approval for this study was received from the Ethics Committee of Karabük University Faculty of Medicine (Number: E-77192459-050.99-209417).

## Funding

None.

## References

1. Rai R, Iwanaga J, Shokouhi G, Loukas M, Mortazavi MM, Oskouian RJ, Tubbs RS. A comprehensive review of the clivus: anatomy, embryology, variants, pathology, and surgical approaches. *Childs Nerv Syst* 2018;34:1451–8.
2. Hofmann E, Prescher A. The clivus. *Clin Neuroradiol* 2012;22:123–39.
3. Cheng Y, Zhang S, Chen Y, Zhao G. Safe corridor to access clivus for endoscopic trans-sphenoidal surgery: a radiological and anatomical study. *PLoS One* 2015;10:e0137962.
4. Stamm AC, Pignatari SS, Vellutini E. Transnasal endoscopic surgical approaches to the clivus. *Otolaryngol Clin of North Am* 2006;39:639–56.
5. Bayrak S, Göller Bulut D, Orhan K. Prevalence of anatomical variants in the clivus: fossa navicularis magna, canalis basilaris medianus, and craniopharyngeal canal. *Surg Radiol Anat* 2019;41:477–83.
6. Patel CR, Fernandez-Miranda JC, Wang WH, Wang EW. Skull base anatomy. *Otolaryngol Clin North Am* 2016;49:9–20.

7. Nardi C, Maraghelli D, Pietragalla M, Scola E, Locatello LG, Maggiore G, Gallo O, Bartolucci M. A practical overview of CT and MRI features of developmental, inflammatory, and neoplastic lesions of the sphenoid body and clivus. *Neuroradiology* 2022;64: 1483–509.
8. Anik I, Koc K, Cabuk B, Ceylan S. Endoscopic transphenoidal approach for fibrous dysplasia of clivus, tuberculum sellae and sphenoid sinus; report of three cases. *Turk Neurosurg* 2012;22: 662–6.
9. Wang SS, Li JF, Zhang SM, Jing JJ, Xue L. A virtual reality model of the clivus and surgical simulation via transoral or transnasal route. *Int J Clin Exp Med* 2014;15:3270–9.
10. Koenigsberg RA, Vakil N, Hong TA, Htaik T, Faerber E, Maiorano T, Dua M, Faro S, Gonzales C. Evaluation of platybasia with MR imaging. *AJNR Am J Neuroradiol* 2005;26:89–92.

**ORCID ID:**

T. Moralı Güler 0000-0003-1083-1601;  
 Ö. F. Ünal 0000-0001-9602-7993;  
 G. Kahiloğulları 0000-0001-8137-0510

**Correspondence to:** Tuğba Moralı Güler, MD

Neurosurgery Unit, Private Medikar Hospital,  
 Karabük, Türkiye  
 Phone: +90 533 425 31 50  
 e-mail: tugbamorali@yahoo.com

*Conflict of interest statement:* No conflicts declared.

This is an open access article distributed under the terms of the Creative Commons Attribution-NonCommercial-NoDerivs 4.0 Unported (CC BY-NC-ND4.0) Licence (<http://creativecommons.org/licenses/by-nc-nd/4.0/>) which permits unrestricted noncommercial use, distribution, and reproduction in any medium, provided the original work is properly cited. *How to cite this article:* Moralı Güler T, Ünal ÖF, Kahiloğulları G. The radiological anatomy of clivus for surgical approaches. *Anatomy* 2022;16(2):51–55.

# Relationship between the carrying angle and some other parameters related to muscle strength and endurance in healthy young adults

Kübra Erdoğan<sup>1</sup> , Mehmet Ali Malas<sup>1</sup> , Deniz Bayraktar<sup>2</sup> , Hilal Uzunlar<sup>2</sup> , Derya Özer Kaya<sup>2</sup> 

<sup>1</sup>Department of Anatomy, Faculty of Medicine, İzmir Katip Çelebi University, İzmir, Türkiye

<sup>2</sup>Department of Physiotherapy and Rehabilitation, Faculty of Health Sciences, İzmir Katip Çelebi University, İzmir, Türkiye

## Abstract

**Objectives:** The present study aimed to determine whether there is a relationship between carrying angle and some parameters such as the middle part of the deltoid muscle strength, hand grip muscle strength, lateral bridge times and push-up repeats for both genders.

**Methods:** This study was carried out on 100 (48 male, 52 female) university students aged between 18–30 years. Individuals with known chronic systemic disease, congenital or acquired anomaly of the skeletal system and a body mass index of 30 and above were excluded. Only right-handed participants were included to eliminate the confusion of dominance. The participants' age, gender, height, body weight, and body mass index were recorded. The carrying angles were measured with a goniometer. The middle part of the deltoid muscle strength and hand grip strength measurements were used to evaluate muscle strength, and the lateral bridge test and push-up test were used for endurance.

**Results:** A statistically significant difference was found between carrying angle values on the right and left sides in males ( $p=0.004$ ), while there was no difference in the females ( $p=0.28$ ). A statistically significant difference was found between the genders on the left carrying angle ( $p<0.001$ ). A statistically significant difference was found in the total group and in both genders on middle part of the deltoid muscle strength and hand grip strength between the sides. In males, a significant positive correlation was found between carrying angle and the middle part of the deltoid muscle strength ( $r=0.29$ ,  $p=0.04$ ) on the right side. In females, a significant negative correlation was found between carrying angle and the hand grip test ( $r=-0.29$ ,  $p=0.04$ ) on the left side. There was no significant correlation between carrying angles and other parameters in both genders.

**Conclusion:** Our results suggest that the carrying angle may be related to the middle part of the deltoid muscle strength in males on the right side and lateral bridge test in females on the right side, even though they are weak.

**Keywords:** carrying angle; deltoid muscle strength; endurance; hand-grip strength; lateral bridge test; push-up test

Anatomy 2022;16(2):56–61 ©2022 Turkish Society of Anatomy and Clinical Anatomy (TSACA)

## Introduction

The carrying angle (CA) is the angle between the longitudinal axes of the humerus and the radially deviated forearm in the anatomical position while the elbow is fully extended and supinated. CA is approximately 17°, but the absolute angle varies between individuals.<sup>[1]</sup> The CA varies depending on age and gender, and also it is considered as one of the secondary sex characteristics in the literature.<sup>[2,3]</sup> The CA difference according to gender may vary due to laxity of articular ligaments, larger breasts and wider pelvis in females.<sup>[4]</sup> In addition, there is no consensus in the literature whether the CA is greater

on the right or left sides. While some studies mentioned lateralization, no consensus was reached about which dominant or non-dominant sides have a greater CA.<sup>[3,5,6]</sup> On the other hand, some studies reported that the CA does not differ between the sides.<sup>[4,6]</sup> Furthermore, in the foetal period, no difference was reported between CA of the right and left sides within both genders, but a significant difference was found between genders.<sup>[7]</sup>

The deltoid muscle arises from the shoulder girdle and attaches to the lateral surface of the humerus. The middle part of the deltoid muscle allows abduction of the arm and it is more effective at higher abduction angles.

The supraspinatus muscle has a synergistic effect on the deltoid muscle during the first 30°. The deltoid muscle stabilizes the humeral head during abduction.<sup>[8]</sup> Muscle strength may differ between genders because males usually have more muscle bulk, and also there are some physiological differences between genders.<sup>[9,10]</sup> Leyk et al.<sup>[10]</sup> reported grip strength of the females is lower than the male counterparts. Upper extremity muscle strength is also affected by hand dominance. Also, many studies reported that the grip strength is more likely to be higher on the dominant side.<sup>[11-13]</sup> Patel and Verma<sup>[14]</sup> reported that grip strength, an indicator of general muscle strength, moderately (Spearman's rho between -0.494 and -0.551) related to CA for both sides. The results of these authors indicate that while CA increases, grip strength decreases, and vice versa. The fact that upper extremity muscle strength and hand grip strength change with hand dominance may raise the question of whether there is a relationship with the CA. However, there is limited evidence regarding the relationships between the CA and upper extremity muscle strength or endurance.

The core of the body includes the abdominals, paraspinals, gluteals, diaphragm, pelvic floor, and hip girdle muscles. Core muscles are central to the functional kinetic chain and these muscles initially power all limb movements.<sup>[15]</sup> This muscle group provides the proximal stability for the distal mobility and function of the limbs.<sup>[16]</sup> Contraction of the abdominal muscles increases intra-abdominal pressure, stabilizing the lumbar spine for postural support before limb movement. The thoracolumbar fascia connects the lower and upper extremities so that the core muscles are used in activities such as throwing.<sup>[16]</sup> Erickson et al.<sup>[17]</sup> conducted a study on baseball players in which they evaluated the CA. In their study, they reported that the mean CA was statistically significantly different ( $p < 0.001$ ) in the throwing arm ( $12.5^\circ \pm 4.2^\circ$ ) compared to the other arm ( $9.9^\circ \pm 2.8^\circ$ ).

The core muscles can be evaluated with different tests. Static muscular endurance is based on the ability to sustain a contraction and can be measured through tests such as flexor endurance, lateral bridge and back extensor tests.<sup>[18,19]</sup> The push-up exercise is one of the exercises used to develop upper body and upper arm muscular endurance. The total number of push-ups is a parameter used as an indicator of upper-arm and shoulder girdle strength and endurance.<sup>[19]</sup> Although we couldn't find strong evidence regarding the relationships of the CA and core muscle or shoulder endurance in the literature, core and shoulder endurance seems to be related to upper extremity movements and positions. Considering all of these, the present study aimed to investigate whether

there is a relationship between CA and some parameters related to muscle strength, shoulder and body endurance.

## Materials and Methods

This study was carried out on 100 (48 males, 52 females) university students aged between 18-30. Individuals with known chronic systemic disease, congenital or acquired anomaly of the skeletal system or a history of trauma and individuals with a body mass index of 30 and above were excluded. The dominant hand was determined as inquired by asking the hand used for writing, and only right-handed participants were included in the study.<sup>[20]</sup>

First, the individuals participating in the study signed an informed consent form. The participants' age, gender, height, body weight, and body mass index (BMI) were recorded in a structured data recording form. While the participants were standing in an anatomical position with their upper extremities fully extended and supinated, the carrying angles were measured with a goniometer (Baseline Stainless Steel Goniometer, USA) as stated in literature.<sup>[2]</sup>

The upper extremities were evaluated by measuring the middle part of the deltoid muscle strength and hand grip strength. And push-up and lateral bridge tests were assessed for endurance. The middle part of the deltoid muscle strength of the participants was measured by using maximal voluntary isometric contractions (make test) with a hand-held dynamometer (Lafayette 12-0380 Manual Muscle Tester, Lafayette, IN, USA) and a belt which attached to a stable table.<sup>[21]</sup> Participants were asked to sit upright on a bed with 90° abduction and forearm pronation and to push the arm to the belt toward the hand-held dynamometer. The evaluation was performed with both upper extremities. A 30-second rest was provided between each measurement. Three measurements were performed and the highest result was used in the analysis.

Hand grip strength was measured with the Jamar hand dynamometer (Jamar®, Patterson Medical, Warrenville, IL, USA). Testing was started with the dominant extremity.<sup>[22]</sup> Measurements were made in a sitting position with the shoulder in adduction and neutral rotation, elbow in 90° flexion, forearm in mid-rotation, and wrist in neutral.<sup>[23]</sup> Participants were asked to squeeze the dynamometer arm as strongly as possible and verbally encouraged during testing until the highest score was observed on the dynamometer screen. Three measurements were performed with 30-second breaks between each measurement, and the highest value was used in the analysis.<sup>[22-24]</sup>

The lateral bridge test, a static endurance test of the lateral trunk muscles, was used to evaluate the endurance

of the trunk muscles.<sup>[18]</sup> Participants were asked to maintain the position for the maximum time by raising their bodies flat on their toes with lower elbows and forearms while in the side-lying position. The time until the deterioration of the position was recorded in seconds.

The push-up test was used in males and the modified push-up test was used in females to measure the endurance of the arm and shoulder girdle muscles. The participants were asked to lift their heads, shoulders and trunk from the ground with the elbows in full extension from a prone position on the bed with their arms and elbows flexed.<sup>[25]</sup> The test was performed with full extension of the trunk and lower extremities in males and with trunk extension and knee flexion in females. The abdomen was not allowed to touch the mat during the assessment and participants were asked to keep the straight position of their back at all times. The test was stopped when the participants were unable to maintain their position. The maximum number of push-ups performed in a row without rest for one minute was used in the analysis.<sup>[26]</sup>

In addition, gender groups were divided into two groups as cases with the CA below and above the mean value. Muscle strengths and endurances in these two groups were compared with an independent samples test.

The statistical analysis was performed using SPSS (Version 25.0, IBM Corp., Armonk, NY, USA). The conformity to normal distribution was examined using the

Shapiro-Wilk test. Mean and standard deviations of the parameters were obtained according to gender groups and right and left sides. Sides and gender groups were compared using the t-test, and non-conforming groups were evaluated using the Mann-Whitney U test. The correlation between measurements was evaluated with the Pearson correlation test. The statistical significance level was determined as  $p < 0.05$ .

## Results

In our study, 100 people (48 males, 52 females) were evaluated in a young population. The mean, standard deviation and p values of demographic data, CA, the middle part of deltoid muscle strength, grip strength, lateral bridge and push-up tests are shown in **Table 1**.

Statistically significant differences were found in the parameters between the genders except for age and right carrying angles (**Table 1**). There was no statistically significant difference between the right and left sides of the whole group CA ( $p=0.10$ ). However, there was a statistically significant difference between CA values on the right and left sides in males ( $p=0.004$ ), while there was no difference in the females ( $p=0.28$ ) (**Table 1**). Middle part of the deltoid muscle strength and hand grip strength between the sides, a statistically significant difference was observed in the total group and in both genders (**Table 1**). In comparing the lateral bridge test between the sides, no statistically significant difference was detected in the whole group

**Table 1**

Comparison of demographic characteristics, carrying angle and other parameters according to genders and right/left sides.

		Male (n=48) Mean±SD	Female (n=52) Mean±SD	Total (n=100) Mean±SD	p-values for gender comparison	p-values for side comparison
Age (year)		19.54±1.11	19.96±1.04	19.76±1.09	0.055	-
Height (cm)		178.45±5.07	163.69±5.67	170.78±9.15	<0.001*	-
Weight (kg)		75.38±13.07	57.86±9.30	66.27±14.24	<0.001*	-
BMI (kg/m <sup>2</sup> )		23.64±3.82	21.57±3.08	22.56±3.59	0.004†	-
Carrying angle (°)	Right	22.06±3.22	23.19±2.77	22.65±3.03	0.064	male p=0.004†
	Left	20.64±3.09	23.55±2.38	22.16±3.10	<0.001*	female p=0.28
Middle part of the deltoid muscle strength (kg)	Right	17.75±6.23	10.38±2.10	13.92±5.86	<0.001*	male p=0.026†
	Left	16.83±5.75	9.73±2.06	13.14±5.53	<0.001*	female p=0.001†
Grip strength (kg)	Right	39.62±6.69	23.71±4.27	31.34±9.71	<0.001*	male p=0.004†
	Left	37.46±7.41	21.68±3.50	29.25±9.75	<0.001*	female p<0.001*
Lateral bridge test (sec)	Right	59.08±23.61	37.96±18.75	48.10±23.63	<0.001*	male p=0.33
	Left	56.74±24.66	38.10±19.55	47.05±23.94	<0.001*	female p=0.94
Push-up test (repeat)		20.62±11.21	15.67±6.52	18.05±9.37	0.009†	-

\* $p < 0.001$ , † $p < 0.005$ . BMI: Body mass index.

and in both genders. Males had higher push-up counts than females (Table 1,  $p=0.009$ ). The correlations between the parameters are shown in Table 2 according to the sides for both genders.

In males, a significant positive correlation was found between CA and the middle part of the deltoid muscle strength ( $r=0.29$ ,  $p=0.04$ ) on the right side. In females, a significant negative correlation was found between CA and the hand grip test ( $r=-0.29$ ,  $p=0.04$ ) on the left side. There was no significant correlation between carrying angles and other parameters in both genders.

In addition, gender groups were divided into cases with the CA below and above the mean value. Muscle strengths and endurances belonging to these two groups were compared. In males, there was a significant difference in the group's middle part of the deltoid muscle strength with a large CA on the right side ( $p=0.003$ ). The male group with larger CA also had a stronger middle part of the deltoid muscle on the right side. There was no significant difference between the male groups in other parameters. In females, there was a significant difference between the larger and smaller CA groups; the lateral bridge test results were higher in the group with a smaller CA ( $p=0.03$ ) on the right side. There was no significant difference between other parameters in females.

## Discussion

Studies in the literature reported that the CA varies according to age, gender, dominant hand side, and body characteristics such as weight and height. In our study, we investigated whether the CA is related to muscle strength and endurance.

Numerous studies have reported that the CA is statistically significantly larger in females than males.<sup>[2,4,6,27]</sup> It was even described as a gender-specific factor. Erdoğan and Malas<sup>[7]</sup> reported that males had greater CA than females in the fetal period. Another study reported

that the CA was greater in males aged between 3–5.<sup>[3]</sup> On the other hand, studies also reported no difference between genders.<sup>[28,29]</sup> In our study, there was a significant difference between genders only in the left side CA ( $p<0.001$ ). CA of the dominant side (right side) were similar in both genders.

Studies in the literature reported that the CA is larger on the right side.<sup>[3,27]</sup> In some studies, the dominant hand was questioned and they reported that the CA was larger on the dominant side.<sup>[17,30,31]</sup> Another study revealed that the CA is larger on the non-dominant side.<sup>[5]</sup> However, studies also report no difference between the CA of both sides.<sup>[4,6,29]</sup> In our study, left-hand dominant individuals were excluded. There was no difference between the right and left sides on the CA in the whole group, regardless of gender ( $p=0.10$ ). When the CA of the right and left sides of male individuals were compared, a significant difference was found ( $p=0.004$ ), but not in females ( $p=0.28$ ). This result is similar to a study conducted on professional baseball players, where the CA on the dominant side was measured larger than on the non-dominant side.<sup>[17]</sup> In contrast, there was a significant difference between males and females on the left side CA ( $p<0.001$ ) but not on the right side ( $p=0.064$ ). The studies in the literature do not seem to have a consensus on which side has a larger CA.

CA was weak and positively correlated to the middle part of the deltoid muscle strength in males in the present study ( $r=0.29$ ,  $p=0.044$ ). However, the correlation between the CA and the hand grip test on the right side was not statistically significant different ( $r=0.28$ ,  $p=0.052$ ) in males. According to these results, there was not a strong relationship between the CA and the strength of the upper extremity muscles. This study can be taken further by measuring the strength of different muscles on the dominant side belonging to the upper extremity. Also, it would be useful to make the measure-

**Table 2**  
Correlations between carrying angle and other parameters (r).

Gender	Sides	Middle part of the deltoid muscle strength		Grip strength		Lateral bridge test		Push-up test
		Right	Left	Right	Left	Right	Left	
Male	Right CA (°)	0.29*		0.28		-0.21		0.16
	Left CA (°)		0.11		0.15		-0.06	-0.06
Female	Right CA (°)	0.12		-0.09		-0.08		0.18
	Left CA (°)		0.19		-0.29*		-0.03	-0.07

\* $p<0.05$ .

ments on a more significant number of subjects to clarify these correlations.

When comparing two groups with CA below and above, the mean value in both genders, in males' middle part of the deltoid muscle strength was higher in the group with a larger CA on the right side ( $p=0.003$ ). In females, the lateral bridge test results were higher in the group with a smaller CA ( $p=0.003$ ). This result might be interpreted as a significant functional relationship between CA and the middle part of the deltoid muscle strength and between CA and body endurance on the right (dominant) side.

In a retrospective study comparing individuals with lateral epicondylitis and the control group, it was reported that there was a significant difference in CA. Lateral epicondylitis was found to be associated with the dominant side. In addition, increased CA has been reported to be associated with lateral epicondylitis. It has been stated that, it may contribute to the etiology of lateral epicondylitis by increasing the extensor carpi radialis brevis tendon tension.<sup>[32]</sup> In our study, a significant relationship between the middle part of the deltoid muscle strength and CA was determined. The middle part of deltoid muscle strength and hand grip strength were evaluated to give an idea about upper extremity muscle strength in general. It seems that the CA may be related to various upper extremity muscles. Examination of the relationship between the other upper extremity muscle strengths and the CA may give an idea about which muscles may have an effect on the CA.

## Conclusion

In our study, we aimed to understand whether muscle strength and endurance affect the CA. A statistically significant difference was observed in the total group and in both genders on middle part of the deltoid muscle strength and hand grip strength between the sides. In males, a significant positive correlation was found between CA and middle part of the deltoid muscle strength ( $r=0.29$ ,  $p=0.04$ ) on the right side. In females, a significant negative correlation was found between CA and the hand grip test ( $r=-0.29$ ,  $p=0.04$ ) on the left side. Although these correlation values were statistically significant, they were weak. Prospective studies may provide more detailed information about whether the change in muscle strength affects the CA. Examination of the relationship between the other upper extremity muscle strengths and the CA may provide insight into which muscles may affect the CA.

## Conflict of Interest

The authors declare no conflict of interest.

## Author Contributions

KE: project development, data collection, data analysis, manuscript writing; MAM: data analysis, manuscript writing; DB: data collection; HU: data collection; DÖK: project development.

## Ethics Approval

Ethics committee approval was obtained from the Clinical Research Ethics Committee of İzmir Katip Çelebi University (2019-KAE-0277).

## Funding

This study was funded by İzmir Katip Çelebi University, Coordinatorship of Scientific Research with the following research number: 2019-GAP-SABF-0005.

## References

1. Johnson D, Ellis H, Collins P. Pectoral girdle and upper limb. In: Standing S, editor. *Gray's anatomy: the anatomical basis of clinical practice*. 29th ed. Edinburgh (Scotland): Elsevier Churchill Livingstone; 2005. p. 846.
2. Chinweife K, Ejimofor O, Ezejindu D. Correlation of carrying angle of the elbow in full extension and hip-circumference in adolescents of Nnewi people in Anambra State. *International Journal of Scientific and Research Publications* 2014;4:547.
3. Dey S, Mandal L, Kundu B, Mondal M, Sett TK. Carrying angle of the elbow: it's changes from childhood to adulthood: morphometric study in Eastern India. *Indian Journal of Basic and Applied Medical Research* 2013;8:823–30.
4. Bari W, Alam M, Omar S. Goniometry of elbow carrying angle: a comparative clinical study on sexual dimorphism in young males and females. *International Journal of Research in Medical Sciences* 2015; 3:3482–4.
5. Sharma K, Mansur D, Khanal K, Haque M. Variation of carrying angle with age, sex, height and special reference to side. *Kathmandu Univ Med J* 2013;11:315–8.
6. Kaewpornawan K, Kamegaya M, Udompunterak S, Ariyawatkul T. The normal reference values of carrying angle from birth to adolescence. *Siriraj Medical Journal* 2018;70:284–8.
7. Erdoğan K, Malas MA. The investigation of the carrying angle of the elbow in fetal period. *Surg Radiol Anat* 2020;42:911–8.
8. Moser T, Lecours J, Michaud J, Bureau NJ, Guillin R, Cardinal É. The deltoid, a forgotten muscle of the shoulder. *Skeletal Radiol* 2013; 42:1361–75.
9. Nicolay CW, Walker AL. Grip strength and endurance: influences of anthropometric variation, hand dominance, and gender. *International Journal of Industrial Ergonomics* 2005;35:605–18.
10. Leyk D, Gorges W, Ridder D, Wunderlich M, Rütger T, Sievert A, Essfeld D. Hand-grip strength of young men, women and highly trained female athletes. *Eur J Appl Physiol* 2007;99:415–21.
11. Incel NA, Ceceli E, Durukan PB, Erdem HR, Yorgancıoğlu ZR. Grip strength: effect of hand dominance. *Singapore Med J* 2002;43: 234–7.
12. Noonari SB, Samejo B, Nonari MH. The association between hand grip strength and hand span of dominant and non-dominant

- hand of undergraduate physiotherapy students. *Journal of Modern Rehabilitation* 2019;13:193–8.
13. Zaccagni L, Toselli S, Bramanti B, Gualdi-Russo E, Mongillo J, Rinaldo N. Handgrip strength in young adults: association with anthropometric variables and laterality. *Int J Environ Res Public Health* 2020;17:4273.
  14. Patel MR, Verma S. Effect of varying carrying angle on grip strength in normal young individuals. *International Journal of Health Sciences and Research* 2018;8:159–66.
  15. Akuthota V, Nadler SF. Core strengthening. *Arch Phys Med Rehabil* 2004;85:S86–92.
  16. Kibler WB, Press J, Sciascia A. The role of core stability in athletic function. *Sports Med* 2006;36:189–98.
  17. Erickson BJ, Chalmers PN, Zajac J, Sgroi T, Eno JJ, Altchek DW, Dines JS, Coleman SH. Do professional baseball players with a higher valgus carrying angle have an increased risk of shoulder and elbow injuries? *Orthop J Sports Med* 2019;7:1–5.
  18. Dejanovic A, Cambridge ED, McGill S. Isometric torso muscle endurance profiles in adolescents aged 15–18: normative values for age and gender differences. *Ann Hum Biol* 2014;41:153–8.
  19. Rozenek R, Byrne JJ, Crussemeyer J, Garhammer J. Male-female differences in push-up test performance at various cadences. *J Strength Cond Res* 2022;36:3324–9.
  20. Shiri R, Varonen H, Heliövaara M, Viikari-Juntura E. Hand dominance in upper extremity musculoskeletal disorders. *J Rheumatol* 2007;34:1076–82.
  21. Kolber MJ, Cleland JA. Strength testing using hand-held dynamometry. *Physical Therapy Reviews* 2005;10:99–112.
  22. Cildan Uysal S, Tonak HA, Kitis A. Validity, reliability and test-retest study of grip strength measurement in two positions with two dynamometers: Jamar® Plus and K-Force® Grip. *Hand Surg Rehabil* 2022;41:305–10.
  23. Fess EE. Clinical assessment recommendations. In: Casanova JS, editor. *Grip strength*. 2nd ed. Chicago: American Society of Hand Therapists; 1992. p. 41–5.
  24. Özyürek S, Aktar B. Investigation of the relationship between handgrip strength and cough strength in healthy individuals. *Journal of Health Science and Profession* 2018;5:39–43.
  25. Baumgartner TA, Oh S, Chung H, Hales D. Objectivity, reliability, and validity for a revised push-up test protocol. *Measurement of Physical Education Exercise Science* 2002;6:225–42.
  26. Ambegaonkar JP, Caswell SV, Winchester JB, Caswell AA, Andre MJ. Upper-body muscular endurance in female university-level modern dancers: a pilot study. *J Dance Med Sci* 2012;16:3–7.
  27. Eliakim-Ikechukwu C, Atu L, Etika M, Udo-affah G. The carrying angle of the Ibo and Yoruba ethnic groups of Nigeria and its relationship with the height of individuals. *Journal of Biology, Agriculture and Healthcare* 2012;2:157–62.
  28. Emami MJ, Abdinejad F, Khodabakhshi S, Amini M, Naseri B. The normal carrying angle of the elbow in Shiraz. *Medical Journal of the Islamic Republic of Iran* 1998;12:37–9.
  29. Kumar B, Pai S, Ray B, Mishra S, Siddaraju K, Pandey A, Binu S. Radiographic study of carrying angle and morphometry of skeletal elements of human elbow. *Rom J Morphol Embryol* 2010;51:521–6.
  30. Paraskevas G, Papadopoulos A, Papaziogas B, Spanidou S, Argiriadou H, Gigis J. Study of the carrying angle of the human elbow joint in full extension: a morphometric analysis. *Surg Radiol Anat* 2004;26:19–23.
  31. Yilmaz E, Karakurt L, Belhan O, Bulut M, Serin E, Avci M. Variation of carrying angle with age, sex, and special reference to side. *Orthopedics* 2005;28:1360–3.
  32. Umur LF, Surucu S. Association between increased elbow carrying angle and lateral epicondylitis. *Cureus* 2022;14:e22981.

**ORCID ID:**

K. Erdoğan 0000-0003-0417-4094; M. A. Malas 0000-0002-1451-0672;  
D. Bayraktar 0000-0002-2852-8910; H. Uzunlar 0000-0002-6870-0770;  
D. Özer Kaya 0000-0002-6899-852X



**Correspondence to:** Kübra Erdoğan, MD  
Department of Anatomy, Faculty of Medicine,  
İzmir Katip Çelebi University, İzmir, Türkiye  
Phone: +90 232 329 35 35  
e-mail: erdkubra@yahoo.com

*Conflict of interest statement:* No conflicts declared.

This is an open access article distributed under the terms of the Creative Commons Attribution-NonCommercial-NoDerivs 4.0 Unported (CC BY-NC-ND4.0) Licence (<http://creativecommons.org/licenses/by-nc-nd/4.0/>) which permits unrestricted noncommercial use, distribution, and reproduction in any medium, provided the original work is properly cited. *How to cite this article:* Erdoğan K, Malas MA, Bayraktar D, Uzunlar H, Özer Kaya D. Relationship between the carrying angle and some other parameters related to muscle strength and endurance in healthy young adults. *Anatomy* 2022;16(2):56–61.

# Evaluation of trabecular structure of hamate using micro-computed tomography

Hakan Ocak<sup>1</sup> , Hakan Hamdi Çelik<sup>2</sup> , Mert Ocak<sup>3</sup> , Ferhat Geneci<sup>4</sup> 

<sup>1</sup>Department of Anatomy, Faculty of Medicine, Ağrı İbrahim Çeçen University, Ağrı, Türkiye

<sup>2</sup>Department of Anatomy, Faculty of Medicine, Hacettepe University, Ankara, Türkiye

<sup>3</sup>Department of Anatomy, Faculty of Dentistry, Ankara University, Ankara, Türkiye

<sup>4</sup>Department of Anatomy, Faculty of Medicine, Ankara Yıldırım Beyazıt University, Ankara, Türkiye

## Abstract

**Objectives:** In this study, we intended to reveal the trabecular structure of hamate by using micro-computed tomography.

**Methods:** This study was carried out on 55 human dry hamates. The bones were scanned with a micro-CT device. Volume, surface, and trabecular parameters (trabecular number, trabecular thickness, trabecular separation) of the scanned bones were analyzed.

**Results:** The mean percentage of the bone volume was  $44.930 \pm 5.859\%$ , trabecular number was  $1.31 \pm 0.150 \text{ mm}^{-1}$ , trabecular thickness was  $0.35 \pm 0.056 \text{ mm}$ , trabecular separation was  $0.57 \pm 0.087 \text{ mm}$ .

**Conclusion:** Hamate has sufficient strength for screw implantation in terms of trabecular thickness and number, but weaker in terms of trabecular separation when compared with other carpal bones. Hamate has the greatest trabecular thickness among the other carpal bones, while it is ranked as the second in terms of trabecular number.

**Keywords:** carpal bones; hamate; micro-computed tomography; microstructure; trabeculae

Anatomy 2022;16(2):62–68 ©2022 Turkish Society of Anatomy and Clinical Anatomy (TSACA)

## Introduction

Hamate is a cuneiform bone with its special unciform process called as hook of hamate projecting from distal part of the palmar surface.<sup>[1]</sup> Hamate articulates with triquetrum, 4th and 5th metacarpal bones, and also with the ulnar side of the capitate. The hook of hamate projects from the volar side 1–2 cm distally and radially to the pisiform bone. It forms the ulnar side of the carpal tunnel and the radial side of Guyon's canal. Its ossification is not completed until the age of 15.<sup>[2]</sup> Several structures attach to the hook of hamate such as pisohamate ligament and transverse carpal ligament. Hamate is prone to subluxation and fractures because of its weak blood supply. Biomechanical factors, such as ligaments and muscles attaching to the bone can lead to fractures and subluxations. Blood supply may affect fracture healing (union-non-union procedure) and occurring avascular necrosis after trauma.<sup>[3]</sup>

Micro-computed tomography (Micro-CT) is a valuable method for the investigation of bone morphometry and microarchitecture. This method uses data sets obtained by

X-ray attenuation for the 3-dimensional representation of material density. In this era resolution of micro-CT devices has increased up to several micrometers.<sup>[4]</sup>

The literature reveals some pathological cases such as fractures,<sup>[5–8]</sup> avascular necrosis,<sup>[9–11]</sup> osteoblastoma,<sup>[12,13]</sup> osteochondroma,<sup>[14,15]</sup> and osteomyelitis<sup>[16]</sup> related to hamate. Hamate fractures occur in the body and hamulus parts of the bone. Both types of fractures are characterized by pain felt on the ulnar side of the wrist, which may be associated with ulnar paresthesia. Delayed diagnosis of the fracture may cause ulnar neuritis, ulnar artery thrombosis, and rupture of the flexor digitorum profundus tendons of 4th and 5th fingers.<sup>[17]</sup>

Clinical CT and micro-CT can be used to determine the bone microstructure. Studies have shown that all the values that can be measured with clinical CT can be measured more precisely with micro-CT. However, despite of the high resolution of micro-CT, its ability to scan only small parts that can be placed in its chamber makes it impossible to use it in a clinical setting.<sup>[18]</sup> This study

aimed to explore the trabecular microstructure of human dry hamates using micro-CT scanning method.

## Materials and Methods

Fifty-five human dry hamates without any external deformity were included in the study. The bones were obtained from collections of Anatomy Departments of Hacettepe and Ankara Universities in Turkey. Scanning and analysis were executed via micro-CT device (SkyScan 1174, SkyScan, Aartselaar, Belgium) at Hacettepe University. The scanning parameters were set as follows: degree of rotation=180°, exposure time=2700 milliseconds, current=800 mA, voltage=50 kVp, projection=33 µm and scanning time=90 minutes.

After the scanning procedure, the raw data in TIF format were reconstructed with Nrecon software (Micro Photonics Inc., Allentown, PA, USA) and axial images were generated in BMP format with 33 µm of projection. Then these reconstructed data were transferred to CTAn software and 2D–3D analysis was performed with this software. In this study we studied 2 groups of parameters; (i) volume-surface and (ii) trabecular properties. In the volume-surface group, we examined the following parameters: tissue volume, bone volume, percent bone volume (bone volume/tissue volume), bone surface, bone surface/volume ratio; while in the trabecular group we examined trabecular number, trabecular thickness, trabecular separation, structure model index and degree of anisotropy.

Statistical analysis was performed with IBM SPSS Statistics Version 23.0 (Armonk, NY, USA) with 95 % confidence interval. The distribution of variables (whether normally distributed or not) was tested via the Kolmogorov-Smirnov test.

## Results

The measurements were performed on 3D reconstruction images of the hamates (Figures 1 and 2). The average percentage of bone volume was  $44.930 \pm 5.859\%$ . There was high range in the average percentage of bone volume ranging between 29.65–60.78%. While the mean trabecular thickness was  $0.350 \pm 0.056$  mm, the average number of trabeculae for each mm was  $1.31 \pm 0.15$ . The average value for the trabecular separation, which indicates the mean space between trabeculae, was  $0.570 \pm 0.087$  mm. For trabecular number, trabecular thickness, and trabecular separation values, there was an up to two-fold difference between the minimum and maximum values (Table 1). While the samples showed a wide scatter in terms of structure-model index, the samples were much more homogeneous in terms of degree of anisotropy.

## Discussion

Bone strength is an important factor for implant treatment. This factor is related to bone integration. In some studies, a relationship is observed between bone quality and the success of implant treatment.<sup>[19,20]</sup> Bone mass, bone mineral density, macro and microarchitecture, and matrix properties are some of the factors which determine bone quality. Cortical bone is the primary determinant of bone robustness while the spongy bone is part of bone-implant integration. Information of trabecular bone structure has some importance for the success of implant treatment and further evaluation of implant surface architecture. Bone/implant integration is dependent upon the bone quality and bone/implant interphase.<sup>[21]</sup> Trabecular bone is the determinant of bone integration and forms the bone/implant interphase. For this reason, the trabecular bone structure should be researched to obtain objective and detailed scientific information. Lee et al.<sup>[22]</sup> scanned bones that had 4 different quality levels with the micro-CT device and revealed a statistically important relationship between bone quality and bone volume density, bone surface/volume ratio. Also, statistically significant correlations were observed between all the parameters. For this reason, in addition to trabecular parameters (trabecular thickness, number, and separation, structure-model index, degree of anisotropy) some other parameters (tissue volume, bone surface, bone volume, bone surface/volume ratio, percentage bone volume) which are affected by trabecular structure were also examined in the present study.

Tissue volume represents both volumes of bone tissue and spaces between these bone tissues while bone volume includes the only volume of bony structure but not spaces between these structures. Tissue volume and bone volume were observed as  $2526.120 \pm 604.615$  mm<sup>3</sup> and  $1137.100 \pm 318.973$  mm<sup>3</sup> subsequently in this study.

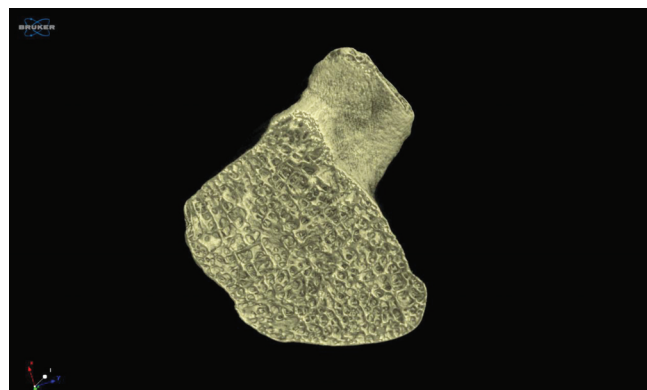
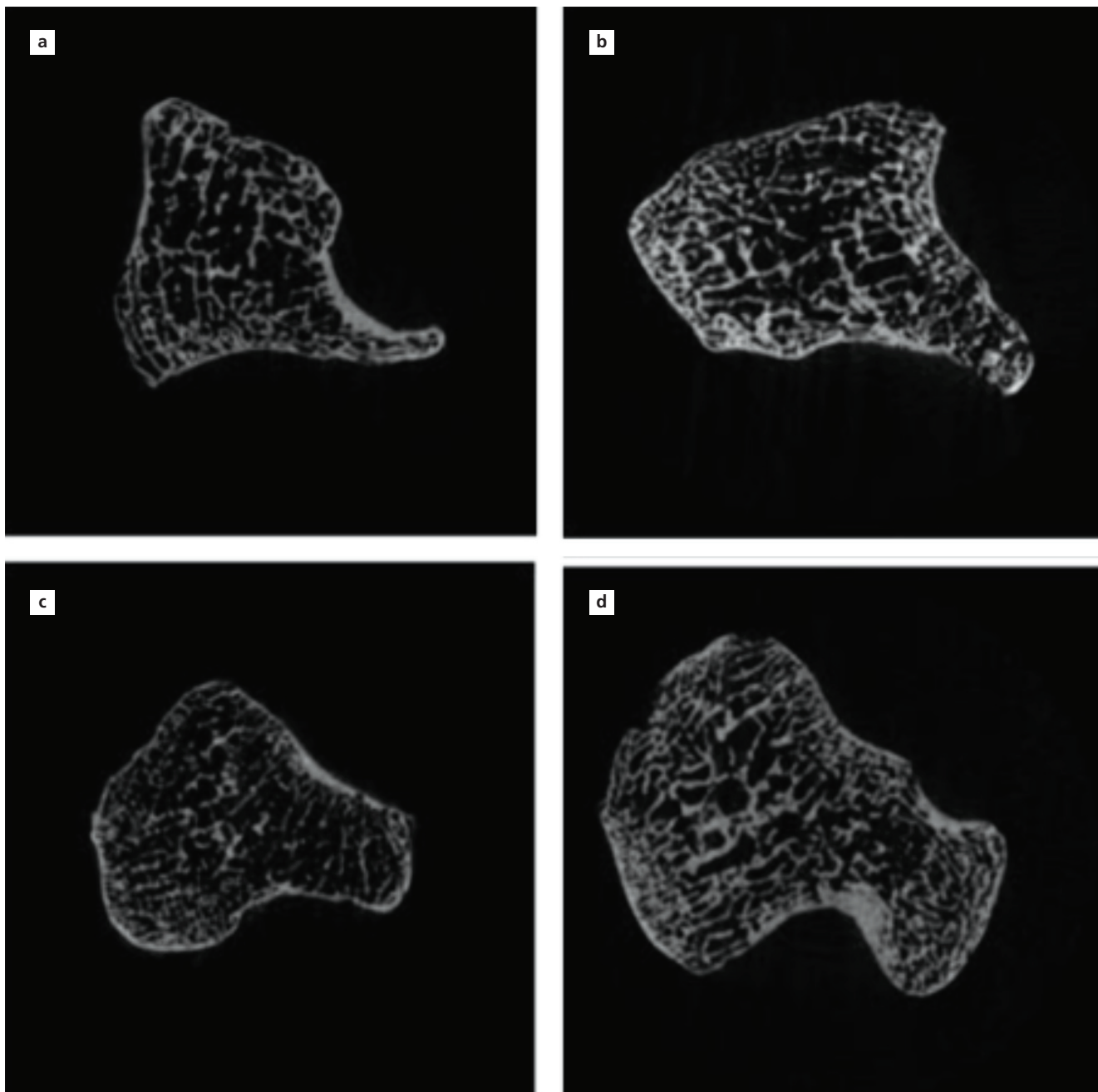


Figure 1. Trabecular structure of hamate.



**Figure 2.** Trabecular number, trabecular thickness, and trabecular separation of different hamates (a-d).

Percentage bone volume is the ratio of bone volume to tissue volume and was observed as  $44.930 \pm 5.859\%$  in our study. Previous studies have revealed data belonging to other carpal bones regarding bone and tissue volumes but since each carpal bone has a different dimension, it is quite an expected result that these bones will have different volume. So, it is not logical to compare these bones with each other in terms of volumes.

The bone surface represents the surface of trabeculae in inspected area. In our study the mean bone surface was measured as  $12149.250 \pm 3738.144 \text{ mm}^2$ . Trabecular number and thickness are parameters that change proportionately with the bone surface. Wurnig et al.<sup>[23]</sup> measured trabecular number and thickness as  $2.24 \pm 0.46 \text{ mm}^{-1}$  and  $0.229 \pm 0.032 \text{ mm}$  for cadaveric hamates. In our study, these values were  $1.31 \pm 0.150 \text{ mm}^{-1}$  and  $0.35 \pm 0.056 \text{ mm}$  for dry

**Table 1**  
Results of the measurements (n=55).

	Mean±SD	Min.–Max.
Tissue volume (mm <sup>3</sup> )	2526.12±604.615	1432.99–4358.62
Bone volume (mm <sup>3</sup> )	1137.10±318.973	540.46–1987.47
Percentage bone volume (%)	44.93±5.859	29.65–60.78
Bone surface (mm <sup>2</sup> )	12149.25±3738.144	6266.40–20443.43
Bone surface/volume ratio (mm <sup>-1</sup> )	10.78±2.006	7.78–17.38
Trabecular number (mm <sup>-1</sup> )	1.31±0.150	0.90–1.61
Trabecular thickness (mm)	0.35±0.056	0.23–0.49
Trabecular separation (mm)	0.57±0.087	0.38–0.83
Structure-model index	-0.12±0.638	-1.40–1.05
Degree of anisotropy	1.30±0.093	1.13–1.49

hamates subsequently. The bone surface/volume ratio represents the proportion of bone surface in the bone volume of the region of interest. Bone surface is also affected by trabecular number and thickness. In the aforementioned study<sup>[23]</sup> bone surface and bone surface/volume ratio parameters were not measured. Although it is not possible to judge the difference of the bone surface and bone surface/volume ratio with our study precisely, it is clear that none of these values (trabecular thickness and number) shows difference when compared with our study.

The trabecular number is the number of trabeculae that are observed in each mm of the sample. The higher number of trabeculae contributes positively to bone strength. We observed this value as  $1.310 \pm 0.150 \text{ mm}^{-1}$  while Wurnig et al.<sup>[23]</sup> as  $2.24 \pm 0.46 \text{ mm}^{-1}$ . In different studies, researchers compared normal carpal bones in various pathological conditions. Han et al.<sup>[24]</sup> compared normal lunates with those lunates which had Kienböck's disease, and they measured trabecular number as  $1.57 \pm 0.41 \text{ mm}^{-1}$  for normal lunates. Nufer et al.<sup>[25]</sup> studied normal trapezium and trapezium bones with osteoarthritis. The trabecular number was revealed as  $1.26 \pm 0.18 \text{ mm}^{-1}$  for non-pathological trapezium bones. Qu et al.<sup>[26]</sup> evaluated normal scaphoids and non-union scaphoids. They measured trabecular numbers for proximal and distal parts as  $0.08 \pm 0.04 \text{ mm}^{-1}$  and  $0.07 \pm 0.05 \text{ mm}^{-1}$  for normal specimens. It is known that bone strength changes proportionately with the trabecular number. Accordingly, it is possible to order the strength of the bones as lunate, hamate, trapezium, and scaphoid in terms of decreasing bone strength.

Trabecular thickness is the mean thickness of trabeculae in inspected area. Bone strength increases with higher trabecular thickness values. The trabecular thickness was

revealed as  $0.35 \pm 0.056 \text{ mm}$  in our study. Wurnig et al.<sup>[23]</sup> found this value as  $229 \pm 32 \mu\text{m}$  ( $0.229 \pm 0.032 \text{ mm}$ ) and Han et al.<sup>[24]</sup> as  $0.160 \pm 0.024 \text{ mm}$  for normal lunates. Nufer et al.<sup>[25]</sup> measured the trabecular thickness as  $0.17 \pm 0.02 \text{ mm}$  for normal trapezia; while Wurnig et al.<sup>[23]</sup> measured  $0.220 \pm 0.036 \text{ mm}$  for normal scaphoids. Increasing trabecular thickness is a factor that contributes to bone strength positively. When the bone strength is compared in terms of trabecular thickness the strength order will be in decreasing order as hamate, scaphoid, trapezium, and lunate.

Trabecular separation is a measure of the mean distance between trabeculae.<sup>[23]</sup> When trabecular number and thickness increase trabecular separation decreases and the behavior of these 3 parameters in this manner would increase the bone strength. In conclusion, the higher value of trabecular separation means the lower strength of the bone. In our study, the trabecular separation value was measured as  $0.57 \pm 0.087 \text{ mm}$ . Han et al.<sup>[24]</sup> revealed this value as  $0.52 \pm 0.21 \text{ mm}$  for lunates, Nufer et al.<sup>[25]</sup>  $0.74 \pm 0.18 \text{ mm}$  for trapezia, Qu et al.<sup>[26]</sup> as  $0.33 \pm 0.04 \text{ mm}$  (for proximal part) and  $0.33 \pm 0.05 \text{ mm}$  (for distal part) for scaphoids. In terms of trabecular separation, the bones can be ordered as the scaphoid, lunate, hamate, and trapezium in decreasing order of bone strength.

By the results of our study and other studies, it may be quite possible to judge differently when only one parameter is considered for determination of strength of the bone. For the diagnosis of some metabolic diseases such as osteoporosis and design of implant treatment for bone fractures, it is vital to consider multiple parameters to choose the correct treatment. And it is necessary to compare the results between samples whether they are statistically important or not.

Structure-model index is a trabeculae related factor. This factor may have -4, -3, 0, 3 and 4 values. “-4” and “-3” values correspond to spherical and cylindrical cavities while 0, 3 and 4 values represent smooth plate, cylindrical and spherical trabeculae. In our study, we measured the mean structure-model index as  $-0.12 \pm 0.638$ . These results indicate that our hamates had smooth plate-like trabeculae. Wurnig et al.<sup>[23]</sup> didn't study this parameter in their study. Han et al.<sup>[24]</sup> showed this value as  $1.99 \pm 0.31$  for normal lunates, Nufer et al.<sup>[25]</sup>  $1.35 \pm 0.44$  for normal trapezia and Qu et al.<sup>[26]</sup>  $0.63 \pm 0.74$  and  $0.63 \pm 1.00$  for proximal and distal parts of normal scaphoids. These results indicate that all the mentioned carpal bones together with hamate have smooth trabeculae. Change of structure-model index shows the changing pattern of trabeculae. For instance, Qu et al.<sup>[26]</sup> compared normal scaphoids with non-union scaphoids and observed that the latter has a higher value of structure-model index at its distal part. They also observed that the trabecular shape of the distal part resembled a cylinder in contrast to the proximal part's trabeculae. However, proximal part has a lower SMI showing its plate-like appearance, which is also an indicator of dense trabecular structure and stronger bone. The plate-like trabecular structure is a result of higher mechanical stress while the cylindrical shape is a result of lower mechanical stress. In conclusion, it can be said that hamates may be exposed to high mechanical stress.

Degree of anisotropy is a representation of trabecular distribution in the region of interest. If it is equal to 1 it means an isotropic trabecular distribution (alignment along the same axes) exists but values greater than 1 show anisotropic distribution. In this study, this value is measured as  $1.30 \pm 0.093$ . This result shows us that our hamate samples have an anisotropic trabeculae distribution. Wurnig et al.<sup>[23]</sup> measured this value as  $1.56 \pm 0.08$ . In previous studies, degree of anisotropy was revealed as  $0.44 \pm 0.86$  for lunates<sup>[24]</sup> and  $1.28 \pm 0.04$  for trapezia.<sup>[25]</sup> Accordingly, we can conclude that hamates and trapezia have an anisotropic trabeculae distribution in contrast to lunates which have an isotropic distribution. The degree of anisotropy is a measure of bone adaptation to the changing conditions of the structure-model index. For instance, Han et al.<sup>[24]</sup> observed that in the case of progressing bone necrosis, nonnecrotic bony tissue changes its trabecular distribution towards anisotropic in response to compressive stress. So, it is important to be aware of changing pattern of trabecular distribution due to different conditions.

Bone quality is so important for screw implantation and lower bone quality affects screw stability in a negative

manner.<sup>[27]</sup> For this reason, it is vital to evaluate the trabecular structure that has important effects on bone quality and strength. It is stated that the bone reorganizes its trabecular structure as a response to increasing force load in the affected region.<sup>[28]</sup> Accordingly, a carpal bone with an inner position, attached structures (muscles, ligaments, etc.), and microarchitecture would respond to different physiological and pathological conditions in a special manner. So, each bone should be evaluated by considering its position relative to other bones. For instance Mc Lean et al.<sup>[29]</sup> observed 2 types of distinct joints between triquetrum and hamate which were named as TqH-1 and TqH-2 respectively depending on articular surfaces of triquetrum and hamate. In another study, it was revealed that depending on the joint surfaces of triquetrum and hamate, a rotational motion occurs instead of helicoidal movement that refers to a saddle joint.<sup>[30]</sup> So in addition to anatomical properties, functional properties should be considered for any medical intervention on carpal bones. In addition to relative positions of the carpal bones, the intrinsic structural dynamics of individual bones should also be evaluated for a proper localization of screws. For instance, in a study documenting the differences of bone volume-surface and trabecular properties between different quadrants of scaphoid bone, no differences in terms of bone quality and density between these 4 quadrants was noted.<sup>[31]</sup> The vascular supply of the carpal bones is another factor affecting the healing process. Hamate is noted to have two regions of vascular entry and without intraosseous anastomoses. This type of vascular supply pattern puts hamate in a low risk group for developing avascular necrosis.<sup>[32]</sup> Another factor that might have a role in healing process could be the bone age. The analysis of images obtained by CT of the carpal bones is a valid method in the evaluation of bone maturity in children. Choi et al.<sup>[33]</sup> stated that capitohamate (CH) planimetry could be a reliable method for determining bone age. Determining the normal anatomy of the carpal bones will also help to determine the most appropriate parameters in the clinic for treating wrist pathologies.<sup>[33-35]</sup>

Our aim in this study was to define the trabecular structure of hamate, which is one of the parameters affecting the bone strength. Trabecular number, thickness, separation, structure-model index, and degree of anisotropy can be regarded among other factors. Examining only the dry bones and inability to identify the age and genders of the samples are two big limitations of our study. Therefore, we suggest carrying out new studies comparing dry bones with cadaveric specimens and trabecular structure changes in different pathological conditions together with the vasculature of hamate.

## Conclusion

It is obvious that hamate bone has sufficient strength for screw implantation in terms of trabecular thickness and number, but weaker in terms of trabecular separation when compared with other carpal bones. Hamate has the greatest trabecular thickness among the other carpal bones, while it is ranked as the second in terms of trabecular number. In terms of trabecular separation, the carpal bones can be ordered as the scaphoid, lunate, hamate, and trapezium in decreasing order of bone strength.

## Conflict of Interest

The authors declare no conflict of interest.

## Author Contributions

HO: protocol/project development, data collection, data analysis, manuscript writing/editing; HHC: supervision; MO: data collection, data analysis; FG: data collection, data analysis.

## Ethics Approval

The study was approved by Ethical Committee of Hacettepe University (No: GO 18/131-12) and performed in accordance with the Helsinki declaration of principles.

## Funding

The authors declare no financial support.

## References

- Ross CA. Wrist and hand. In: Standring S, editor. *Gray's anatomy: the anatomical basis of clinical practice*. 41st ed. Edinburgh (Scotland): Elsevier Churchill Livingstone; 2016. p. 869.
- Walsh JJ 4th, Bishop AT. Diagnosis and management of hamate hook fractures. *Hand Clin* 2000;16:397-403.
- Foucher G, Schuind F, Merle M, Brunelli F. Fractures of the hook of the hamate. *J Hand Surg Br* 1985;10:205-10.
- Boussein ML, Boyd SK, Christiansen BA, Guldberg RE, Jepsen KJ, Müller R. Guidelines for assessment of bone microstructure in rodents using micro-computed tomography. *J Bone Miner Res* 2010; 25:1468-86.
- De Schrijver F, De Smet L. Fracture of the hook of the hamate, often misdiagnosed as "wrist sprain". *J Emerg Med* 2001;20:47-51.
- Evans MW. Hamate hook fracture in a 17-year-old golfer: importance of matching symptoms to clinical evidence. *J Manipulative Physiol Ther* 2004;27:516-8.
- Cano Gala C, Pescador Hernández D, Rendón Díaz DA, López Olmedo J, Blanco Blanco J. Fracture of the body of hamate associated with a fracture of the base of fourth metacarpal: A case report and review of literature of the last 20 years. *Int J Surg Case Rep* 2013;4: 442-5.
- How Kit N, Malherbe M, Hulet C. Hamate hook stress fracture in a professional bowler: case report of an unusual causal sport. *Hand Surg Rehabil* 2017;36:62-5.
- Van Demark RE, Parke WW. Avascular necrosis of the hamate: a case report with reference to the hamate blood supply. *J Hand Surg Am* 1992;17:1086-90.
- De Smet L. Avascular necrosis of multiple carpal bones. A case report. *Chir Main* 1999;18:202-4.
- Peters SJ, Verstappen C, Degreef I, Smet LD. Avascular necrosis of the hamate: three cases and review of the literature. *J Wrist Surg* 2014;3:269-74.
- van Dijk M, Winters HA, Wuisman PI. Recurrent osteoblastoma of the hamate bone. A two-stage reconstruction with a free vascularized iliac crest flap. *J Hand Surg Br* 1999;24:501-5.
- Gdoura F, Trigui M, Ellouze Z, Hamed YB, Ayadi K, Keskes H. Hamatum osteoblastoma. *Orthop Traumatol Surg Res* 2010;96: 712-6.
- Ayan I, Serinsöz E. Osteoblastoma in the os hamatum: a rare case report. [Article in Turkish] *Eklemler Hastalıkları Cerrahisi* 2014;25:56-9.
- Koti M, Honakeri SP, Thomas A. A multilobed osteochondroma of the hamate: case report. *J Hand Surg Am* 2009;34:1515-7.
- Cha SM, Shin HD, Kim DY. A solitary unilobed osteochondroma of the hamate: a case report. *J Pediatr Orthop B* 2017;26:274-6.
- Santoshi JA, Pallapati SC, Thomas BP. Haematogenous pseudomonas osteomyelitis of the hamate--treatment by radical debridement and bone grafting. *J Plast Reconstr Aesthet Surg* 2010;63:189-90.
- Geneci F, Denk CC, Uzuner MB, Ocak M, Doğan İ, Sayacı EY, Gürses İA, Çay N, Baykal D, Çelik HH, Cömert A. Morphometric evaluation of coccyx with microcomputed tomography (micro CT) and computed tomography (CT) technology. *Journal of Innovative Approaches in Medicine* 2022;3:1-19.
- Jemt T, Lekholm U. Oral implant treatment in posterior partially edentulous jaws: a 5-year follow-up report. *Int J Oral Maxillofac Implants* 1993;8:635-40.
- Drago CJ. Rates of osseointegration of dental implants with regard to anatomical location. *J Prosthodont* 1992;1:29-31.
- Puleo DA, Nanci A. Understanding and controlling the bone-implant interface. *Biomaterials* 1999;20:2311-21.
- Lee JH, Kim HJ, Yun JH. Three-dimensional microstructure of human alveolar trabecular bone: a micro-computed tomography study. *J Periodontal Implant Sci* 2017;47:20-9.
- Wurnig MC, Calcagni M, Kenkel D, Vich M, Weiger M, Andreisek G, Wehrli FW, Boss A. Characterization of trabecular bone density with ultra-short echo-time MRI at 1.5, 3.0 and 7.0 T - comparison with micro-computed tomography. *NMR Biomed* 2014;27:1159-66.
- Han KJ, Kim JY, Chung NS, Lee HR, Lee YS. Trabecular microstructure of the human lunate in Kienbock's disease. *J Hand Surg Eur Vol* 2012;37:336-41.
- Nufer P, Goldhahn J, Kohler T, Kuhn V, Müller R, Herren DB. Microstructural adaptation in trapezium bone due to subluxation of the thumb. *J Orthop Res* 2008;26:208-16.
- Qu G, von Schroeder HP. Trabecular microstructure at the human scaphoid nonunion. *J Hand Surg Am* 2008;33:650-5.
- Alonso-Vázquez A, Lauge-Pedersen H, Lidgren L, Taylor M. The effect of bone quality on the stability of ankle arthrodesis. A finite element study. *Foot Ankle Int* 2004;25:840-50.
- Wolff J. *Das Gesetz der Transformation der Knochen*. Berlin: Hirschwald; 1892. p. 281.
- McLean J, Bain G, Eames M, Fogg Q, Pourgiez N. An anatomic study of the triquetrum-hamate joint. *J Hand Surg Am* 2006;31: 601-7.

30. Moritomo H, Goto A, Sato Y, Sugamoto K, Murase T, Yoshikawa H. The triquetrum-hamate joint: an anatomic and in vivo three-dimensional kinematic study. *J Hand Surg Am* 2003;28:797–805.
31. Huntington LS, Mandaleson A, Hik F, Ek ETH, Ackland DC, Tham SKY. Measurement of scaphoid bone microarchitecture: a computed tomography imaging study and implications for screw placement. *J Hand Surg Am* 2020;45:1185.e1-1185.e8.
32. Panagis JS, Gelberman RH, Taleisnik J, Baumgaertner M. The arterial anatomy of the human carpus. Part II: the intraosseous vascularity. *J Hand Surg Am* 1983;8:375–82.
33. Choi A, Kim YC, Min SJ, Khil EK. A simple method for bone age assessment: the capitohamate planimetry. *European Radiol* 2018;28:2299–307.
34. Canovas F, Roussanne Y, Captier G, Bonnel F. Study of carpal bone morphology and position in three dimensions by image analysis from computed tomography scans of the wrist. *Surg Radiol Anat* 2004;26:186–90.
35. Canovas F, Banegas F, Cyteval C, Jaeger M, DiMéglio A, Bonnel F, Sultan C. Carpal bone maturation assessment by image analysis from computed tomography scans. *Horm Res* 2000;54:6–13.

**ORCID ID:**

H. Ocak 0000-0002-0288-4167;  
H. H. Çelik 0000-0002-7909-7604;  
M. Ocak 0000-0001-6832-6208;  
F. Geneci 0000-0002-5039-4664



**Correspondence to:** Hakan Ocak, PhD

Department of Anatomy, Faculty of Medicine,  
Ağrı İbrahim Çeçen University, Ağrı, Türkiye  
Phone: +90 553 608 89 13  
e-mail: hocak@agri.edu.tr

*Conflict of interest statement:* No conflicts declared.

This is an open access article distributed under the terms of the Creative Commons Attribution-NonCommercial-NoDerivs 4.0 Unported (CC BY-NC-ND4.0) Licence (<http://creativecommons.org/licenses/by-nc-nd/4.0/>) which permits unrestricted noncommercial use, distribution, and reproduction in any medium, provided the original work is properly cited. *How to cite this article:* Ocak H, Çelik HH, Ocak M, Geneci F. Evaluation of trabecular structure of hamate using micro-computed tomography. *Anatomy* 2022;16(2):62–68.

# Morphometric relationship of nasolacrimal duct with maxillary sinus and nasal septum

Aycan Canlı<sup>1</sup> , Alper Vatanserver<sup>2</sup> , Emrah Akay<sup>3</sup> 

<sup>1</sup>Department of Anatomy, Faculty of Medicine, Balıkesir University, Balıkesir, Türkiye

<sup>2</sup>Department of Anatomy, Faculty of Medicine, Bursa Uludağ University, Bursa, Türkiye

<sup>3</sup>Department of Radiology, Faculty of Medicine, Balıkesir University, Balıkesir, Türkiye

## Abstract

**Objectives:** The aim of this study was to evaluate the morphometric properties of the bony part of the nasolacrimal duct and its relationship with nasal septum and maxillary sinus.

**Methods:** High resolution three-dimensional paranasal sinus computed tomography images of 115 individuals (39 women, 76 men) with a mean age of 39.08 years (min: 20, max: 79) were evaluated retrospectively. Individuals with any pathology, trauma or history of surgery were excluded from the study. Volume of bony nasolacrimal duct and maxillary sinus was calculated with free licensed Osirix Lite software. Nasal septum was evaluated according to MLADINA classification.

**Results:** Volume of maxillary sinus was higher in men while volume of bony nasolacrimal duct had no significant differences between genders. There was significant correlation between maxillary sinus volume and anteroposterior cranial distance, however volume of bony nasolacrimal duct had no significant correlation with anteroposterior cranial distance. Relation between volume of maxillary sinus and bony nasolacrimal duct was significant. The nasal septum deviation had no effect on volume of maxillary sinus and bony nasolacrimal duct.

**Conclusion:** A detailed knowledge on morphometric relationship of nasolacrimal duct with maxillary sinus and nasal septum is important for physicians during sinus surgeries and treatment of nasolacrimal duct obstructions. We suggest that there is a significant correlation between volume of maxillary sinus and bony nasolacrimal duct. This information may be useful for explaining one of the etiological factors of acquired nasolacrimal duct obstruction.

**Keywords:** computed tomography; maxillary sinus; nasal septum; nasolacrimal duct; radiological anatomy

Anatomy 2022;16(2):69–75 ©2022 Turkish Society of Anatomy and Clinical Anatomy (TSACA)

## Introduction

Nasolacrimal duct (NLD) is located in maxilla and anterior to the maxillary sinus. The NLD is a bony canal containing a mucous membrane. This mucous membrane continues proximally and forms the lacrimal sac.<sup>[1]</sup> The NLD begins to form with the thickening of the ectoderm in the groove between the maxillary and nasal ridges at about the 5th week of pregnancy and this process is completed at birth.<sup>[2]</sup> The mucous membrane then extends from lacrimal sac and opens into inferior nasal meatus within the bony NLD. The most common pathology of lacrimal system is obstruction of the NLD. The obstruction can be congenital or acquired. Acquired NLD obstruction is classified as primary or secondary. Although primary acquired NLD obstruction could be caused by various reasons, it was reported that volume of

the NLD may be one of the important factors.<sup>[3,4]</sup> Moreover, NLD obstruction could be listed as an important reason of epiphora.<sup>[5]</sup> Treatment protocols must be selected according to the shape and trajectory of NLD. However, surgeons should be aware about anatomical differences among various population to achieve successful results of surgeries. Therefore, comparisons of NLD volume between different populations were reported in previous studies.<sup>[4,6–9]</sup>

Maxillary sinus, the largest paranasal sinus, is located in body of the maxilla.<sup>[1]</sup> This sinus begins to form at the 17th gestational week and is visible at birth. However, its development continues after birth until 18–20 ages.<sup>[10]</sup> It has different variations which can be related with sinonasal pathologies.<sup>[11]</sup> Furthermore, nasal septum deviation could decrease ventilation and development of

maxillary sinus.<sup>[12]</sup> It was demonstrated that an excessive nasal septum deviation could block the osteomeatal complex and effect development of the maxillary sinus.<sup>[13]</sup> Additionally, a recent study demonstrated that nasal septum deviation could increase the risk of development maxillary sinusitis.<sup>[14]</sup> A previous study evaluated effects of craniometric features on NLD morphometry in healthy participants.<sup>[15]</sup> An another clinical study compared the NLD's morphometric properties between healthy and primary acquired NLD obstruction patients.<sup>[16]</sup> On the other hand, since the inferior wall of maxillary sinus is formed by a thin cortical bone layer, it is in close relation with the roots of maxillary molar teeth. Tooth extraction or missing teeth may change the volume of maxillary sinus by time.<sup>[17,18]</sup>

The clinical studies were mostly focused on mucous canal pathologies of the NLD, however, we hypothesize that the morphometric properties of bony part of the NLD may also effect on the pathological conditions. Therefore, the aim of this study was to evaluate morphometric properties of the bony NLD and duct and its relationship with nasal septum and maxillary sinus using three-dimensional paranasal sinus computed tomography.

## Materials and Methods

Computed tomography (CT) images of paranasal sinuses belonging to 244 patients were analyzed. Patients with neoplasia, infection, trauma or previous paranasal surgery were excluded. Accordingly, paranasal CT images of 115 healthy individuals (39 women; 76 men) were included to the study. The mean age of women was  $40.08 \pm 15.27$  (range: 20–76) years, while of men was  $38.58 \pm 13.57$  (range: 20–79) years. CT image series were reconstructed three-dimensionally using free licensed Osirix-Lite software.

Three-dimensional paranasal sinus CTs were performed with a 64 slice detector CT scanner (Toshiba Aquillon 64, Otawara, Japan). The collimation had a slice thickness of 1 mm, 0.8 mm spacing and a pitch of 1.0, 120 kV (peak) and 150 effective mA s. All participants' CT image series were obtained from the picture archiving and communication system (PACS) of the Balikesir University Hospital. All measurement were completed by a 15-year experienced radiologist and a 10-year experienced anatomist using Osirix-Lite software (Pixmeo, SARL, Switzerland).

All CT procedures were completed while the participants were in supine position. To standardize measurements, hard palate was arranged parallel to transverse section and all parameters were measured according to this position. The anteroposterior cranial distance was mea-

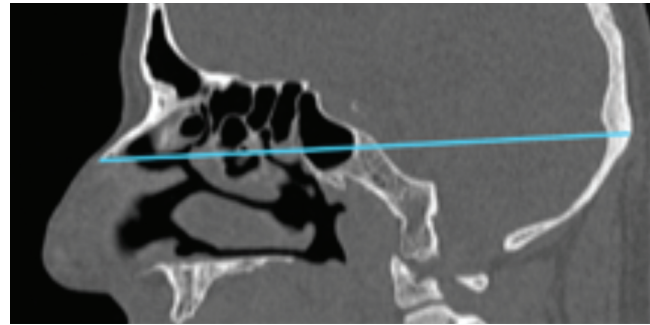


**Figure 1.** Anteroposterior cranial distance from tip of the nasal bone to the externa occipital protuberance.

red from the tip of nasal bone to the external occipital protuberance in sagittal sections (**Figure 1**). For calculating maxillary sinus volume, a region of interest (ROI) was created by drawing borders of the maxillary sinus using pencil function of Osirix-Lite software in axial sections. Then, the volume of selected ROI was calculated (**Figure 2**). This process was repeated separately for right and left sides. The same volume calculation protocol was used for calculating NLD volume bilaterally (**Figure 3**). The deviation in the nasal septum was classified according to MLADINA classification system in coronal sections.<sup>[19]</sup> (**Figure 4**) Additionally, the maxillary dental status of participants were grouped as; complete and missing. Then

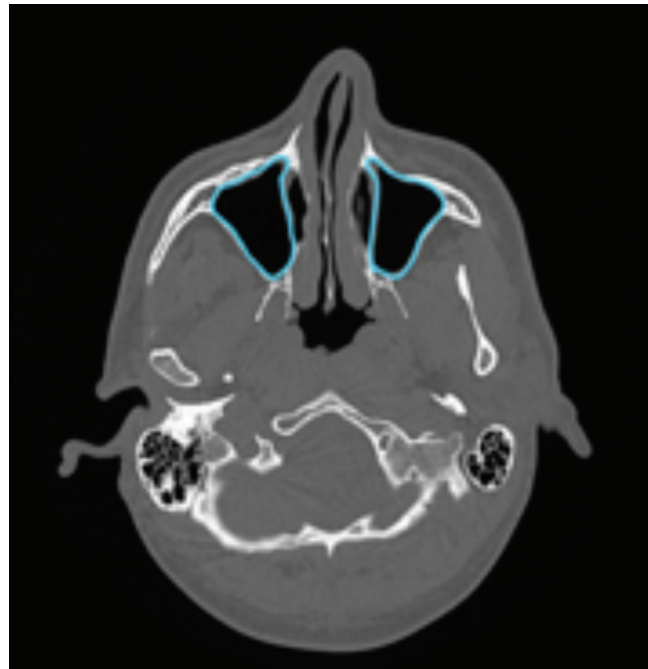


**Figure 2.** Selecting region of interest (ROI) for calculating maxillary sinus volume.

the volume of maxillary sinus between two groups were compared.

Statistical analysis was performed with SPSS (Version 26, Armonk, NY, USA) with 95% confidence interval. All variables were investigated using histograms and probability plots. Kolmogorov-Smirnov and Shapiro-Wilk test was used to define whether the variables distributed normally or not. The student's t-test was used for normally distributed variables, and Mann-Whitney U test was used for non-normally distributed variables for comparison between genders. Pearson or Spearman's rho correlation analyses were performed according to suitability of values' distributions. Paired sample t-test or Wilcoxon test were used for comparing right and left sides. One-way ANOVA or Kruskal-Wallis tests were used for comparing variables between the groups with nasal septum deviation.

## Results

The results of the measurements were summarized in **Table 1**.

The maxillary sinus volume had a wide range between  $6.84 \text{ cm}^3$  and  $35.85 \text{ cm}^3$ . The mean volume of maxillary sinus was  $16.41 \pm 4.53$  (range:  $6.84\text{--}24.15$ )  $\text{cm}^3$  in women, while it was  $20.85 \pm 5.97$  (range:  $10.02\text{--}35.85$ )  $\text{cm}^3$  in men on the right side. The mean volume of the sinus was  $15.98 \pm 4.37$  (range:  $7.64\text{--}22.99$ )  $\text{cm}^3$  in women, while it was  $20.35 \pm 5.91$  (range:  $8.85\text{--}34.75$ )  $\text{cm}^3$  in men on the left side.

The NLD volume was  $0.23 \pm 0.07$  (range:  $0.1\text{--}0.49$ )  $\text{cm}^3$  in women, while it was  $0.25 \pm 0.08$  (range:  $0.11\text{--}0.5$ )  $\text{cm}^3$  in

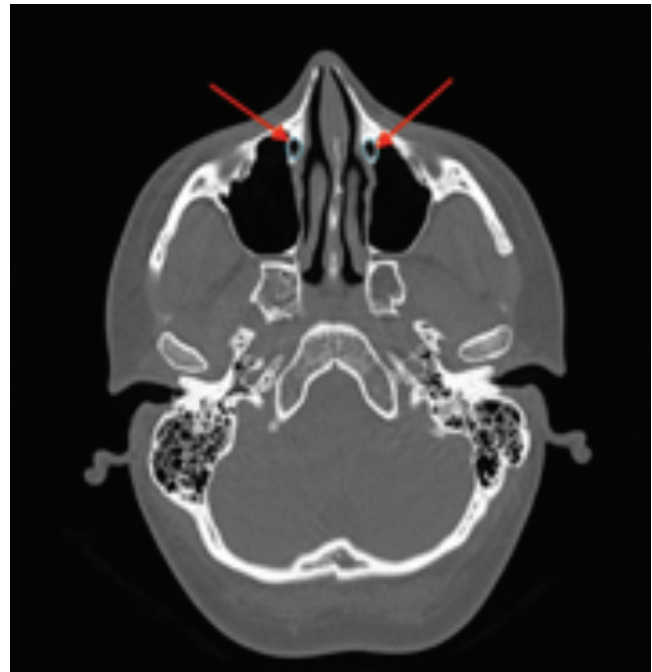


**Figure 3.** Selecting region of interest (ROI) for calculating the volume of nasolacrimal duct (arrows).

men on the right side. It was  $0.23 \pm 0.09$   $\text{cm}^3$  (range:  $0.11\text{--}0.5$ ) in women, while it was  $0.24 \pm 0.08$  (range:  $0.12\text{--}0.53$ )  $\text{cm}^3$  in men on the left side.

After evaluating nasal septum classification according to MLADINA classification,<sup>[19]</sup> our results demonstrated that 12 of the participants (10.4%) had no septal devia-



**Figure 4.** MLADINA classification<sup>[19]</sup> of nasal septum deviation in coronal section.

**Table 1**  
Summary of the results.

	Gender	n	Mean±SD	Min.	Max.
Anteroposterior cranial distance (cm)	Women	39	17.50±0.66	16.43	19.15
	Men	76	18.45±0.67	16.88	19.90
Volume of right maxillary sinus (cm <sup>3</sup> )	Women	39	16.41±4.53	6.84	24.15
	Men	76	20.85±5.97	10.02	35.85
Volume of left maxillary sinus (cm <sup>3</sup> )	Women	39	15.98±4.37	7.64	22.99
	Men	76	20.35±5.91	8.85	34.75
Volume of right NLD (cm <sup>3</sup> )	Women	39	0.23±0.07	0.10	0.49
	Men	76	0.25±0.08	0.11	0.50
Volume of left NLD (cm <sup>3</sup> )	Women	39	0.23±0.09	0.11	0.50
	Men	76	0.24±0.08	0.12	0.53

NLD: nasolacrimal duct.

tion. Type 1, type 2, type 3, type 4, type 5 and type 7 nasal septum deviations were seen in 9 (7.8%), 9 (7.8%), 34 (29.6%), 29 (25.2%), 17 (14.8%) and 5 (4.3%) of the participants, respectively. It was seen that none of participants had type 6 nasal septum deviation in our study.

After volume of right and left maxillary sinus evaluated within genders, it was seen that there was no significant differences between right and left maxillary sinus in women and men ( $p=0.149$  in women;  $p=0.117$  in men). Maxillary sinus was larger in men than women on right side ( $p<0.001$ ) and left side ( $p<0.001$ ). Maxillary sinus volume comparison between right and left sides without regarding gender, showed that right maxillary sinus was larger than left maxillary sinus ( $p<0.05$ ).

Correlation analyses between maxillary sinus volume and age showed no significant correlations between volume of maxillary sinus and age of participants on both sides (right side  $p=0.16$ ; left side  $p=0.8$ ).

The volume of right and left NLDs demonstrated no significant differences in women ( $p=0.399$ ) and in men ( $p=0.134$ ). Furthermore, volume of the NLD had no significant differences on both sides between genders (right side  $p=0.413$ ; left side  $p=0.485$ ). Besides that, NLD volume comparison between right and left sides without regarding gender, it was demonstrated that there was no significant difference between right and left sides ( $p=0.093$ ).

Correlation analyses between NLD volume and age of participants demonstrated no significant correlation on both side (right side  $p=0.368$ ; left side  $p=0.707$ ). Men had longer anteroposterior cranial distance than women ( $p<0.05$ ). However, maxillary sinus volume had no significant correlation with anteroposterior cranial diameter in women (right side  $p=0.171$ ; left side  $p=0.131$ ) and in men (right side  $p=0.229$ ; left side  $p=0.068$ ). Furthermore, cor-

relations between anteroposterior cranial distance and maxillary sinus volumes without regarding genders, it was seen that there were significant correlations on both sides (right side  $r=0.376$ ,  $p<0.001$ ; left side  $r=0.37$ ,  $p<0.001$ ).

The NLD volumes had no significant correlations with anteroposterior cranial distance on both sides in women (right side  $p=0.693$ ; left side  $p=0.561$ ) and men (right side  $p=0.153$ ; left side  $p=0.411$ ). Beside these, correlations between anteroposterior cranial distance and NLD volumes without regarding genders showed that there was no significant correlation on both sides (right side  $p=0.06$ ; left side  $p=0.1$ ).

The correlations between maxillary sinus and NLD volumes showed a significant correlation between maxillary sinus and NLD volumes in men on both sides (right side  $r=0.277$ ,  $p<0.05$ ; left side  $r=0.241$ ,  $p<0.05$ ). Evaluating correlations between maxillary sinus and NLD volumes without regarding genders demonstrated that there was a significant correlation between maxillary sinus and NLD volumes on the right side ( $r=0.244$ ,  $p<0.05$ ).

The relation nasal septum deviation groups with maxillary and NLD volumes demonstrated no significant difference between nasal septum classification group and maxillary sinus volume on both sides (right side  $p=0.591$ ; left side  $p=0.527$ ). Furthermore, there was no significant difference between nasal septum deviation group and NLD volume on both sides (right  $p=0.949$ ; left side  $p=0.694$ ). No significant difference was found between dental status of the participants and gender groups ( $p<0.05$ ).

## Discussion

The main purpose of this study was to evaluate the morphometric properties of the bony NLD, maxillary sinus

and their relations with nasal septum. We included participants older than 20 years in the current study since these structures complete development at about 18-19 years of age.<sup>[10]</sup> Additionally, we investigated effects of age and anteroposterior cranial distance on the anatomical characteristics of these structures.

Our results demonstrated that age had no effect on morphometric properties on the bony NLD and maxillary sinus. Furthermore, anteroposterior cranial distance had no significant effect on anatomy of bony NLD and maxillary sinus, as well. We expected some possible effects of nasal septum deviation on bony NLD and maxillary sinus morphometry, but our results demonstrated that it had no significant effect on the morphometry of these structures. We also questioned whether morphometric properties of maxillary sinus and bony NLD could affect each other. Our results showed a positive and statistically significant correlation between these structures in men.

With development of endoscopic surgical techniques, endoscopic resection is widely used for the treatment of sinonasal tumors. The NLD could be damaged or opened carefully during sinus surgeries.<sup>[20,21]</sup> Furthermore, treatment of congenital or acquired obstructions is commonly focused by physicians.<sup>[22-26]</sup> Recent morphometric studies mainly focused on patients who had any pathology in their lacrimal system.<sup>[27-31]</sup> A clinical study revealed that patients with primary acquired NLD obstruction had narrower duct than healthy participants, although there were no morphometric differences between obstructed side and non-obstructed side.<sup>[16]</sup> The structural characteristics of the lacrimal system were also examined in healthy participants or cadavers.<sup>[9,32-37]</sup> In a previous study on patients with or without osteomeatal complex variations demonstrated that the NLD volume was higher in presence of variations such as agger nasi, concha bullosa and pneumatized uncinate process.<sup>[38]</sup> This study suggested that not only pathologies, but also anatomical variations should be considered while planning surgeries. It was demonstrated that morphometric properties of proximal end of the NLD had significant positive correlation with anteroposterior distance of cranium.<sup>[15]</sup> This result indicated that types and morphometric properties of cranium could be the key factor for determining surgical techniques for treatment of NLD obstructions.

Pneumatization of maxillary sinus is depended on various factors such as tooth extraction. Pathological tooth loss may also effect maxillary sinus volume. Inferior wall of maxillary sinus may collapse into the alveolar spaces at region of missing teeth, therefore sinus volume increases.<sup>[39-41]</sup> However, our results did not demonstrate any significant effect of missing teeth on

the maxillary sinus volume. Nevertheless, our results may not indicate a precise result since we had limited data about dental status of participants.

There are anatomical studies that evaluated maxillary sinus morphometry in relation with the presence of nasal septum deviation.<sup>[42-45]</sup> Furthermore, other studies focused on relationship between nasal septum deviations and maxillary sinus pathologies.<sup>[13,14,46-48]</sup> However, effects of nasal septum deviation on NLD were investigated mainly on patients with NLD obstruction.<sup>[49-53]</sup> In our study, we examined the morphometric characteristic of NLD in relation with nasal septum deviation in participants who had no NLD obstruction, therefore, it may be useful for surgeons while deciding surgical technique for treatment of any pathology in NLD or maxillary sinus. Thus, the risk of unexpected iatrogenic injuries may be avoided and recovery period could be shorter.

Since this study was designed as a retrospective study, participants' body measurement data such as height, weight, body mass index could not be evaluated. Although we evaluated maxillary sinus volumes with dental status, our results may not demonstrate a precise result, since we did not have any data about for how long and why the participants lost their teeth.

## Conclusion

Our results demonstrated morphometric relations between maxillary sinus and NLD which may be important and helpful for physicians during an accurate diagnosis and planning surgical techniques. Comparing our results with clinical studies may contribute to selecting criteria for an ideal surgical technique. Thus, it may improve post-operative life quality of patients who would need surgery against paranasal sinuses and NLD, as well.

## Conflict of Interest

Authors have no conflict of interests to declare.

## Author Contributions

AC: protocol/project development, data collection, data analysis; AV: protocol/project development, data analysis, writing the manuscript; EA: data collection, data analysis.

## Ethics Approval

The study was approved by Ethical Board of Balikesir University (No: 2021/154).

## Funding

None.

## References

1. Standring S. Gray's anatomy: the anatomical basis of clinical practice. Forty-first ed. New York: Elsevier Limited; 2016. p. 1562.
2. Bewes T, Sacks R, Sacks PL, Chin D, Mrad N, Wilcsek G, Tumuluri K, Harvey R. Incidence of neoplasia in patients with unilateral epiphora. *J Laryngol Otol* 2015;129 Suppl 3:S53-7.
3. Ali MJ, Paulsen F. Etiopathogenesis of primary acquired nasolacrimal duct obstruction: what we know and what we need to know. *Ophthalmic Plast Reconstr Surg* 2019;35:426-33.
4. Fasina O, Ogbole GI. CT Assessment of the nasolacrimal canal in a black African population. *Ophthalmic Plast Reconstr Surg* 2013;29:231-3.
5. Avdagic E, Phelps PO. Nasolacrimal duct obstruction as an important cause of epiphora. *Dis Mon* 2020;66:101043.
6. Gore SK, Naveed H, Hamilton J, Rene C, Rose GE, Davagnanam I. Radiological comparison of the lacrimal sac fossa anatomy between black Africans and Caucasians. *Ophthalmic Plast Reconstr Surg* 2015;31:328-31.
7. Lin Z, Kamath N, Malik A. High-resolution computed tomography assessment of bony nasolacrimal parameters: variations due to age, sex, and facial features. *Orbit* 2021;40:364-9.
8. Yong AMY, Zhao DB, Siew SC, Goh PS, Liao JM, Amrith S. Assessment of bony nasolacrimal parameters among asians. *Ophthalmic Plast Reconstr Surg* 2014;30:322-7.
9. Lin Z, Kamath N, Malik A. Morphometric differences in normal bony nasolacrimal anatomy: comparison between four ethnic groups. *Surg Radiol Anat* 2021;43:179-85.
10. Lorkiewicz-Muszynska D, Kociemba W, Rewekant A, Sroka A, Jonczyk-Potoczna K, Patelska-Banaszewska M, Przystanska A. Development of the maxillary sinus from birth to age 18. Postnatal growth pattern. *Int J Pediatr Otorhinolaryngol* 2015;79:1393-400.
11. Ayyildiz H, Akgunlu F. Are maxillary sinus variations related to maxillary sinus diameters? *Oral Radiol* 2023;39:425-36.
12. Zhu JH, Lim KM, Thong KTM, Wang DY, Lee HP. Assessment of airflow ventilation in human nasal cavity and maxillary sinus before and after targeted sinonasal surgery: a numerical case study. *Resp Physiol Neurobiol* 2014;194:29-36.
13. Jadia S, Qureshi S, Agrawal S, Singh SG. Effect of deviated nasal septum on maxillary sinus volume and occurrence of sinusitis. *Indian J Otolaryngol Head Neck Surg* 2019;71:1871-5.
14. Karatas D, Koc A, Yuksel F, Dogan M, Bayram A, Cihan MC. The Effect of nasal septal deviation on frontal and maxillary sinus volumes and development of sinusitis. *J Craniofac Surg* 2015;26:1508-12.
15. Erçakmak Güneş B, Vatanserver A, Demiryürek D, Gümeler E. Morphometric evaluation of nasolacrimal duct. *Anatomy* 2021;15:64-8.
16. Bulbul E, Yazici A, Yanik B, Yazici H, Demirpolat G. Morphometric evaluation of bony nasolacrimal canal in a caucasian population with primary acquired nasolacrimal duct obstruction: a multidetector computed tomography study. *Korean J Radiol* 2016;17:271-6.
17. Belgin CA, Bayrak S, Atakan C. Determination of alveolar bone height according to the relationship between molar teeth and maxillary sinus. *Oral Maxillofac Surg* 2021;25:175-80.
18. Yamaguchi K, Munakata M, Kataoka Y, Uesugi T, Shimoo Y. Effects of missing teeth and nasal septal deviation on maxillary sinus volume: a pilot study. *Int J Implant Dent* 2022;8:19.
19. Mladina R, Skitarelic N, Poje G, Subaric M. Clinical implications of nasal septal deformities. *Balkan Med J* 2015;32:137-46.
20. Rotsides JM, Franco A, Albader A, Casiano RR, Lieberman SM. Nasolacrimal duct management during endoscopic sinus and skull base surgery. *Ann Otol Rhinol Laryngol* 2019;128:932-7.
21. Sadeghi N, Joshi A. Management of the nasolacrimal system during transnasal endoscopic medial maxillectomy. *Am J Rhinol Allergy* 2012;26:e85-8.
22. Avram E. Insights in the treatment of congenital nasolacrimal duct obstruction. *Rom J Ophthalmol* 2017;61:101-6.
23. Eustis HS, Nguyen AH. The treatment of congenital nasolacrimal duct obstruction in children: a retrospective review. *J Pediatr Ophthalmol Strabismus* 2018;55:65-7.
24. Gazit I, Pras E, Or L, Hartstein ME. Balloon catheter dilation as the primary treatment of congenital nasolacrimal duct obstruction. *Eur J Ophthalmol* 2021;31:334-9.
25. Petris C, Liu D. Probing for congenital nasolacrimal duct obstruction. *Cochrane Database Syst Rev* 2017;7:CD011109.
26. Keilani C, Keller P, Piaton JM. Incision of Hasner's valve under endoscopic intranasal surgery for the treatment of nasolacrimal duct obstruction in children. *J Laryngol Otol* 2020;134:56-62.
27. Alakus MF, Dag U, Balsak S, Erdem S, Oncul H, Akgol S, Diri H. Is there an association between congenital nasolacrimal duct obstruction and cesarean delivery? *Eur J Ophthalmol* 2020;30:1228-31.
28. Arnold RW, Olitsky SE, Suh DW, Wasserman BN. Management of congenital nasolacrimal duct obstruction with anatomic anomalies. *J Pediatr Ophthalmol Strabismus* 2017;54:6-9.
29. Lee S, Lee UY, Yang SW, Lee WJ, Kim DH, Youn KH, Kim YS. 3D morphological classification of the nasolacrimal duct: anatomical study for planning treatment of tear drainage obstruction. *Clin Anat* 2021;34:624-33.
30. Vatanserver M, Argin MA, Gorur K. Effect of facial parameters in primary acquired nasolacrimal duct obstruction. *J Craniofac Surg* 2017;28:e752-6.
31. Zhang C, Wu Q, Cui Y, Yu G. Anatomy of nasolacrimal canal in congenital nasolacrimal duct obstruction - 18 cases retrospective study. *Acta Ophthalmol* 2015;93:e404-5.
32. Groell R, Schaffler GJ, Uggowitz M, Szolar DH, Muellner K. CT-anatomy of the nasolacrimal sac and duct. *Surg Radiol Anat* 1997;19:189-91.
33. Kim YH, Park MG, Kim GC, Park BS, Kwak HH. Topography of the nasolacrimal duct on the lateral nasal wall in Koreans. *Surg Radiol Anat* 2012;34:249-55.
34. Takahashi Y, Kakizaki H, Nakano T. Bony nasolacrimal duct entrance diameter: gender difference in cadaveric study. *Ophthalm Plast Reconstr* 2011;27:204-5.
35. Tatlisumak E, Aslan A, Comert A, Ozlugedik S, Acar HI, Tekdemir I. Surgical anatomy of the nasolacrimal duct on the lateral nasal wall as revealed by serial dissections. *Anat Sci Int* 2010;85:8-12.
36. Valencia MRP, Takahashi Y, Naito M, Nakano T, Ikeda H, Kakizaki H. Lacrimal drainage anatomy in the Japanese population. *Ann Anat* 2019;223:90-9.
37. Wang XD, Chen XJ, Zheng M, Liu CY, Wang CS, Zhang L. The relationships between the nasolacrimal duct and the anterior wall of the maxillary sinus. *Laryngoscope* 2019;129:1030-4.
38. Khojastepour L, Dokohaki S, Paknahad M. Are of osteomeatal complex variations related to nasolacrimal canal morphometry. *Iran J Otorhinolaryngol* 2022;34:17-26.
39. Esposito M, Grusovin MG, Rees J, Karasoulos D, Felice P, Alissa R, Worthington HV, Coulthard P. Interventions for replacing missing teeth: augmentation procedures of the maxillary sinus. *Cochrane Database Syst Rev* 2010;17:CD008397.

40. Lim HC, Kim S, Kim DH, Herr Y, Chung JH, Shin SI. Factors affecting maxillary sinus pneumatization following posterior maxillary tooth extraction. *J Periodontal Implant Sci* 2021;51:285–95.
41. Oz AZ, Oz AA, El H, Palomo JM. Maxillary sinus volume in patients with impacted canines. *Angle Orthod* 2017;87:25–32.
42. Al-Rawi NH, Uthman AT, Abdulhameed E, Al Nuaimi AS, Seraj Z. Concha bullosa, nasal septal deviation, and their impacts on maxillary sinus volume among Emirati people: a cone-beam computed tomography study. *Imaging Sci Dent* 2019;49:45–51.
43. Asantogrol F, Cosgunarslan A. The effect of anatomical variations of the sinonasal region on maxillary sinus volume and dimensions: a three-dimensional study. *Braz J Otorhinolaryngol* 2022;88Suppl1: S118–27.
44. Atsal G, Demir E, Yildirim O, Edizer DT, Olgun L. The relationship between degree of nasal septum deviation with sinonasal structures and variations. *J Craniofac Surg* 2022;33:e447–9.
45. Orhan I, Ormeci T, Aydin S, Altin G, Urger E, Soyulu E, Yilmaz F. Morphometric analysis of the maxillary sinus in patients with nasal septum deviation. *Eur Arch Otorhinolaryngol* 2014;271:727–32.
46. Arslan IB, Uluyol S, Demirhan E, Kozcu SH, Pekcevik Y, Cukurova I. Paranasal sinus anatomic variations accompanying maxillary sinus retention cysts: a radiological analysis. *Turk Arch Otorhinol* 2017; 55:162–5.
47. Aydin S, Taskin U, Orhan I, Altas B, Oktay MF, Toksoz M, Albayrak R. The analysis of the maxillary sinus volumes and the nasal septal deviation in patients with antrochoanal polyps. *Eur Arch Otorhinolaryngol*. 2015;272:3347–52.
48. Kalabalik F, Ertaş ET. Investigation of maxillary sinus volume relationships with nasal septal deviation, concha bullosa, and impacted or missing teeth using cone-beam computed tomography. *Oral Radiol* 2019;35:287–95.
49. Dikici O, Ulutaş HG. Relationship between primary acquired nasolacrimal duct obstruction, paranasal abnormalities and nasal septal deviation. *J Craniofac Surg* 2020;31:782–6.
50. Lee JS, Lee H, Kim JW, Chang M, Park M, Baek S. Association of facial asymmetry and nasal septal deviation in acquired nasolacrimal duct obstruction in East Asians. *J Craniofac Surg* 2013;24:1544–8.
51. Samarei R, Samarei V, Aidenloo NS, Fateh N. Sinonasal anatomical variations and primary acquired nasolacrimal duct obstruction: a single centre, case-control investigation. *Eurasian J Med* 2020;52:21–4.
52. Singh S, Alam MS, Ali MJ, Naik MN. Endoscopic intranasal findings in unilateral primary acquired nasolacrimal duct obstruction. *Saudi J Ophthalmol* 2017;31:128–30.
53. Taban M, Jarullazada I, Mancini R, Hwang C, Goldberg RA. Facial asymmetry and nasal septal deviation in acquired nasolacrimal duct obstruction. *Orbit* 2011;30:226–9.

**ORCID ID:**

A. Canlı 0000-0003-4497-5427;  
 A. Vatansever 0000-0002-3632-1020;  
 E. Akay 0000-0002-8586-3571

**Correspondence to:** Alper Vatansever, PhD

Department of Anatomy, Faculty of Medicine,  
 Bursa Uludağ University, Bursa, Türkiye  
 Phone: +90 538 368 13 12  
 e-mail: avatansever@uludag.edu.tr

*Conflict of interest statement:* No conflicts declared.

This is an open access article distributed under the terms of the Creative Commons Attribution-NonCommercial-NoDerivs 4.0 Unported (CC BY-NC-ND4.0) Licence (<http://creativecommons.org/licenses/by-nc-nd/4.0/>) which permits unrestricted noncommercial use, distribution, and reproduction in any medium, provided the original work is properly cited. *How to cite this article:* Canlı A, Vatansever A, Akay E. Morphometric relationship of nasolacrimal duct with maxillary sinus and nasal septum. *Anatomy* 2022;16(2):69–75.

# Total anomalous pulmonary venous connection: preoperative anatomy, physiology, preoperative evaluation, surgical considerations and single centre clinical experiences

Başak Soran Türkcan , Mustafa Yılmaz , Atakan Atalay 

Department of Pediatric Cardiovascular Surgery, Ankara Bilkent City Hospital, Ankara, Türkiye

## Abstract

**Objectives:** The aim of the present study was to document the anatomical subtypes of total anomalous pulmonary venous connection (TAPVC) since it is critical in the surgical and medical management of this cardiac anomaly.

**Methods:** This retrospective study was conducted at a paediatric heart centre between February 2019 and December 2021. The study included 27 patients who underwent intracardiac repair of total anomalous pulmonary venous connection.

**Results:** The mean age of the patients were found  $159.37 \pm 411.29$  (range: 7.00–2160) days, the mean weight of patients were  $4756.67 \pm 2988.78$  grams. Mean oxygen saturation at the arrival of the hospital was  $84.89 \pm 7.98$  (range: 60–96) %. Mortality was seen in 7 (25.9%) patients. 2 of 7 patients (28.6%) had supracardiac type, 2 of 7 patients had (28.6%) cardiac type, 2 of 7 (28.6%) patients had infracardiac type and 1 of 7 patients (14.3%) had mixt type anomaly. Only 3 (11.1%) patients needed ECMO. One of these 3 patients (33.3%) had supracardiac type, and the remaining 2 of 3 patients (66.7%) had infracardiac type anomaly.

**Conclusion:** Total anomalous pulmonary venous connection is a rare cardiac anomaly seen in 7/100,000 live births. It constitutes approximately 1% of all congenital heart diseases. It can be found as an isolated cardiac defect or accompany other diseases; usually accompanying cardiac lesions are associated with the severity of the disease and poor prognosis. Understanding the anatomical subtypes of TAPVC is critical in the surgical and medical management of this disease.

**Keywords:** cardiac anomaly; pulmonary venous hypertension; total anomalous pulmonary venous connection

Anatomy 2022;16(2):76–80 ©2022 Turkish Society of Anatomy and Clinical Anatomy (TSACA)

## Introduction

Total anomalous pulmonary venous connection (TAPVC) is a spectrum of cardiac anomalies that occurs when all of the pulmonary veins drain to a structure other than the left atrium.<sup>[1]</sup> The pulmonary veins return either to one of the systemic veins such as the brachiocephalic vein, ductus venosus, hepatic vein, the coronary sinus, or directly to the right atrium. In this pathology, there is a complete mixture of pulmonary and systemic venous return in the right atrium and an obligate right to left atrial shunting to sustain life.<sup>[2]</sup> There are multiple anatomical subtypes, and the presentation and outcomes are largely influenced by any point of obstruction to the pulmonary venous return to the heart. The aim of the

present study was to document the anatomical subtypes of this pathology since it is critical in the surgical and medical management of this disease.

## Materials and Methods

This retrospective study was conducted at a paediatric heart center, between February 2019 and December 2021. The study included twenty-seven patients who underwent intracardiac repair of total anomalous pulmonary venous connection.

Data including age, sex, type of TAPVC, surgical technique, preoperative right ventricle systolic pressure, oxygen saturation at the arrival of the hospital, duration of cardiopulmonary bypass (CPB) and cross-clamp (CC)

time, postoperative pulmonary artery pressure, duration of inotropic support, duration of ventilation, duration of stay in the intensive care unit (ICU), duration of stay in hospital as well as mortality rate, was all retrieved from the institutional databases and medical records of the patients.

Interquartile range (IQR) was used to express continuous data, whereas frequency and percentages were used to represent categorical variables. A p-value of less than 0.05 was considered statistically significant for all statistical analyses, which were carried out using the SPSS for Windows (Version 25.0, IBM Corp., Armonk, NY, USA).

## Results

The mean age (day) of the patients were found to be  $159.37 \pm 411.29$  (range: 7.00–2160) days, the mean weight (g) of patients was  $4756.67 \pm 2988.78$  g, the mean of CC time (minutes) was  $55.85 \pm 23.23$  (range: 32–173) and the CPB time (minutes) mean was  $96.74 \pm 37.12$  (range: 41–226) minutes.

Mean oxygen saturation (%) of the patients at the arrival of the hospital was  $84.89 \pm 7.98$  (range: 60–96). The mean preoperative right ventricular systolic pressure (RVSP), mechanical ventilation time and inotropic support time was  $63.59 \pm 27.37$  (range: 25–150),  $69.59 \pm 76.78$  (range: 12–360), and  $69.59 \pm 74.42$  (range: 12–360) minutes respectively.

Finally, the mean postoperative oxygen saturation (%) of the patients was  $93.07 \pm 0.08$  (range: 80–100), and the mean postoperative pulmonary artery pressure (PAB) was  $27.59 \pm 12.94$  (range: 17–85) mmHg.

Nine of the twenty-seven patients (33.3%) had supracardiac type, 11 of 27 patients (40.7%) had cardiac type, 6 of 27 patients (22.2%) had infracardiac type and 1 of 27 patients (3.7%) had mixed type anomaly.

Mortality was seen in seven patients (25.9%). Two of these patients (28.6%) had supracardiac type, 2 of 7 patients (28.6%) had cardiac type, 2 of 7 patients (28.6%) had infracardiac type and 1 of 7 patients (14.3%) had mixed type anomaly.

The distribution of the patients according to the number of inotropes that they received was as follows: seven patients (25.9%) received 2 types, 12 patients (44.4%) received 3 types, 8 patients (29.6%) received 4 types of inotropes.

Only three patients (11.1%) needed extracorporeal membrane oxygenator (ECMO). One of these 3 patients (33.3%) had supracardiac type, and the remaining two patients (66.7%) had infracardiac type anomaly.

## Discussion

TAPVC is a rare cardiac anomaly seen in 7/100,000 live births.<sup>[3]</sup> It constitutes approximately 1% of all congenital heart diseases.<sup>[4]</sup> It can be found as an isolated cardiac defect or accompany other diseases. Accompanying cardiac lesions (heterotaxy syndrome, atrial isomerism, anatomical lesions with single ventricular physiology, etc.) are associated with the severity of the disease and poor prognosis.<sup>[5]</sup> Most patients do not have a family history of congenital heart disease, but case reports showing that it is seen in siblings and first-degree relatives have been described in the literature. In the case series published by Lucas et al.,<sup>[6]</sup> TAPVC opening into the portal vein was found to be more common in men (3.6:1). There is no known environmental fetal factor for TAPVC.

The failure of all pulmonary veins to separate from the splanchnic venous system and the concomitant leftward placement of the atrial septum, are thought to be the primary defect in the formation of TAPVC. Unilateral formation of the defect throughout development results in partial pulmonary venous return anomaly, and its occurrence in later stages results in common pulmonary vein atresia, cor triatriatum or abnormal union of the common vein with the left atrium, resulting in congenital pulmonary vein stenosis and an abnormal number of pulmonary veins.<sup>[7–10]</sup>

TAPVC consists of four anatomical subtypes: supracardiac, cardiac, infracardiac and mixed type, where the supracardiac type accounts for approximately 45% of all cases. All pulmonary veins form a sac and this common sac drains through the vertical vein into the brachycephalic vein, superior vena cava or azygos vein. This vertical vein typically courses anterior to the left pulmonary artery and enters the systemic venous circulation.<sup>[2]</sup> Although supracardiac TAPVCs are nonobstructive, obstruction can occur at two main points. In 40% of supracardiac TAPVCs, the vertical vein passes between the left pulmonary artery and the left pulmonary bronchus, and creates a stenosis. The second possible site of obstruction occurs where the vertical vein opens directly into the superior vena cava (SVC) or azygos vein, and may cause obstruction at different levels. The innominate vein and SVC are enlarged due to increased blood flow.<sup>[1,2]</sup> In our study 33.3% of the patients had supracardiac type anomaly.

Infracardiac TAPVC accounts for 25% of all cases and is the most common type of obstruction. After the pulmonary veins open into the common venous sac, they open into the ductus venosus, hepatic artery, inferior vena cava or portal vein at a level below the diaphragm via the vertical vein. Since the ductus venosus begins to regress

with birth, it causes obstruction that develops over time. In cases without stenosis, pulmonary venous return comes to the right side of the heart via the inferior vena cava (IVC) and passes through the patent foramen ovale (PFO) to reach the left side of the heart.<sup>[2]</sup> In our study, 22.2% of the patients had an infracardiac type anomaly.

Cardiac TAPVC occurs in approximately 20% of all cases. The common venous sac opens into the right atrium via the coronary sinus, which is dilated. In some cases, it can open directly into the right atrium. These cases are usually associated with heterotaxy syndrome and complex cardiac malformations. Oxygenated blood enters the left atrium via the PFO and this type of TAPVC is the least obstructed type. In our study, 40.7% of the patients had cardiac type anomaly.

The mixed type TAPVC is the rarest type of TAPVC, occurring in approximately 5% of patients. Such patients present in a severe and often severe form. Accurate preoperative diagnosis and clear anatomical definition are critical in planning the surgical strategy in these patients. The confusion in the diagnosis is usually due to the wide anatomical variations in mixed type TAPVC.<sup>[11]</sup> In our study 3.7% of the patients had mixed type anomaly.

At least fifteen different anatomical variations have been described. The most common form is the type in which the left upper lobe lung drains into the left vertical vein and all the remaining venous drainage of the lung into the coronary sinus. In the other most common form, the entire right lung drains into the coronary sinus, while the left lung drains into the vertical vein.<sup>[12]</sup> Chowdhury et al.<sup>[12]</sup> basically classified mixed type TAPVCs into three general groups. Two by two pattern, three by one pattern and the bizarre pattern. The most common anatomical configuration is the latter, followed by 2 by 2, and the least common is the bizarre pattern. Obstruction occurs in approximately 40% of mixed-type TAPVCs.

In patients with TAPVC, obstructed or non-obstructed pulmonary venous drainage or the degree of obstruction dramatically changes the neonatal presentation of the disease. In patients with junctional obstruction, the main presentation is profound hypoxia and pulmonary hypertension. This pulmonary hypertension can sometimes be thought of as a persistence of the fetal circulation. X-ray radiograph shows pulmonary edema without cardiomegaly. The risk of developing circulatory collapse is high in patients with insufficient mixing at the atrium level. These patients may need ECMO until the correct diagnosis is made and surgical correction is made. Obstructed TAPVC is a surgical emergency. In non-obstructive types, varying degrees of desaturation are seen in the presence of heart failure and cardiomegaly; this is

due to the wide left-right shunt. In some cases, the diagnosis is missed in the neonatal period.<sup>[11,12]</sup>

Two-dimensional echocardiography (ECHO) is sufficient to demonstrate anatomy in most TAPVC patients. Cardiac catheterization is rarely needed: in fact, it is often avoided as it may delay corrective cardiac surgery. Magnetic resonance and tomographic angiography may be useful for understanding the anatomy of the pulmonary connection. After diagnosis, surgical correction should be performed without delay for obstructed and non-obstructed TAPVCs. Because the disease does not have the potential to regress and palliative medical strategies do not provide an effective solution. Prostaglandins can be used to maintain ductal patency and provide systemic circulation, but they have no place in the correction of hypoxia or in the treatment of resistant acidosis. Similarly, nitric oxide is not effective in increasing oxygenation. Mueller performed the first surgical correction of TAPVC with pulmonary venous sac and left atrial appendage anastomosis in 1951, without using a cardiopulmonary bypass. In 1956, Lewis and Varco made the first complete correction of TAPVC, using the inflow occlusion technique. In the same year, Kirklin performed a TAPVC repair using cardiopulmonary bypass. Although all correction surgeries are performed using cardiopulmonary bypass today, there are surgical and central differences between the techniques.<sup>[13,14]</sup>

Patients with pulmonary venous obstruction should be operated immediately as soon as the diagnosis is made. Non-obstructive cases should be operated within the first two months. In patients with non-obstructive pulmonary venous connections, medical treatment is given for right ventricular failure, hypoxia and congestive heart failure. These patients are provided with inotropic support, effective diuresis and avoidance of high oxygen, as it reduces pulmonary vascular resistance and increases pulmonary congestion. Medical treatments are limited in obstructive type TAPVC. These patients are frequently intubated, the goal being to create respiratory alkalosis by keeping partial CO<sub>2</sub> levels below 30 mmHg. These reasons generally require hyperventilation with 100% oxygen. To prevent metabolic acidosis, together with sodium bicarbonate, an inotrope is used to support ventricular functions and effective diuresis is provided for the treatment of pulmonary edema. In patients with insufficient right-left shunt, cardiac output is increased by increasing duct patency, by starting prostaglandin-E1. In some centers, cardiac catheterization is performed in patients with obstructive type TAPVC, both for diagnostic procedures and for palliation. These interventions are dilation of the restricted

atrial septum with balloon atrial septostomy and stenting of the obstructed vertical vein.<sup>[9,15,16]</sup>

In surgical repair of supracardiac TAPVC, the vertical vein is ligated through the innominate vein or SVC junction, freeing it from the surrounding tissues. In the presence of severe preoperative obstruction, sometimes leaving the vertical vein open may be beneficial for the prevention of postoperative pulmonary hypertension, but re-intervention may be required after significant residual left-right shunt. A horizontal incision is made in the posterior wall of the left atrium and the pulmonary venous sac, and these two structures are anastomosed to each other as wide as possible. The most critical factor here is proper anastomosis of the pulmonary veins without distortion to ensure long-term patency.<sup>[9]</sup>

In surgical repair of cardiac TAPVC, there is a vertical vein opening into the coronary sinus. The atrial septal defect (ASD) is first expanded towards the coronary sinus. An unroofed coronary sinus is created. If there is stenosis in the opening of the coronary sinus to the pulmonary venous sac, this area is widened and the stenosis is relieved. The large interatrial defect formed is closed with a patch, leaving the coronary sinus and pulmonary venous drainage to the left of the septum. In cases where the TAPVC opens into the right atrium, pulmonary venous drainage is diverted to the left atrium via the PFO by baffle.<sup>[9]</sup>

In infracardiac TAPVC, the vertical vein is typically extrapericardial and passes through the esophageal hiatus into the abdomen. The pulmonary venous sac extends vertically in a Y shape. When the pulmonary venous sac is reached, the vertical vein is ligated. After the pouch is opened with a vertical and Y-shaped incision, the supradiaphragmatic portion of the vertical vein is segmented and used to widen the left atrial anastomosis.<sup>[9,17]</sup>

The most common type of mixed type TAPVC is the type in which three veins drain posterior to the junction of the pulmonary veins and one drains separately into the systemic venous system. The repair is often in the form of establishing the connection of the left atrium to the pulmonary venous sac. Sometimes a single pulmonary vein that opens into the systemic veins can be left in place to prevent postoperative stenosis.<sup>[17]</sup>

Pulmonary hypertension may complicate the postoperative period in newborns with TAPVC, especially in patients with pulmonary venous obstruction in the preoperative period. There may be a need for nitric oxide during separation from CPB. Even in advanced cases, ECMO support may be needed due to failure to exit the CPB. In our study only 3 (11.1%) patients needed ECMO.

It is very important that there is no residual stenosis in the pulmonary venous anastomosis in these patients. In some cases, pulmonary hypertension may persist despite a non-obstructed anastomosis. In these patients, lymphangiectasias can be seen in lung biopsies. It is thought that the most important factor causing this situation is exposure to long-term pulmonary venous hypertension in the intrauterine period. These patients usually have diffused small pulmonary veins that are detected intraoperatively.<sup>[13,18]</sup>

## Conclusion

TAPVC is a set of congenital cardiac defects with a wide range of anatomical characteristics that are linked by a shared pathophysiology, mostly determined by the presence or absence of pulmonary venous obstruction. An early diagnosis makes proper preoperative treatment and surgical correction easier.

## Conflict of Interest

The authors declare no conflict of interest.

## Author Contributions

All authors contributed equally to protocol/project development, data collection, data analysis, manuscript writing/editing.

## Ethics Approval

The study was carried out in compliance with the Declaration of Helsinki's guiding principles and the protocol was accepted by the ethics committee of the Institution (No: E2-22-3047).

## Funding

The authors declare no financial support.

## References

1. Shaw FR, Chen JM. Surgical considerations in total anomalous pulmonary venous connection. *Semin Cardiothorac Vasc Anesth* 2017; 21:132–7.
2. Hines MH, Hammon JW. Anatomy of total anomalous pulmonary venous connection. *Operative Techniques in Thoracic and Cardiovascular Surgery* 2001;6:2–7.
3. Seale AN, Uemura H, Webber SA, Partridge J, Roughton M, Ho SY, McCarthy KP, Jones S, Shaughnessy L, Sunnegardh J, Hansens K, Berggren H, Johansson S, Rigby ML, Keeton BR, Daubney PEF; British Congenital Cardiac Association. Total anomalous pulmonary venous connection: morphology and outcome from an international population-based study. *Circulation* 2010;122:2718–26.
4. Correa-Villasenor A, Ferencz C, Boughman JA, Neill CA. Total anomalous pulmonary venous return: familial and environmental factors. The Baltimore-Washington Infant Study Group. *Teratology* 1991;44:415–28.

5. Raisher BD, Dowton SB, Grant JW. Father and two children with total anomalous pulmonary venous connection. *Am J Med Genet* 1991;40:105–6.
6. Lucas RV Jr, Adams P Jr, Anderson RC, Varco RL, Edwards JE, Lester RG. Total anomalous pulmonary venous connection to the portal venous system: a cause of pulmonary venous obstruction. *Am J Roentgenol Radium Ther Nucl Med* 1961;86:561–75.
7. Becker AE, Anderson RH. Pathology of congenital heart disease. 2nd ed. London: Butterworths; 1981. p. 498.
8. Herlong JR, Jagers JJ, Ungerleider RM. Congenital heart surgery nomenclature and database project: pulmonary venous anomalies. *Ann Thorac Surg* 2000;69:S56–S69.
9. Viola N, Caldarone CA. Total anomalous pulmonary venous connection. In: Mavroudis C, Backer CL, editors. *Pediatric cardiac surgery*, 4th ed. West Sussex, UK: John Wiley & Sons; 2013. p. 659–73.
10. Moorman A, Webb S, Brown NA, Lamers W, Anderson RH. Development of the heart: (1) formation of the cardiac chambers and arterial trunks. *Heart* 2003;89:806–14.
11. Files MD, Morray B. Total anomalous pulmonary venous connection: preoperative anatomy, physiology, imaging, and interventional management of postoperative pulmonary venous obstruction. *Semin Cardiothorac Vasc Anesth* 2017;21:123–31.
12. Chowdhury UK, Malhotra A, Kothari SS, Reddy SK, Mishra AK, Pradeep KK, Venugopal P. A suggested new surgical classification for mixed totally anomalous pulmonary venous connection. *Cardiol Young* 2007;17:342–53.
13. Kanter K. Surgical repair of total anomalous pulmonary venous connection. *Semin Thorac Cardiovasc Surg Pediatr Card Surg Annu* 2006;40–4.
14. Jonas RA. Total anomalous pulmonary venous connection. *Operative Techniques in Thoracic and Cardiovascular Surgery* 2006;11:286–94.
15. Kyser JP, Bengur AR, Siwik ES. Preoperative palliation of newborn obstructed total anomalous pulmonary venous connection by endovascular stent placement. *Catheter Cardiovasc Interv* 2006;67:473–6.
16. Meadows J, Marshall AC, Lock JE, Scheurer M, Laussen PC, Bacha EA. A hybrid approach to stabilization and repair of obstructed total anomalous pulmonary venous connection in a critically ill newborn infant. *J Thorac Cardiovasc Surg* 2006;131:e1–2.
17. Kouchoukos NT, Blackstone EH, Hanley FL, Kirklin JK. *Kirklin/Barratt-Boyes cardiac surgery*. 4th ed. Philadelphia (PA): Elsevier/Saunders; 2013. Volume 1. Chapter 31, Total anomalous pulmonary venous connection; p. 1182–208.
18. Bando K, Turrentine MW, Ensing GJ, Sun K, Sharp TG, Sekine Y, Girod DA, Brown JW. Surgical management of total anomalous pulmonary venous connection. Thirty-year trends. *Circulation* 1996;94:II12–6.

**ORCID ID:**

B. Soran Türkcan 0000-0002-0694-5211;  
 M. Yılmaz 0000-0002-3212-2673;  
 A. Atalay 0000-0002-2527-2665



**Correspondence to:** Başak Soran Türkcan, MD  
 Department of Pediatric Cardiovascular Surgery,  
 Ankara Bilkent City Hospital, Ankara, Türkiye  
 Phone: +90 532 477 66 27  
 e-mail: basaksoran@gmail.com

*Conflict of interest statement:* No conflicts declared.

This is an open access article distributed under the terms of the Creative Commons Attribution-NonCommercial-NoDerivs 4.0 Unported (CC BY-NC-ND4.0) Licence (<http://creativecommons.org/licenses/by-nc-nd/4.0/>) which permits unrestricted noncommercial use, distribution, and reproduction in any medium, provided the original work is properly cited. *How to cite this article:* Soran Türkcan B, Yılmaz M, Atalay A. Total anomalous pulmonary venous connection: preoperative anatomy, physiology, preoperative evaluation, surgical considerations and single centre clinical experiences. *Anatomy* 2022;16(2):76–80.

# Determination of knee joint line in relation to bony landmarks: a CT study in Turkish population

Cem Özcan<sup>1</sup> , Ali Şahin<sup>2</sup> 

<sup>1</sup>Department of Orthopedics and Traumatology, School of Medicine, İzmir Katip Çelebi University, İzmir, Türkiye

<sup>2</sup>Department of Orthopedics and Traumatology, Ankara Etilik City Hospital, Ankara, Türkiye

## Abstract

**Objectives:** Evaluation of the knee joint line is important in terms of clinical outcomes in lower extremity alignment surgeries. Since there are a limited number of studies examining the relationship between the normal knee joint line and the bony landmarks around the knee in Turkish society, we evaluated the relationship between the knee joint line and the bone landmarks in the Turkish population.

**Methods:** Knee CT images of 100 patients (50 females, 50 males) aged between 18–50 years were retrospectively evaluated. The distance between the joint line and the medial epicondyle, lateral epicondyle, apex of head of fibula, patella lower pole, tuberositas tibia and interepicondylar distance of the femur was evaluated.

**Results:** With the exception of lateral epicondyle/femoral transepicondylar width, tibial tubercle distance/femoral transepicondylar width, tibial width /femoral transepicondylar width, and tibial width/tibial tubercle distance; all ratios differed between the genders with statistical significance ( $p < 0.005$ ).

**Conclusion:** CT evaluation of the knee joint allows making precise measurements in the coronal, axial and sagittal planes. We believe that the values we determined will help surgeons to determine the joint line during total knee replacement and revision knee replacement surgery in Turkish patients.

**Keywords:** bony landmarks; femoral interepicondylar width; knee, knee joint line

Anatomy 2022;16(2):81–87 ©2022 Turkish Society of Anatomy and Clinical Anatomy (TSACA)

## Introduction

The importance of the orientation of the joint line of the knee joint has been demonstrated in many clinical studies.<sup>[1,2]</sup> Defining the joint line is crucial in terms of clinical outcomes in lower extremity alignment surgeries. The importance of restoration of the knee joint line in total knee replacement and revision knee replacement surgeries has also been emphasized in many studies. It has been reported that a change of more than 4 mm in the joint line will affect the clinical outcome.<sup>[3–6]</sup> Particularly determining the intraoperative joint line is an important challenge for surgeons while operating patients with bone loss and osteolysis. In general, the joint line is evaluated radiologically during preoperative planning. In this evaluation process, certain anatomical bony landmarks are marked and the level of the joint line is calculated, and efforts are made to place the femoral and tibial components in accordance with the normal joint line during the operation. It has

been reported that bony landmarks are reliable and widely used in determining the joint line during revision knee replacement surgery.<sup>[7–9]</sup>

The distances between the bony landmarks and the joint line have been found to be significantly affected by variables such as gender, ethnicity, and the height of the patient.<sup>[10]</sup> Some researchers have suggested that the ratio of the distance from bony landmarks to the joint line and the femoral transepicondylar width, also called the epicondylar ratio, is more reliable than the distances of the bony landmarks to the articular line.<sup>[8,9,11]</sup> However, studies conducted among specific ethnic populations have yielded differences in the recommended values.<sup>[12]</sup>

Since there is a limited number of studies examining the relationship between the normal knee joint line and the bony landmarks around the knee in the Turkish population, we aimed to evaluate the relationship between

the knee joint line and bony landmarks in the Turkish population using computerized tomography (CT) images of normal knees.

## Materials and Methods

Knee CT images of 100 patients (50 females, 50 males) aged between 18–50 years were evaluated retrospectively. The images of the patients with fractures around the knee, degenerative changes in the articular cartilage, osteochondral defects, and patients with a history of previous knee surgery were not included.

All exams were performed with a 16-slice multidetector-row scanner (Toshiba Alexion, Toshiba Medical Systems Corporation, Otawara, Japan). The acquired 2-mm-thick axial images and reformatted coronal and sagittal images were observed independently with electronic calipers at a picture archiving and communication system (PACS) station by an orthopedic surgeon. First, the joint line of the knee (JL) was determined as the line passing through the most distal points of the medial and lateral femoral condyles in the coronal plane and/or as

the line passing through the most distal point of the femur perpendicular to the anatomical axis of the tibial shaft in the sagittal plane. Subsequently, the following parameters were measured.

### In the Coronal Plane

- **Medial epicondylar distance (MED):** The distance between the JL and the most medial point of the femur where the medial collateral ligament attached (**Figure 1**).
- **Lateral epicondylar distance (LED):** The distance between the JL and the most lateral point of the femur where the lateral collateral ligament attached (**Figure 1**).
- **Proximal tibiofibular joint distance (PTFJD):** The distance between the JL and the center of the horizontal portion of the proximal tibiofibular joint (**Figure 2**).
- **Apex of head of fibula distance (AFD):** The distance between the JL and the superior point of the apex of head of fibula (**Figure 3**).

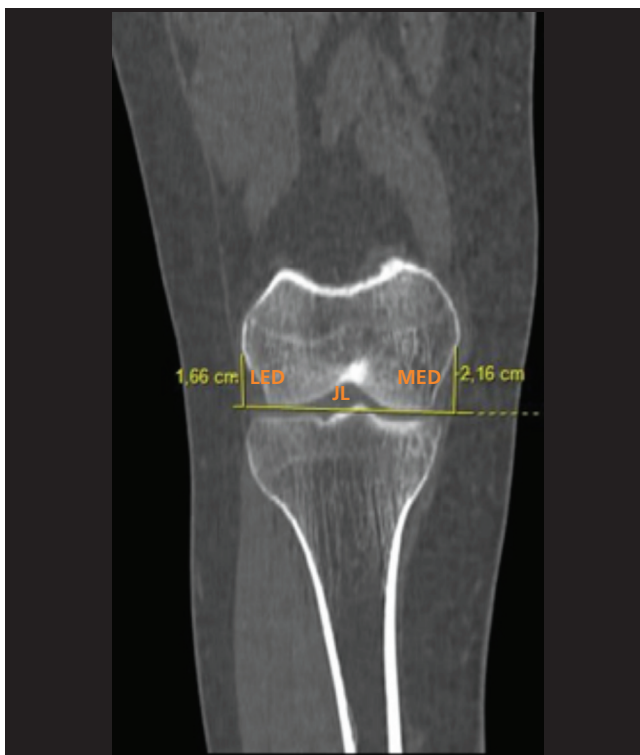


**Figure 1.** Coronal CT image. Medial epicondylar distance (MED) is the distance between joint line (JL) and the most medial point of the femur where the medial collateral ligament originated and the lateral epicondylar distance (LED) is the distance between JL and the most lateral point of the femur where the lateral collateral ligament originated.

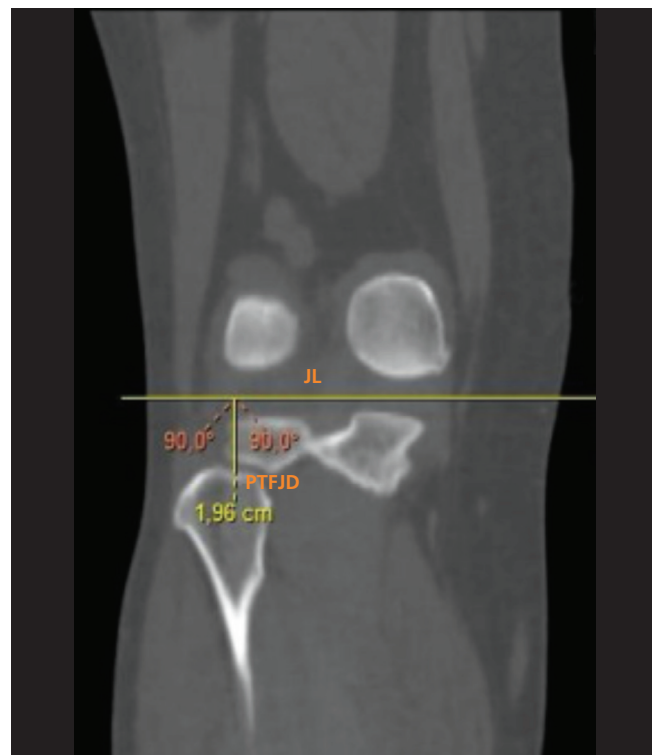


**Figure 2.** Coronal CT image. Proximal tibio-fibular joint distance (PTFJD) is the distance between JL and the center of the horizontal portion of the proximal tibiofibular joint.

In the Sagittal Plane

- **Tibial width (TW):** The diameter of the tibia at the level of the tibial tubercle (TT) or the most proximal point where the patellar tendon is attached to the tibial tubercle (Figure 4).
- **Tibial tubercle distance (TTD):** The distance between the JL and the level of the TT or the most proximal point where the patellar tendon is attached to the tibial tubercle (Figure 5).
- **Patellar distance (PD):** The distance between the JL and the most inferior point of the inferior pole of the patella (Figure 5).

In the Axial Plane

- **Femoral transepicondylar width (FW):** The distance between the most prominent point of the medial femoral epicondyle and the most prominent point of the lateral femoral epicondyle (Figure 6).

Femoral ratios, taken as the ratios of the femoral width to JL-MED, JL-LED, PJL-TFJD, JL-AFD, JL-TTD, and JL-PD were evaluated. The tibial ratio, as the ratio of

the tibial width to to the JL-TTD, was also calculated. All measurements were repeated twice by a single observer. The mean values of these measurements were used.

Categorical variables were presented as frequencies and percentages. The chi-square test was used for comparisons of categorical variables. The Shapiro-Wilk test was used to test the normality of distribution. All continuous variables were normally distributed; therefore, when comparing clinical characteristics, the Student t-test was used for continuous variables and values were presented as mean± standard deviation (SD). The data obtained in the study were analyzed using SPSS (Statistical Package for Social Sciences) for Windows (Version 26, IBM Corp., Armonk, NY, USA). For all analyses; p<0.05 was considered as significant.

Results

The mean age of the of the participants was 43.56±7.0 in males and 45.4±10.1 years in females (p=0.294). The distances between the anatomical landmarks and the joint line of the knee and the tibial and femoral diameters are pre-



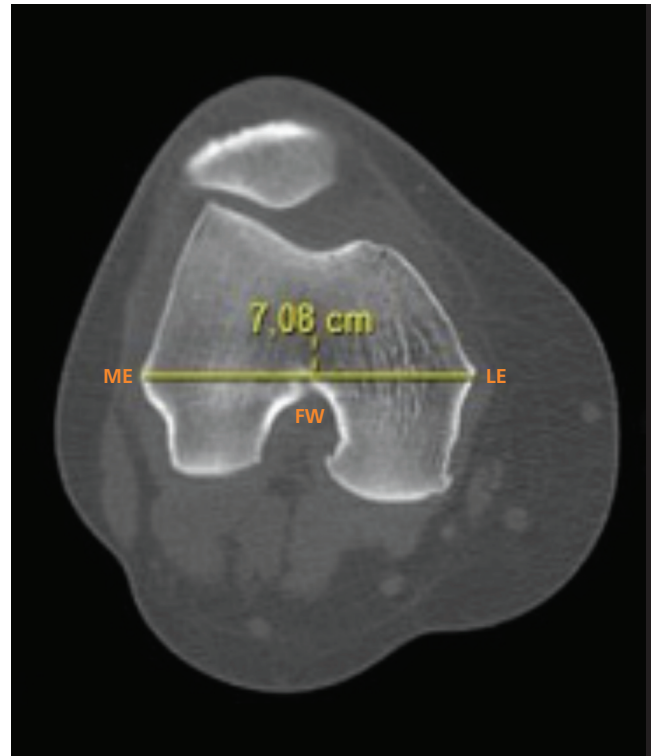
Figure 3. Coronal CT image. Apex of head of fibula distance (AFD) is the distance between joint line (JL) and the superior point of the apex of head of fibula.



Figure 4. Sagittal CT image. Tibial width (TW) is the diameter of the tibia at the level of the tibial tubercle (TT) or the most proximal point where the patella tendon is inserted into the tibial tubercle (TT).



**Figure 5.** Sagittal CT image. Tibial tubercle distance (TTD) is the distance between the joint line (JL) and the level of the tibial tubercle (TT) or the most proximal point where the patella tendon is inserted into the tibial tubercle (TT) and the patellar distance (PD) is the distance between the joint line (JL) and the most inferior point of inferior pole of patella.



**Figure 6.** Axial CT image. Femoral transepicondylar width (FW) is the distance between the most prominent point of medial femoral epicondyle (ME) and the most prominent point of the lateral femoral epicondyle (LE).

sented in **Table 1**. All distances and diameters differed between the genders with statistical significance ( $p < 0.005$ ). The mean and SD values of the femoral and tibial ratios for all landmarks are presented in **Table 2**. With the exception of LED/FW, TTD/FW, TW/FW, and TW/TTD, all ratios differed between the genders with statistical significance.

## Discussion

The medial epicondyle, lateral epicondyle, tibial tubercle, apex of head of fibula, and lower pole of the patella are commonly used bone reference points in clinical settings. Surgeons can evaluate these points in preoperative radiological examinations or intraoperatively with palpation. In the current CT study, we investigated the distances between bony landmarks such as the medial epicondyle, lateral epicondyle, apex of head of fibula, proximal tibiofibular joint, tibial tubercle, and lower pole of the patella and the knee joint line as well as the ratios of these distances to femoral width and tibial width in the Turkish population. Knowing the normal range of values for the

knee joint line in a society is of great importance in planning knee arthroplasty and especially revision surgery because slippage of the joint line may disrupt the biomechanics of the knee, resulting in complications such as decreased strength of the extensor mechanism, increased patellofemoral joint pressure, anterior knee pain, and decreased range of motion.<sup>[13-15]</sup> Although it is necessary to restore the normal joint line for both primary and revision total knee arthroplasty, there is still no consensus on how to determine the normal joint line.<sup>[10]</sup> During primary total knee arthroplasty, surgeons can estimate the normal joint line position based on the thickness of the femoral osteotomy. However, in the case of revision total knee arthroplasty, reliable references are needed to find the normal articular line because of bone loss in the distal femur and proximal tibia due to previous surgery. The use of anatomical landmarks to determine the position of the joint line is well accepted in clinical practice.<sup>[8]</sup> However, the mean distances from the bony reference points to the knee joint line are strongly correlated with body build, gender and race.<sup>[7]</sup> To overcome this disadvantage, Servien et al.<sup>[8]</sup> proposed evaluation of the ratios of these measured distances

**Table 1**

Summary of the measurements and gender difference.

Distance (mm)	Overall (Mean±SD)	Males (Mean±SD)	Females (Mean±SD)	p-value*
MED	27.8±1.1	28.1±0.6	27.5±1.4	0.007
LED	23.6±1.8	24.3±1.7	22.8±1.6	<0.001
PTJFD	26.0±2.5	27.8±0.9	24.1±2.2	<0.001
AFD	19.1±5.0	22.8±2.6	15.4±3.9	<0.001
PD	13.3±1.7	14.4±0.7	12.2±1.7	<0.001
TTD	23.0±1.7	23.7±0.3	22.3±2.1	<0.001
FW	77.3±2.3	78.9±0.9	75.8±2.3	<0.001
TW	43.5±4.0	44.9±3.5	42.1±3.9	<0.001

\*Distances and diameters differed between the genders with statistical significance ( $p < 0.005$ ). AFD: apex of head of fibula distance; FW: femoral transepicondylar width; LED: lateral epicondylar distance; MED: medial epicondylar distance; PT: patellar distance; PTJFD: proximal tibiofibular joint distance; TTD: tibial tubercle distance; TW: tibial width.

to the femoral transepicondylar width and claimed that these ratios would be less affected by variables such as gender, race, or body mass index (BMI). The use of ratios has proven to be more reliable. It has been shown that ratios are less affected by the variations caused by age, BMI, and gender, and they can be used easily with information obtained from both radiological examinations and intraoperative measurements.<sup>[11,16-18]</sup> In our study, we considered the epicondylar ratio as well as the distances of the bone reference points to the joint line.

The results of our study revealed the mean FW as 77.3 mm. This value was previously reported by Romero et al.<sup>[19]</sup> as 79.9 mm, by Servien et al.<sup>[8]</sup> as 81.7 mm, by Lee et al.<sup>[20]</sup> as 75 mm, by Seedhom et al.<sup>[21]</sup> as 77.2 mm, and by Iacono et al.<sup>[22]</sup> as 89.7 mm. Differences between our results and previous studies can be explained by differences

in the patients' ethnicities, participant selection, measurement methodology or observer differences. The mean distance between the head of the fibula and the joint line was reported as 20.5 mm by Gurbuz et al.,<sup>[12]</sup> while Mason et al.<sup>[23]</sup> found it as 20 mm. We found this mean value to be 19.1 mm, similar to the reported ranges in the literature. In our study, the mean MED was 27.8 mm and the mean LED was 23.6 mm. These values were determined as 28.95 mm and 23.97 mm, respectively by Ozkurt et al.<sup>[11]</sup> in a cadaver study. Iacono et al.<sup>[22]</sup> reported a correlation between the medial epicondyle-joint line distance and femur interepicondylar width, calculating a ratio value of 0.343. This value was 0.327 in a study conducted by Fan et al.<sup>[9]</sup> among the Chinese population, while it was 0.34 in the study of Servien et al.<sup>[8]</sup> and 0.35 in the study of Ozkurt et al.<sup>[11]</sup> Similarly, we determined this value as 0.35. This

**Table 2**

Mean ratios and gender difference.

Ratio	Overall (Mean±SD)	Males (Mean±SD)	Females (Mean±SD)	p-value
MED/FW	0.35±0.01	0.35±0.0	0.36±0.01	0.007
LED/FW	0.30±0.02	0.31±0.02	0.30±0.02	0.116
PD/FW	0.17±0.01	0.18±0.0	0.16±0.02	<0.001*
TTD/FW	0.29±0.02	0.30±0.0	0.29±0.02	0.122
AFD/FW	0.24±0.06	0.28±0.03	0.2±0.05	<0.001*
PTJFD/FW	0.33±0.02	0.35±0.01	0.31±0.02	<0.001*
TW/FW	0.56±0.04	0.57±0.04	0.55±0.04	0.120
TW/TTD	1.9±0.2	1.8±0.1	1.9±0.3	0.759

\*Ratios differed between the genders with statistical significance ( $p < 0.005$ ). AFD: apex of head of fibula distance; FW: femoral transepicondylar width; LED: lateral epicondylar distance; MED: medial epicondylar distance; PT: patellar distance; PTJFD: proximal tibiofibular joint distance; TTD: tibial tubercle distance; TW: tibial width.

ratio does not reflect significant differences between the genders and its standard deviation is low; therefore, we think that it can guide surgeons with high reliability.

Computed tomography, magnetic resonance imaging, and direct radiographs are used to determine the location of the joint line.<sup>[24–26]</sup> We used CT in our study because CT is known to be superior in evaluating bony structures and we anticipated that it would be possible to locate the bone reference points from coronal, sagittal, and axial sections with higher reliability. While CT has disadvantages such as higher radiation load compared to conventional radiographs and magnetic resonance imaging and being more costly than conventional radiographs, these disadvantages were not reflected in our study because our study entailed a retrospective review of CT images taken in the emergency room and outpatient clinic for different reasons.

One of the limitations of the present study may be that the measurements were made by one observer. We thought that measurements made by a single observer would ensure standardization among slices. Repeated measurements performed at two different times were used to overcome the possible limitation. Since our study was a CT-based study, it allowed us to make precise measurements in the coronal, axial, and sagittal planes.

## Conclusion

There are few publications in the literature examining the relationship between the knee joint line and the bony landmarks around the knee in the Turkish population. We anticipate that the values we determined will help surgeons who often perform total knee replacement and revision knee replacement surgeries for Turkish patients to determine the joint line.

## Conflict of Interest

The authors declare no conflict of interest.

## Author Contributions

CÖ: conceiving and designing the analysis, collecting the data; AS: analyzing the data, writing the manuscript.

## Ethics Approval

The study was approved by the non-interventional clinical research ethics committee of Izmir Katip Çelebi University (No: 0086/0107) and carried out in compliance with the Declaration of Helsinki's guiding principles.

## Funding

The authors did not and will not receive any funding for this study.

## References

- Clave A, Le Henaff G, Roger T, Maisongrosse P, Mabit C, Dubrana F. Joint line level in revision total knee replacement: assessment and functional results with an average of seven years follow-up. *Int Orthop* 2016;40:1655–62.
- Martin JW, Whiteside LA. The influence of joint line position on knee stability after condylar knee arthroplasty. *Clin Orthop Relat Res* 1990;(259):146–56.
- Singerman R, Heiple KG, Davy DT, Goldberg VM. Effect of tibial component position on patellar strain following total knee arthroplasty. *J Arthroplast* 1995;10:651–6.
- Fornalski S, McGarry MH, Bui CN, Kim WC, Lee TQ. Biomechanical effects of joint line elevation in total knee arthroplasty. *Clin Biomech* 2012;27:824–9.
- Partington PF, Sawhney J, Rorabeck CH, Barrack RL, Moore J. Joint line restoration after revision total knee arthroplasty. *Clin Orthop Relat Res* 1999;(367):165–71.
- Khan WS, Bhamra J, Williams R, Morgan-Jones R. “Meniscal” scar as a landmark for the joint line in revision total knee replacement. *World J Orthop* 2017;8:57–61.
- Griffin FM, Math K, Scuderi GR, Insall JN, Polivache PL. Anatomy of the epicondyles of the distal femur: MRI analysis of normal knees. *J Arthroplasty* 2000;15:354–9.
- Servien E, Viskontas D, Giuffre BM, Coolican MRJ, Parker DA. Reliability of bony landmarks for restoration of the joint line in revision knee arthroplasty. *Knee Surg Sports Traumatol Arthrosc* 2008;16:263–9.
- Fan A, Xu T, Li X, Lei L, Fan L, Yang D, Li G. Using anatomical landmarks to calculate the normal joint line position in Chinese people: an observational study. *J Orthop Surg Res* 2018;13:261–70.
- Pereira GC, von Kaeppeler E, Alaia MJ, Montini K, Lopez MJ, Di Cesare PE, Amanatullah DF. Calculating the position of the joint line of the knee using anatomical landmarks. *Orthopedics* 2016;39:381–6.
- Ozkurt B, Sen T, Cankaya D, Kendir S, Basarir K, Tabak Y. The medial and lateral epicondyle as a reliable landmark for intra-operative joint line determination in revision knee arthroplasty. *Bone Joint Res* 2016;5:280–6.
- Gurbuz H, Cakar M, Adas M, Tekin AC, Bayraktar MK, Esenyel CZ. Measurement of the knee joint line in Turkish population. *Acta Orthop Traumatol Turc* 2015;49:41–4.
- Laskin RS. Management of the patella during revision total knee replacement arthroplasty. *Orthop Clin North Am* 1998;29:355–60.
- Laskin RS. Joint line position restoration during revision total knee replacement. *Clin Orthop Relat Res* 2002;(404):169–71.
- König C, Sharenkov A, Matziolis G, Taylor WR, Perka C, Duda GN, Heller MO. Joint line elevation in revision TKA leads to increased patellofemoral contact forces. *J Orthop Res* 2010;28:1–5.
- Bieger R, Huch K, Kocak S, Jung S, Reichel H, Kappe T. The influence of joint line restoration on the results of revision total knee arthroplasty: comparison between distance and ratio-methods. *Arch Orthop Trauma Surg* 2014;134:537–41.
- Rajagopal TS, Nathwani D. Can interepicondylar distance predict joint line position in primary and revision knee arthroplasty? *Am J Orthop (Belle Mead NJ)* 2011;40:175–8.
- Sadaka C, Kabalan Z, Hoyek F, Abi Fares G, Lahoud JC. Joint line restoration during revision total knee arthroplasty: an accurate and reliable method. *SpringerPlus* 2015;4:736.

19. Romero J, Seifert B, Reinhardt O, Ziegler O, Kessler O. A useful radiologic method for preoperative joint-line determination in revision total knee arthroplasty. *Clin Orthop Relat Res* 2010;468:1279–83.
20. Lee IS, Choi JA, Kim TK, Han I, Lee JW, Kang HS. Reliability analysis of 16-MDCT in preoperative evaluation of total knee arthroplasty and comparison with intraoperative measurements. *AJR Am J Roentgenol* 2006;186:1778–82.
21. Seedhom BB, Longton EB, Wright V, Dowson D. Dimensions of the knee. Radiographic and autopsy study of sizes required by a knee prosthesis. *Ann Rheum Dis* 1972;31:54–8.
22. Iacono F, Lo Presti ML, Bruni D, Raspugli GF, Bignozzi S, Sharma B, Marcacci. The adductor tubercle: a reliable landmark for analysing the level of the femorotibial joint line. *Knee Surg Sports Traumatol Arthrosc* 2013;21:2725–9.
23. Mason M, Belisle A, Bonutti P. An accurate and reproducible method for locating the joint line during a revision total knee arthroplasty. *J Arthroplasty* 2006;21:1147–53.
24. Sato T, Koga Y, Sobue T, Omori G, Tanabe Y, Sakamoto M. Quantitative 3-dimensional analysis of preoperative and postoperative joint lines in total knee arthroplasty: a new concept for evaluation of component alignment. *J Arthroplasty* 2007;22:560–8.
25. Howell SM, Chen J, Hull ML. Variability of the location of the tibial tubercle affects the rotational alignment of the tibial component in kinematically aligned total knee arthroplasty. *Knee Surg Sports Traumatol Arthrosc* 2013; 21:2288–95.
26. Herzog RJ, Silliman JF, Hutton K, Rodkey WG, Steadman JR. Measurements of the intercondylar notch by plain film radiography and magnetic resonance imaging. *Am J Sports Med* 1994; 22:204–10.

**ORCID ID:**

C. Özcan 0000-0002-1541-2484;  
A. Şahin: 0000-0002-2399-404X

**Correspondence to:** Ali Şahin, MD

Department of Orthopedics and Traumatology,  
Ankara Etlik City Hospital, Ankara, Türkiye  
Phone: +90 533 548 66 98  
e-mail: ortdralisahin@gmail.com

*Conflict of interest statement:* No conflicts declared.

This is an open access article distributed under the terms of the Creative Commons Attribution-NonCommercial-NoDerivs 4.0 Unported (CC BY-NC-ND4.0) Licence (<http://creativecommons.org/licenses/by-nc-nd/4.0/>) which permits unrestricted noncommercial use, distribution, and reproduction in any medium, provided the original work is properly cited. *How to cite this article:* Özcan C, Şahin A. Determination of knee joint line in relation to bony landmarks: a CT study in Turkish population. *Anatomy* 2022;16(2):81–87.

# Effects of the position of uncinete process on olfactory fossa depth and lateral lamella length

Ömer Hızlı<sup>1</sup> , Serkan Kayabaşı<sup>2</sup> , Deniz Özkan<sup>3</sup> 

<sup>1</sup>Department of Otolaryngology, Faculty of Medicine, Balıkesir University, Balıkesir, Türkiye

<sup>2</sup>Department of Otolaryngology, Middle East Private Hospital, Ankara, Türkiye

<sup>3</sup>Department of Radiology, Faculty of Medicine, Aksaray University, Aksaray, Türkiye

## Abstract

**Objectives:** To investigate the variations of olfactory fossa and lateral lamella by reference to the attachment site of uncinete process.

**Methods:** To perform the comparison of the olfactory fossa depth, 250 patients were categorized into three groups. Patients with bilateral type A uncinete process were included in the group A, patients with a unilateral type A uncinete process were included in the group B, and the patients with a type B or C uncinete process on both sides were included in the group C. To compare the lateral lamella length, we used the categorization of 500 uncinete processes from 250 patients, based on the attachment site of uncinete: lamina papyracea, skull base and middle turbinate.

**Results:** The mean olfactory fossa depth did not significantly differ between the group A and B ( $p=0.503$ ), however, it was significantly greater in the group C, compared to both to the group A ( $p<0.001$ ) and B ( $p=0.003$ ). The mean lateral lamella length did not significantly differ between the lamina papyracea group and middle turbinate group ( $p=0.387$ ) however, it was significantly greater in the skull base group, compared both to lamina papyracea ( $p<0.001$ ) and middle turbinate groups ( $p<0.001$ ).

**Conclusion:** Patients with uncinete processes attached to skull base and/or middle turbinate on both sides had a lower olfactory fossa, and the uncinete process attached to the skull base is associated with longer lateral lamella.

**Keywords:** lateral lamella; middle turbinate; olfactory fossa; skull base; uncinete process

Anatomy 2022;16(2):88–92 ©2022 Turkish Society of Anatomy and Clinical Anatomy (TSACA)

## Introduction

The anatomical variations of lateral nasal wall and paranasal sinuses may affect the position of the skull base. During endoscopic sinus surgery, surgeons should pay attention on the depth of olfactory fossae and length of lateral lamella of the cribriform plate (LLCP) to avoid the well-known complication of this surgical procedure; skull base injury. The olfactory fossae are the grooves of the cribriform plate and contains the olfactory bulb and LLCP serves to separate this anterior cranial fossa from ethmoid air cells. The depth of the olfactory fossa is determined by the length of the LLCP and may be asymmetric.<sup>[1-3]</sup> Thus, pre-operative evaluation of the skull base and adjacent structures upon paranasal computed tomography (CT) is crucial.

A categorization based on the olfactory fossa depth was performed by Keros<sup>[1]</sup> previously. Individuals with a

deeper olfactory fossa usually have a longer LLCP. LLCP is a thin and weak bone plate constituting the lateral boundary of cribriform plate as a bridge between cribriform plate and fovea ethmoidalis, which is an extension of the orbital plate of the frontal bone forming the lateral part of the ethmoid roof. Considering that the uncinete process of ethmoid bone has three different attachment sites,<sup>[2]</sup> the position of the skull base may have an association with the status of uncinete process. Several studies investigated the association of olfactory fossa depth and/or LLCP length with adjacent anatomic structures,<sup>[3,4]</sup> however; to the best of our knowledge, only a limited number of studies thus far has focused on the association between the skull base and uncinete process. Therefore, in this study we aimed to investigate the variations of olfactory fossa and LLCP by reference to the attachment site of uncinete process.

## Materials and Methods

After a detailed search of paranasal CT archives of our tertiary institution, we included paranasal CT sections of 250 patients. We compiled the data using a Toshiba Alexion CT unit (Canon Medical Systems Corp., Otawara, Tochigi, Japan) with a radiologic archiving and imaging system (Probel, İzmir, Turkey). The parameters of the CT scanner were 130 kVp, 1.2 mm slice thickness, 0.8-s rotation time, and 1 mm pitch. Patients with any history of sinus surgery, facial trauma, paranasal sinus tumors including inverted papilloma, cystic fibrosis, and generalized nasal polyposis that might alter the anatomy of uncinate process and ethmoid roof were excluded from the study. To compare the olfactory fossa depth and LLCP length based on the attachment site of the uncinate process, two different categorizations were performed. To perform these categorizations, we utilized the classical previous description of the attachment of uncinate process by Wormald<sup>[2]</sup> as; uncinate process with a superior attachment to lamina papyracea (Type A-considered as normal position), skull base (Type B), and middle turbinate (Type C).

To perform the comparison of the olfactory fossa depth, 250 patients were categorized into three groups. The patients with bilateral type A uncinate process were included in the group A, the patients with a unilateral type A uncinate process were included in the group B, and the patients with a type B or C uncinate process on both sides were included in the group C. We measured the olfactory fossa depth of the patients on the coronal CT sections in which crista galli was most prominent, in accordance with the previous description by Keros,<sup>[1]</sup> based on the position of cribriform plate relative to ethmoid roof. In accordance with the Keros<sup>[1]</sup> classification, olfactory fossa depth between 1–3 mm was determined as type 1, 4–7 mm as type 2 and 8–16 mm as type 3. Then, the mean olfactory fossa depth values of the groups were compared statistically.

To compare the LLCP length, we used the categorization of 500 uncinate processes from 250 patients, based on the attachment site of uncinate. We measured

LLCP length as the lateral boundary of cribriform plate, between horizontal cribriform plate and fovea ethmoidalis. Then, the mean LLCP lengths of three groups (lamina papyracea, skull base and middle turbinate) were compared statistically.

Results of the analysis were presented as mean±standard deviation. The normal distribution of the data was confirmed using Kolmogorov-Smirnov normality test ( $p>0.2$ ). The olfactory fossa depth and LLCP length of three groups were compared using one-way analysis of variance (ANOVA) test. The homogeneity of the data was investigated using Levene's test. Post-hoc analyzes were performed using Tukey's test. All statistical analysis was performed using SPSS 23.0 software on MacOS 12.2.1 (IBM Corp, Armonk, NY, USA). A p-value under 0.05 was considered statistically significant.

## Results

In total, paranasal CT sections from 250 patients were included. For the comparison of olfactory fossa depth, the patients were categorized as three group. Group A consisted of 85 patients [43 males and 42 females, median age: 29 (18–76) years], group B consisted of 66 patients [34 males and 32 females, median age: 29 (18–70) years], and group C consisted of 99 patients [40 males and 59 females, median age: 28 (18–66) years]. The groups were age and gender-matched ( $p=0.889$  and  $p=0.258$ , respectively). The distribution of the groups based on Keros<sup>[1]</sup> classification was presented in **Table 1** and comparison of the mean olfactory fossa depth values of the groups was presented in **Table 2**. One way ANOVA revealed that olfactory fossa depth did significantly differ between three groups ( $p<0.001$ ). According to the post-hoc tests, the mean olfactory fossa depth did not significantly differ between the group A and B ( $p=0.503$ ), however, the mean olfactory fossa depth was significantly greater in the group C, compared to both to the group A ( $p<0.001$ ) and B ( $p=0.003$ ) (**Figure 1**). Thus, we found that patients with uncinate processes with a superior attachment to skull base and/or middle turbinate (abnormal position) on both sides had a lower olfactory fossa.

**Table 1**

Keros distribution of the groups.

Groups	Type 1	Type 2	Type 3
A (n=85)	19 (22.4%)	64 (75.3%)	2 (2.3%)
B (n=66)	9 (13.63%)	55 (83.33%)	2 (3.04%)
C (n=99)	9 (9.09%)	71 (71.71%)	19 (19.2%)

**Table 2**  
Comparison of olfactory fossa depth.

Groups	Olfactory fossa depth (mm)
A (patients with bilateral type A uncinate process) (n=85)	5.05±1.41
B (patients with unilateral type A uncinate process) (n=66)	5.32±1.37
C (patients with type B or C uncinate process on both sides) (n=99)	6.11±1.6
p-value*	<0.001

\*of one-way ANOVA.

For the comparison of LLCP lengths, 500 uncinate processes from 250 patients were categorized based on attachment site; lamina papyracea group (n=265), skull base group (n=135) and middle turbinate group (n=100). One way ANOVA revealed that the mean LLCP length did significantly differ among three groups ( $p<0.001$ ) (Table 3). According to the post-hoc tests, the mean LLCP length did not significantly differ between the lamina papyracea group and middle turbinate group ( $p=0.387$ ), however, it was significantly greater in the skull base group, compared both to lamina papyracea ( $p<0.001$ ) and middle turbinate groups ( $p<0.001$ ) (Figure 2). Thus, we found that attachment of the uncinate process into skull base might be associated with a longer LLCP.

## Discussion

In this radiological and anatomical investigation, we focused on the association between the attachment site of the uncinate process and the position of skull base. We found that patients with uncinate processes with a superior attachment to skull base and/or middle turbinate on both sides had a lower olfactory fossa. Additionally, the patients with an uncinate process attached to the skull base had a longer LLCP.

The position of skull base has a surgical implication for patients undergoing endoscopic sinus surgery: the lower the olfactory fossa, the longer the LLCP.<sup>[1,4]</sup> It is known that the LLCP is the weakest area of the skull base, and the patients with a lower olfactory fossa has a greater risk of skull base injury with a longer LLCP. Thus, we can speculate that patients with an uncinate process attached to the skull base carries an increased risk of skull base injury because of their longer lateral lamellas compared to the patients with an uncinate process attached to the lamina papyracea and middle turbinate.

When the previous literature is reviewed, there exist several studies investigating the relationships of the skull base and adjacent anatomical structures.<sup>[3,4,6]</sup> Additionally, authors focused on the angle between LLCP and the crib-

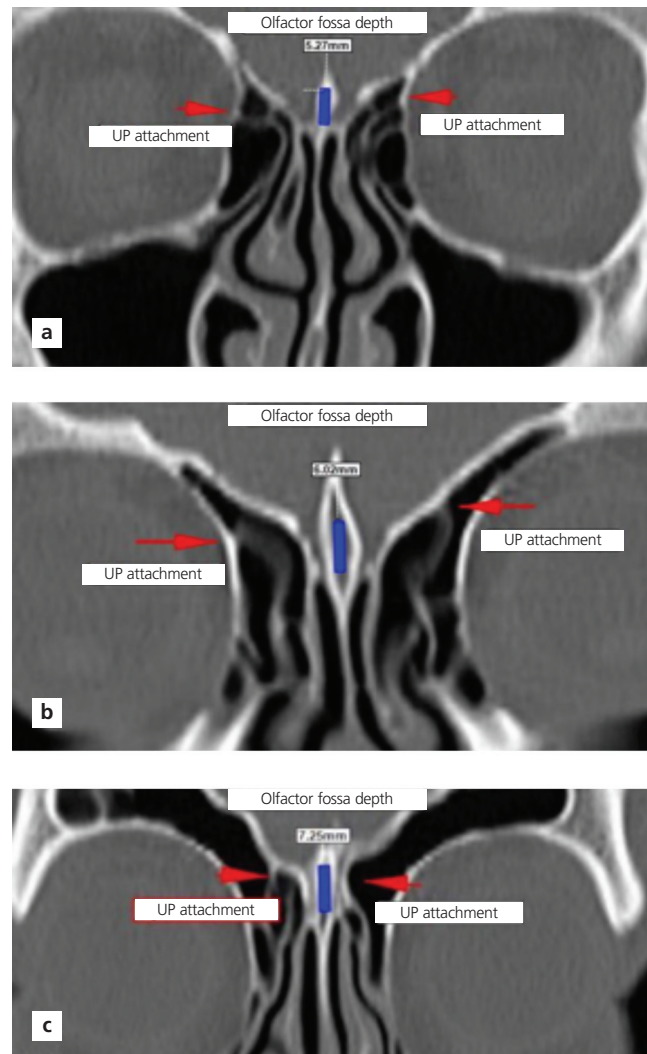


**Figure 1.** (a) Measurement of olfactory fossa depth on a patient from group A (with bilateral type A uncinate process); (b) measurement of olfactory fossa depth on a patient from group B (with a type A uncinate process on right); (c) measurement of olfactory fossa depth on a patient from group C (with a type B/C uncinate process on both sides).

iform plate in recent publications.<sup>[7,8]</sup> Moreover, the LLCP was reported as being an anatomical risk factor for iatrogenic cerebrospinal fluid leak.<sup>[9,10]</sup> Barroso et al.<sup>[11]</sup>

**Table 3**  
Comparison of lateral lamella length.

Groups*	Lateral lamella length (mm)
Lamina papyracea (n=265)	5.08±1.31
Middle turbinate (n=100)	6.01±1.42
Skull base (n=135)	6.99±1.51
p-value†	<0.001

\*Based on the superior attachment point of uncinate process; †of one-way ANOVA.

reported that the variations of attachment of the uncinate process did not affect the development of frontal sinus mucocoeles. However, to the best of our knowledge, only a limited number of studies study thus far have investigated the effects of the different attachment types of uncinate process on the development of the skull base, olfactory fossa depth and LLCP length.

The embryologic associations of the anatomical structures around paranasal sinuses are well-known. Ozcan et al.<sup>[12]</sup> reported the effects of paranasal sinus development on the position of orbital medial wall. Additionally, a coexistence between the hypoplasia of maxillary and frontal sinuses are known.<sup>[13]</sup> As reported by Kayabasi et al.,<sup>[4]</sup> maxillary sinus hypoplasia might be associated with a lower olfactory fossa and longer LLCP, bringing about an increased risk of skull base injury. Thus, superior attachment of uncinate process might affect the olfactory fossa depth and LLCP length. This study revealed the significant effect of uncinate process with a superior attachment to skull base on the LLCP length, however, as being a radiologic study, it has a disadvantage against cadaveric studies, considering as the major limitation of the study. In addition, according to the Keros<sup>[1]</sup> classification, olfactory fossa depth was determined as measurement only on crista galli, thus we added LLCP data on both sides to rule out this limitation. Nevertheless, surgeons should keep in mind that patients with uncinate processes attached to skull base or middle turbinate may have a deeper olfactory fossa, associated with an increased risk of iatrogenic skull base injury.

## Conclusion

In conclusion, patients with uncinate processes with a superior attachment to skull base and/or middle turbinate on both sides had a lower olfactory fossa, and the uncinate process attached to the skull base is associated with longer LLCP and increased risk of iatrogenic skull base injury during endoscopic sinus surgery.

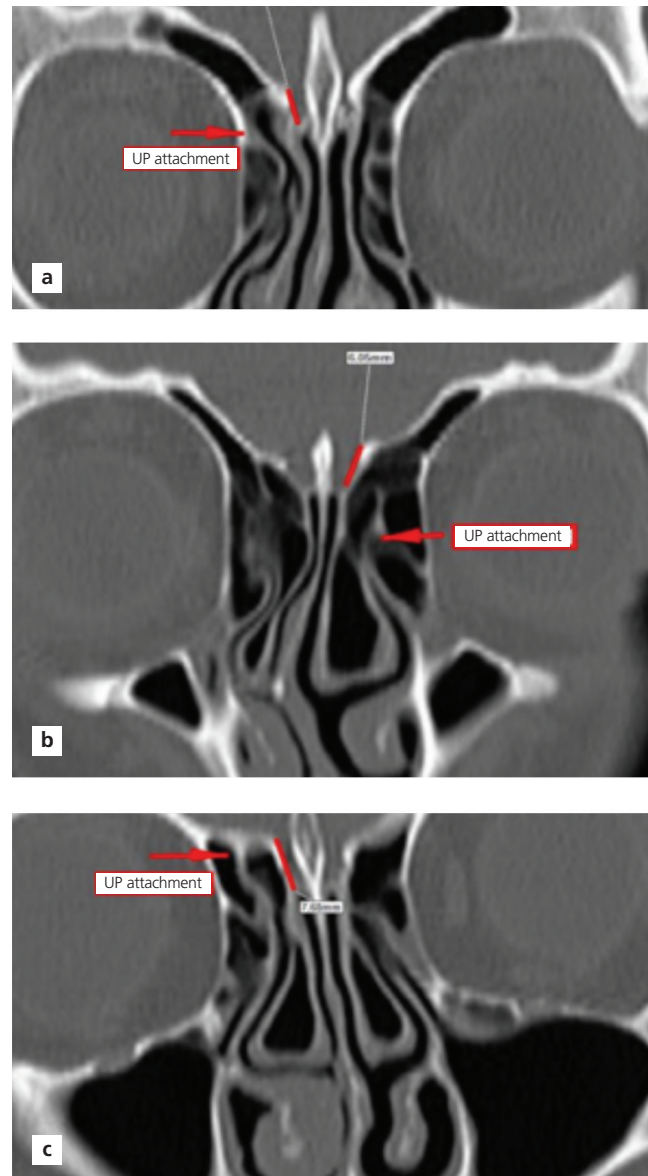


**Figure 2.** (a) Measurement of lateral lamella length on a type A uncinate process (attached to lamina papyracea); (b) measurement of lateral lamella length on a type B uncinate process (attached to middle turbinate); (c) measurement of lateral lamella length on a type C uncinate process (attached to skull base).

### Conflict of Interest

The authors declare that there is no conflict of interest.

### Author Contributions

ÖH: designing the study, data collection and analysis, writing the manuscript, SK: data analysis, revising the manuscript, supervision of the study, DÖ: data collection and analysis, revising the manuscript.

### Ethics Approval

This retrospective investigation was conducted in line with the dictates of Helsinki Declaration and approved by the local ethics committee of Aksaray University (IRB No: 2021/04-08).

### Funding

None.

### References

1. Keros P. On the practical value of differences in the level of the lamina cribrosa of the ethmoid. *Z Laryngol Rhinol Otol* 1962;41:809-13.
2. Wormald PJ. The agger nasi cell: the key to understanding the anatomy of the frontal recess. *Otolaryngol Head Neck Surg* 2003;129:497-507.
3. Gumus C, Yildirim A. Radiological correlation between pneumatization of frontal sinus and height of fovea ethmoidalis. *Am J Rhinol* 2007;21:626-8.
4. Kayabasi S, Hizli O, Ozkan D. Does paranasal sinus development affect olfactory fossa depth and lateral lamella length? *Laryngoscope* 2019;129:2458-63.
5. Kansu L. The relationship between superior attachment of the uncinat process of the ethmoid and varying paranasal sinus anatomy: an analysis using computerised tomography. *ENT Updates* 2019;9:81-9.
6. Çomoğlu Ş, Şahin B, Sönmez S, Değer K. Frontal sinus pneumatization affects height of the lateral lamella and position of anterior ethmoidal artery. *J Craniofac Surg* 2017;28:265-9.
7. Gera R, Mozzanica F, Karligkiotis A, Preti A, Bandi F, Gallo S, Schindler A, Bulgheroni C, Ottaviani F, Castelnuovo P. Lateral lamella of the cribriform plate, a keystone landmark: proposal for a novel classification system. *Rhinology* 2018;56:65-72.
8. Özeren Keşkek C, Aytuğar E. Radiological evaluation of olfactory fossa with cone-beam computed tomography. *J Oral Maxillofac Res* 2021;12:e3.
9. Fadda GL, Petrelli A, Martino F, Succo G, Castelnuovo P, Bignami M, Cavallo G. Anatomic variations of ethmoid roof and risk of skull base injury in endoscopic sinus surgery: statistical correlations. *Am J Rhinol Allergy* 2021;35:871-8.
10. Preti A, Mozzanica F, Gera R, Gallo S, Zocchi J, Bandi F, Guidugli G, Ambrogi F, Yakirevitch A, Schindler A, Dragonetti A, Castelnuovo P, Ottaviani F. Horizontal lateral lamella as a risk factor for iatrogenic cerebrospinal fluid leak. *Clinical retrospective evaluation of 24 cases. Rhinology* 2018;56:358-63.
11. Barroso MS, Araujo BC, Jacinto J, Marques C, Gama I, Barros E. Association between the insertion type of uncinat process and the development of frontal sinus mucocoeles - is there a relationship? *Acta Otorrinolaringol Esp (Engl Ed)* 2021;72:246-51.
12. Ozcan KM, Hizli O, Ulusoy H, Coskun ZU, Yildirim G. Localization of orbit in patients with maxillary sinus hypoplasia: a radiological study. *Surg Radiol Anat* 2018;40:1099-104.
13. Ozcan KM, Hizli O, Sarisoy ZA, Ulusoy H, Yildirim G. Coexistence of frontal sinus hypoplasia with maxillary sinus hypoplasia: a radiological study. *Eur Arch Otorhinolaryngol* 2018;275:931-5.

#### ORCID ID:

Ö. Hızlı 0000-0001-6822-2679;  
S. Kayabaşı 0000-0002-5292-5940;  
D. Özkan 0000-0002-4882-2922

deomed®

#### Correspondence to: Ömer Hızlı, MD

Department of Otolaryngology, Faculty of Medicine,  
Balıkesir University, Balıkesir, Türkiye  
Phone: +90 505 519 59 71  
e-mail: hizliomer@gmail.com

*Conflict of interest statement:* No conflicts declared.

This is an open access article distributed under the terms of the Creative Commons Attribution-NonCommercial-NoDerivs 4.0 Unported (CC BY-NC-ND4.0) Licence (<http://creativecommons.org/licenses/by-nc-nd/4.0/>) which permits unrestricted noncommercial use, distribution, and reproduction in any medium, provided the original work is properly cited. *How to cite this article:* Hızlı Ö, Kayabaşı S, Özkan D. Effects of the position of uncinat process on olfactory fossa depth and lateral lamella length. *Anatomy* 2022;16(2):88-92.

# A review of the anatomy of soft tissues associated with sexually dimorphic landmarks on the cranium

Jade S. De La Paz , Hallie R. Buckley , Siân E. Halcrow , Stephanie J. Woodley 

*Department of Anatomy, School of Biomedical Sciences, University of Otago, Dunedin, New Zealand*

## Abstract

**Objectives:** This review systematically assesses literature relating to five muscles and one ligament connected to sexually dimorphic cranial landmarks – the nuchal crest and mastoid process – used for sex estimation in anthropology: the upper trapezius, semispinalis capitis, sternocleidomastoid, splenius capitis, and longissimus capitis muscles and the nuchal ligament. Although these soft tissues are not commonly grouped together in anatomical literature, they are anthropologically relevant in relation to cranial sex estimation. This review demonstrates how anatomical analyses can inform anthropological research and illustrates the benefit of multidisciplinary studies.

**Methods:** A systematic literature review was conducted following PRISMA (preferred reporting items for systematic reviews and meta-analyses) guidelines and included journal articles and texts that discussed attachment sites, muscle architecture, function, and sexual dimorphism of the soft tissues in of interest.

**Results:** A total of 804 publications were assessed with a final number of 64 relevant texts, including 53 primary scientific articles and 11 textbooks. Upper trapezius and sternocleidomastoid were the most widely studied, while longissimus capitis and the nuchal ligament were the least. Additionally, there was limited consistent data on muscle architecture, attachment site morphology (entheses), sexual dimorphism, and population variation in these studies.

**Conclusion:** This paper highlights the need for more detailed architectural and entheses data from diverse sex and population groups, and interdisciplinary research that will improve understanding of sexual dimorphism in humans. This can be applicable in clinical anatomy when assessing injury rates between males and females, and in anthropology, when estimating sex from the skeleton.

**Keywords:** anthropology; mastoid process; muscle architecture; nuchal crest; sexual dimorphism

Anatomy 2022;16(2):93–107 ©2022 Turkish Society of Anatomy and Clinical Anatomy (TSACA)

## Introduction

In biological anthropology, biological sex is often estimated from the skeleton using the pelvis;<sup>[1–3]</sup> however, in its absence, robusticity of certain skeletal landmarks on the cranium may be used to estimate sex in forensic and archaeological situations.<sup>[1,4]</sup> Humans show sexual dimorphism (morphological differences between males and females) in these areas, with males typically demonstrating greater robusticity compared with females. Two of these cranial landmarks – the nuchal crest and mastoid process – are sites of muscle attachment. Although anthropological analyses consider each of these landmarks as a single, generalized muscle or ligament attach-

ment site, these skeletal features actually represent the location of several soft tissue attachments.<sup>[5]</sup> In the anthropological literature, it is assumed that the robusticity of these skeletal landmarks is associated with the robusticity of the muscles attached at these sites.<sup>[1]</sup> However, this hypothesis has not been specifically tested and assumes anatomical knowledge of these attachment sites, which are not well understood in the anthropological literature.<sup>[1,4]</sup> To better identify why these cranial skeletal landmarks are sexually dimorphic, it is essential to study the nuances of the attached soft tissue anatomy, including any presence of sex differences in these areas. This is important because observation of sexual dimorphism in the associated soft tissues may help improve sex

estimation methods using these landmarks, when working with unidentified human skeletal remains.

Collectively, five muscles and one ligament span the cervical spine and have attachments associated with the nuchal crest and mastoid process. These include the upper trapezius and semispinalis capitis muscles and the nuchal ligament – associated with the nuchal crest – and sternocleidomastoid, splenius capitis, and longissimus capitis – associated with the mastoid process.

The overall objective of this review was to systematically evaluate research on the morphology of the relevant soft tissues to better understand musculoskeletal relationships and how this may relate to anthropological research in sex estimation. To achieve this, the literature covering muscle and ligament morphology, including attachment sites, size (physiological cross-sectional area [PCSA], cross sectional area [CSA], and mass or volume), and pennation angle was examined. Muscle and ligament function were also considered, alongside any findings that indicated evidence of sexual dimorphism.

**Materials and Methods**

A systematic search of the primary literature was conducted in December 2020 and updated June and November 2021, following the PRISMA (preferred reporting items for systematic reviews and meta-analyses) guidelines and using the keywords summarized in **Figure 1**.<sup>[6]</sup> Although neurovascular supply has been included in similar reviews of soft tissue,<sup>[7]</sup> this study focused on muscle and ligament morphology and function, which is most relevant to its overall aim. Studies that did not appear in the database search, but were found during general research (forwards search) or through screening the reference lists (backwards search), were also included (**Figure 2**). During this general search, five books and/or book chapters with information relevant to this study were also found and included. An additional six text books (three modern, three historical) that provided relevant information on this topic were also selected for a total of 11 books. Exclusion criteria are outlined in **Figure 2**. All literature was screened by the first author.

**Results**

A total of 65 publications, consisting of 54 primary scientific articles and 11 books or book chapters were included. A review of each muscle, grouped by the two skeletal landmarks of interest (nuchal crest and mastoid process), is presented below.

**Nuchal Crest**

The soft tissues associated with the nuchal crest are the upper trapezius and semispinalis capitis muscles, and the nuchal ligament. Trapezius is the most superficial, with semispinalis capitis lying deep to the trapezius and splenius muscles.<sup>[8]</sup> From its proximal to distal extent, the nuchal ligament runs superficial to deep, extending along the midline of the posterior neck. It is an attachment site for the upper trapezius, among other muscles.<sup>[9–11]</sup>

Nine studies (five dissection, four imaging) contained information relating to upper trapezius, and nine (four dissection, six imaging) were also reviewed for semispinalis capitis. Although the nuchal ligament was described in a number of resources, only one provided quantitative data.

**Upper trapezius:** The trapezius is a large, flat, triangle shaped muscle in the cervical, thoracic, and shoulder regions<sup>[8,12,13]</sup> and is described as the most superficial muscle of the posterior neck.<sup>[14–16]</sup> The area of interest in this study is the upper trapezius,<sup>[10]</sup> also termed the clavotrapezius<sup>[17]</sup> or the pars descendens or descending part.<sup>[18,19]</sup> The upper trapezius is smaller than the middle trapezius, being one-fifth of its mass.<sup>[20]</sup>

**Attachment sites:** The upper trapezius muscle attaches proximally at the superior nuchal line and the ligamentum nuchae, wrapping around the neck to attach distally at the lateral third of the clavicle.<sup>[8,10,13,16,17,21,22]</sup> Proximal attach-

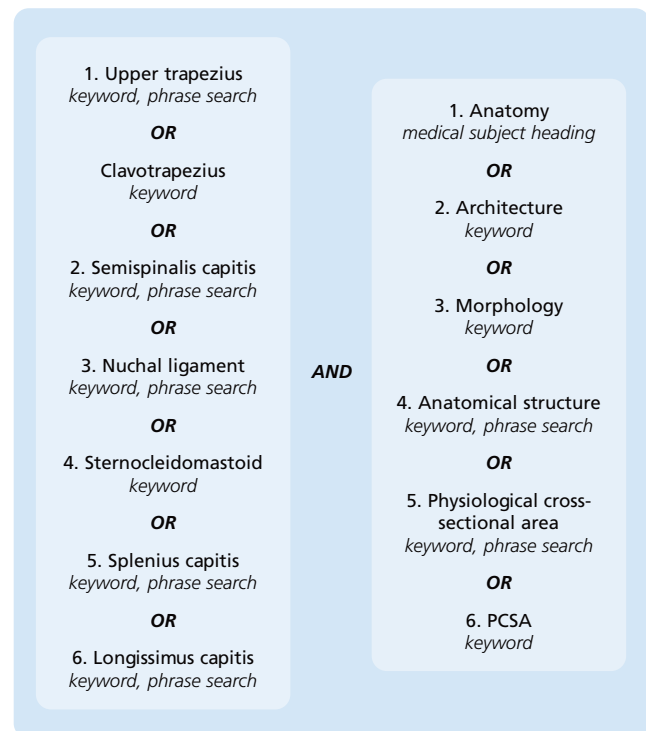


**Figure 1.** Search terms and keywords.

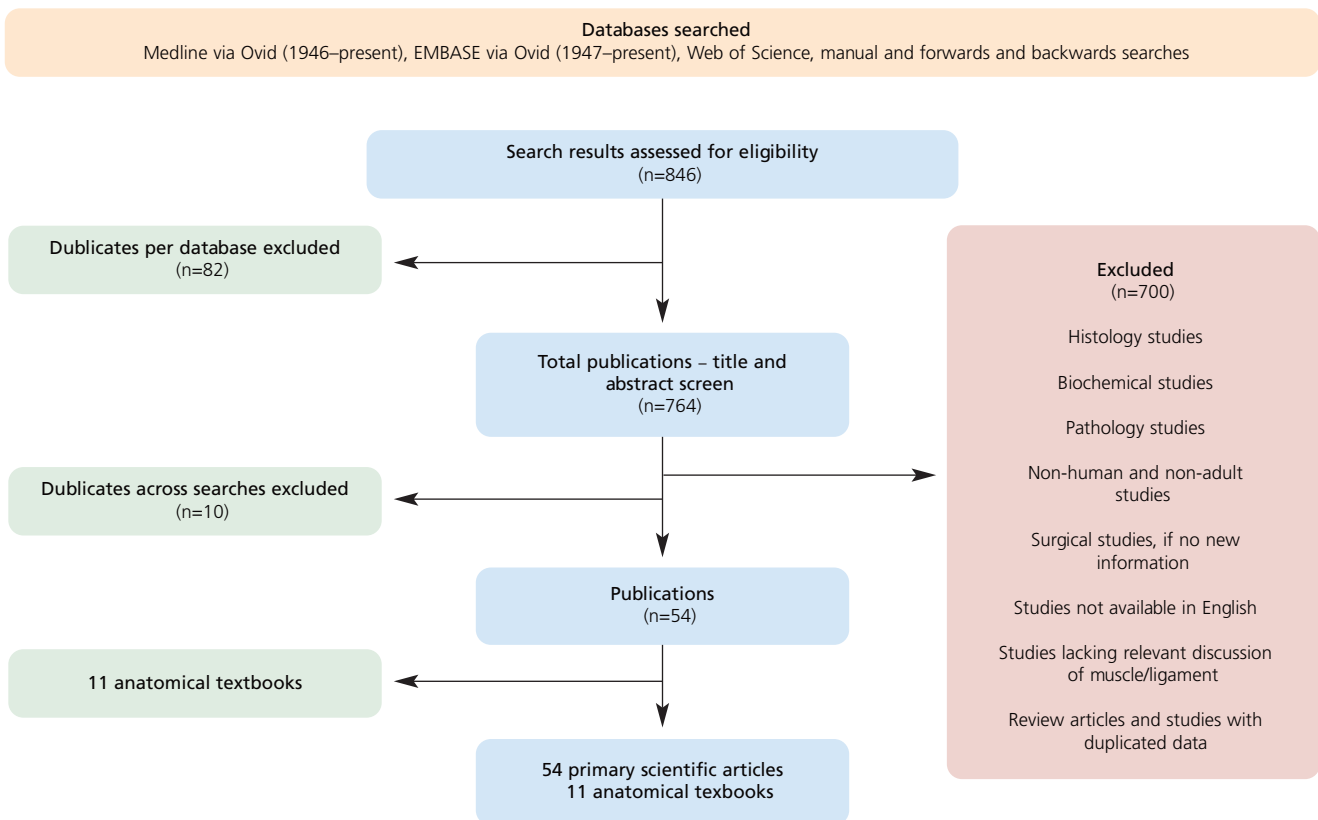


**Figure 2.** PRISMA flow chart of the review process.

ment sites may vary although they are generally within the upper cervical/occipital area of the neck and head region: occiput and C1–C5,<sup>[18]</sup> C2–C3,<sup>[19]</sup> posterior border of the nuchal ligament,<sup>[23]</sup> occipital and nuchal ligament as far as the level of C7,<sup>[11]</sup> medial third of the superior nuchal line, external occipital protuberance, and nuchal ligament,<sup>[24]</sup> and occiput and nuchal ligament.<sup>[12,20]</sup> Additionally, the midline muscle fibers of upper trapezius attach to the nuchal ligament and pass over the midline connecting with the contralateral muscle fibers.<sup>[25]</sup> The distal attachment is described as the clavicle, specifically the superior posterior surface of its lateral third.<sup>[12,18–20,26–30]</sup> Variation may occur, with extension to the medial clavicle and occasional overlapping with the sternocleidomastoid attachment.<sup>[12,13]</sup> None of the literature reviewed discussed enthesal (muscle attachment) measurements or morphology, for either the proximal or distal attachments of the upper trapezius.

**Muscle architecture:** Architectural data from dissection, magnetic resonance imaging (MRI), and ultrasound studies for upper trapezius are presented in **Table 1**. Mean fascicle length was fairly consistent at around 8 cm, although one study, which reported data from only one individual, showed a larger value of 12 cm.<sup>[18]</sup> Pennation

angle ranged from 0–30° for all studies, although some did not provide detailed methods for how these data were collected.<sup>[19]</sup> Two other studies described the measurement as the angle at which the muscle fibers lay in relation to the line of action for the muscle.<sup>[17,18]</sup> Interestingly, these two studies report different pennation angles (0° compared to 0–30°), but as the proximal attachments of upper trapezius span the length of the neck, it is possible that there is some variation across this part of the muscle. Muscle mass was provided in all studies, except Johnson et al.,<sup>[10]</sup> which reported volume. All measurements fell within a range of approximately 18.7–37.6 g, with volume reported as 30 ml. Although different units of measurement, mass and volume are comparable, as absolute values do not vary greatly when converting between the two using standard muscle density measures.<sup>[31]</sup> The largest value of 37.6 g is likely because trapezius was split into two segments,<sup>[18]</sup> rather than the standard three.<sup>[10]</sup>

The PCSA values obtained from dissection show a range of 2.0–3.8 cm<sup>2</sup> and CSA values from imaging ranged between 3.1–36.0 cm<sup>2</sup>. In two studies, PCSA was larger (>3.5 cm<sup>2</sup>) than others, as the muscle was divided into two segments, rather than three.<sup>[18,32]</sup> Additionally, in an MRI

**Table 1**  
Muscle architecture data for upper trapezius.

Study	Sample/sex/age	Fascicle <sup>1</sup>		Muscle <sup>1</sup>			
		Length (cm)	Pennation angle (°)	Volume (ml) or mass (g)	P CSA (cm <sup>2</sup> )	CSA (cm <sup>2</sup> )	
Dissection studies	Bayoglu et al. (2017)	n=1 Male 79 years	8.9	0	25.7 (g)	2.9	-
	Borst et al. (2011) <sup>2</sup>	n=1 Male 86 years	12	0	37.6 (g)	3.5	-
	Johnson et al. (1994) <sup>3</sup>	n=8 Unknown >65 years	8–11	-	30 (ml)	3.3	-
	Kamibayashi and Richmond (1998)	n=9 <sup>4</sup> 7 M / 3 F 66–92 years	8.1 (1.6)	0–30	18.7 (4.5) (g)	2.0 (0.6)	-
	Van Ee et al. (2000)	n=6 4 M / 2 F 70–83 years	-	0–5	-	3.8 <sup>2</sup>	-
Imaging studies - MRI	Dawson et al. (2013)	n=10 Male 26–54 years	-	-	-	-	3.2 (1.0)
	De Loose et al. (2009)	n=25 Male 20–40 years	-	-	-	-	4.3 (1.4) <sup>5</sup>
	Li et al. (2014)	n=16 11 M / 5 F 23–33 years	-	-	-	-	36.0 <sup>6</sup>
Imaging studies - Ultrasound	Valera-Calero et al. (2020)	n=15 Male 22.5±4.5 years	-	-	-	-	13.1 (3.8)
		n=10 Female 25.5±6 years	-	-	-	-	7.6 (1.8)

CSA: cross-sectional area; F: female, M: male; MRI: magnetic resonance imaging; PSCA: physiological cross-sectional area. <sup>1</sup>Mean values presented where relevant (standard deviation) given where available. <sup>2</sup>Trapezius considered as two segments instead of the standard three. <sup>3</sup>Upper trapezius split into three segments; these data represent a range or total mean for each measurement (standard deviation not recalculated). <sup>4</sup>Ten cadavers were included (seven males, three females) with nine used for the analysis of trapezius; however, the representation of each sex is not clear. <sup>5</sup>Data given for right side only. Fighter pilot neck pain study. Data show control group with no neck pain. <sup>6</sup>Study gave maximum CSA of the trapezius at C6–C7.

study, Li et al.<sup>[33]</sup> reported a much larger CSA (36.0 cm<sup>2</sup>), likely due to the study reporting the maximum CSA of the muscle rather than values from a specified anatomical location, such as C4.<sup>[34]</sup>

**Function:** Trapezius is a major extensor muscle of the head and neck,<sup>[8,35]</sup> providing stability to the scapula through the clavicle.<sup>[26,27]</sup> Specifically, upper trapezius produces lateral flexion and extension of the head.<sup>[13]</sup> It also contributes to shoulder elevation and upward scapula rotation (in conjunction with lower trapezius), as well as scapula retraction.<sup>[15,16,21,22,24,30]</sup>

**Sexual dimorphism:** One study addressed sex differences, reporting that males had a significantly larger upper trapezius CSA than females.<sup>[36]</sup> The authors also noted that

larger weight, height, and body mass index were significantly correlated with larger CSA, an association that corresponded with male sex. They suggest that overall sexual dimorphism was apparent in their sample for physical size characteristics as well as muscle CSA.<sup>[36]</sup>

**Semispinalis capitis:** Semispinalis capitis, also called semispinalis complexus in historical texts,<sup>[12,21,30]</sup> is a long and thick muscle, located in the third layer of the neck,<sup>[14,15,37,38]</sup> deep to the trapezius and splenius muscles.<sup>[8,12,16]</sup> Semispinalis capitis is consistently described as a digastric muscle which is divided into two sections by internal aponeuroses,<sup>[37]</sup> or alternatively described as being interspersed with internal tendons that connect the muscle bellies.<sup>[12,17,19]</sup>

**Table 2**  
Muscle architecture data for semispinalis capitis.

Study	Sample/sex/age	Fascicle <sup>1</sup>		Muscle <sup>1</sup>			
		Length (cm)	Pennation angle (°)	Volume (cm <sup>3</sup> ) or mass (g)	PSCSA (cm <sup>2</sup> )	CSA (cm <sup>2</sup> )	
Dissection studies	Bayoglu et al. (2017)	n=1 Male 79 years	8.4	0	20.3 (g)	3.1	-
	Borst et al. (2011)	n=1 Male 86 years	10.3	0	45.3 (g)	4.3	-
	Kamibayashi and Richmond (1998)	n=9 <sup>2</sup> 7 M / 3 F 66–92 years	6.2 (1.1)	0–20	38.5 (9.4) (g)	5.4 (1.3)	-
	Van Ee et al. (2000)	n=6 4 M / 2 F 70–83 years	-	>3	-	5.5	-
Imaging studies - MRI	Elliot et al. (2014) <sup>3</sup>	n=34 Female 26.9±5.6 years	-	-	-	-	1.5 (1.4-1.6)
	Li et al. (2014)	n=16 11 M / 5 F 23–33 years	-	-	-	-	4.5 <sup>4</sup>
	Reddy et al. (2021)	n=13 Male 30.5±1.7 years	-	-	M: 60.6 (3.2) (cm <sup>3</sup> )	M: 5.5 (0.2) <sup>5</sup>	M: 9.9 (0.3) <sup>6</sup>
		n=17 Female 30.8±1.7 years	-	-	F: 38.2 (1.5) (cm <sup>3</sup> )	F: 3.7 (0.1) <sup>5</sup>	F: 6.7 (0.2) <sup>6</sup>
Uthaikhup et al. (2017) <sup>7</sup>	n=14 Female 64.2±4 years	-	-	-	-	1.9 (0.3)	
Imaging studies - Ultrasound	Rankin et al. (2005)	n=46 Male 20–72 years	-	-	-	-	M: 1.8 (0.4)
		n=53 Female 18–70 years	-	-	-	-	F: 1.3 (0.4)
	Rezasoltani et al. (1998) <sup>8</sup>	n=46 18 M / 28 F 19–34 years	-	-	-	-	M: 2.0 (0.4) F: 1.6 (0.4)

CSA: cross-sectional area; F: female, M: male; MRI: magnetic resonance imaging; PSCSA: physiological cross-sectional area. <sup>1</sup>Mean values presented where relevant (standard deviation) given where available. <sup>2</sup>Ten cadavers were included (seven males, three females) with nine used for the analysis of semispinalis capitis; however, the representation of each sex is not clear. <sup>3</sup>Study looks at whiplash-associated disorders measuring CSA at both C2–C3 and C5–C6. Data here given for healthy control group measured at the level of C5–C6. <sup>4</sup>Study gave maximum CSA of the semispinalis capitis at C1–C2, which may account for the large number. <sup>5</sup>Study estimated PSCSA by dividing reconstructed muscle length by muscle volume and reporting RCSA (reconstruction-based cross-sectional area) as the equivalent of PSCSA. <sup>6</sup>Study reported ACSA (anatomical cross-sectional area), which was the maximum CSA of each muscle and may account for the large numbers. <sup>7</sup>Cervicogenic headache study of older female sample. Data show control group with no neck pain. <sup>8</sup>Study compares right and left side for males and females in sitting and prone positions. Data here given for right side in prone position.

**Attachment sites:** Semispinalis capitis attaches distally at the transverse processes of the lower cervical and upper thoracic vertebrae and proximally at the mid-occipital region.<sup>[12,13,16,20,21,30]</sup> The proximal attachment is described consistently in most studies with some variation: at the mid-occipital level inferior to the superior nuchal line,<sup>[20]</sup> between the superior and inferior nuchal lines,<sup>[37]</sup> or at the linea nuchae.<sup>[18]</sup> There is some variability in the exact ver-

tebrae included as the distal attachment sites: C3–T4,<sup>[18]</sup> C4–T6,<sup>[19]</sup> and C3–T6,<sup>[37]</sup> although this is likely related to standard anatomical variation. Despite details about the proximal and distal attachments of this muscle, none of the included studies discussed enthesal morphology.

**Muscle architecture:** Table 2 summarizes the data relating to muscle architecture. The mean fascicle length

of semispinalis capitis ranged from 6.2–10.3 cm. As described above, the individual from Borst et al.<sup>[18]</sup> had larger values, yet it is unclear why this individual is an outlier. Pennation angle ranged from 0–20°, which reflects the morphology of this muscle attaching distally to a number of transverse processes in the cervical and thoracic regions of the spine. With respect to muscle size, mass was reported in three studies, ranging between 20.3–45.3 g. In two of these, data were collected from one individual<sup>[18,19]</sup> and fell nearly within the reported values from the third study (mean: 38.5, range: 21.3–55.8 g), which included 10 specimens.<sup>[17]</sup> Volume was reported in one imaging study,<sup>[39]</sup> with a mean value of 60.6 cm<sup>3</sup> for males and 38.2 cm<sup>3</sup> for females. PCSA ranged between 3.1–5.5 cm<sup>2</sup> and CSA was 1.3–9.9 cm<sup>2</sup>, although the larger values for CSA were based on maximum CSAs.<sup>[33,39]</sup> Similar to upper trapezius a limited number of studies provided architectural data for semispinalis capitis. Additionally, there were differences in which architectural parameters were examined. For example, an ultrasound study reported the mean lateral dimension (3.73 cm for males and 3.27 for females) and muscle thickness (0.53 cm for males and 0.48 cm for females).<sup>[14]</sup> Further, a computed tomography (CT) study<sup>[15]</sup> provided measurements for thickness and depth, describing semispinalis capitis as a thin layer of muscle with a mean thickness of 1 cm for males and 0.8 cm for females. The depth measurements were taken from both the inner and outer muscle border to the skin giving mean depth measurements of 3.3 cm (inner) and 2.4 cm (outer) for males and 2.9 cm (inner) and 2.1 cm (outer) for females.<sup>[15]</sup>

**Function:** Acting bilaterally, semispinalis capitis is a major extensor of the head and neck while also stabilizing the head,<sup>[13,16,21,22,35,40,41]</sup> although Rankin et al.<sup>[14]</sup> state that there are varying opinions on whether or not the muscle is active at rest. Acting unilaterally, it extends the head ipsilaterally.<sup>[21]</sup> Despite multiple studies mentioning the presence of interspersed tendons within semispinalis capitis,<sup>[17,19,37]</sup> their function is not discussed in the literature.

**Sexual dimorphism:** Significant differences were found between males and females in three studies.<sup>[14,15,39]</sup> These studies found sex differences when analysing various muscle architecture parameters, including overall size and strength, muscle CSA, lateral dimension, and thickness of the semispinalis capitis. In general, they found that muscles were larger in males than females.

**Nuchal ligament:** The nuchal ligament, or ligamentum nuchae, described as a triangular fibrous septum positioned along the midsagittal plane of the neck, serves as an attachment site for surrounding posterior cervical muscles.<sup>[9–12,21–23]</sup> These include the upper trapezius where, as previously described, the right and left aponeuroses inter-

digitate across the nuchal ligament.<sup>[16,23,25,42,43]</sup> Johnson et al.,<sup>[42]</sup> in a detailed dissection study describe that the posterior portion of the ligament is formed by the bilateral aponeuroses of trapezius, splenius capitis, rhomboid minor, and serratus posterior superior, with the anterior portion composed of thin connective tissue. They also state that the ligament is fragile and difficult to dissect, as it cannot be clearly differentiated from the surrounding muscles and tendons.

**Attachment sites:** The ligamentum nuchae attaches to the external occipital protuberance<sup>[30]</sup> and the posterior spinal dura mater at C1 and C2.<sup>[9]</sup> With respect to variation, three publications state that the ligament attaches to the C2–C6 spinous processes,<sup>[11,42,44]</sup> while one reports that it does not.<sup>[9]</sup> Most studies agree that, generally, the nuchal ligament attaches proximally at the occiput, specifically the external occipital protuberance, and distally at C7.<sup>[12,13,21,23,25,42,43,45,46]</sup> Some studies provide additional descriptions that suggest that the anterior portion of the ligament attaches at the foramen magnum<sup>[23,46]</sup> or the posterior tubercle of the atlas.<sup>[42]</sup>

Both dissection and imaging studies report a connection between the nuchal ligament and cervical dura mater in the occipital region,<sup>[9,45,47]</sup> however, this connection was not observed by Nash et al.<sup>[48]</sup> in plastinated cadaveric sections. Additionally, Mitchell et al.<sup>[45]</sup> found that the proximal attachment site can extend bilaterally along the occiput as far as the temporal bone, suggesting a complex morphology, possibly similar to the “fan-like” portions described in Allia and Gorniak.<sup>[25]</sup>

**Ligament architecture:** The architecture of the nuchal ligament is described differently in various literature having two to four parts. Allia and Gorniak<sup>[25]</sup> define four parts: a cord-like portion, running from the occiput to the C7 spinous process in the midline; a septum that connects this cord anteriorly to the spinous processes; a large “fan-like” portion attaching to the occiput; an additional small “fan-like” portion, inferior to the large one, also attaching to the occiput. Fielding et al.<sup>[23]</sup> similarly describe it as triangular shaped, attaching anteriorly to the cervical spinous processes, and composed of two portions: lamellar (anterior) and funicular (posterior), similar to the descriptions of Kadri and Al-Mefty<sup>[43]</sup> and Takeshita et al.<sup>[46]</sup> Kadri and Al-Mefty<sup>[43]</sup> further describe the lamellar portion as superficial at the level of C6 and C7, but deep at the level of C1. The lamellar and funicular portions are described in Standing<sup>[13]</sup> as the median septal and dorsal raphe portions, respectively.

One study identified part of the nuchal ligament as a separate entity, which they referred to as the “to be named

ligament".<sup>[49]</sup> They defined it as a band of fibrous tissue arising from the nuchal ligament and extending anteriorly at C1 and C2. However, the description of this fibrous band is consistent with definitions of the lamellar portion in four other studies and is likely referring to this segment of the ligament.<sup>[23,25,46,48]</sup>

No data were found that discuss the standard length, width, thickness, mass, volume, or CSA of the nuchal ligament. A dissection study of 30 individuals is the only publication that provides some measurements, which are related to the width (several mm to 1.5 cm) and length (0.03–1.0 cm) of the occipital attachment.<sup>[9]</sup> These data are more appropriately associated with the enthesis rather than the architecture of the ligament itself.

**Function:** The nuchal ligament comprises strong, elastic connective tissue<sup>[12,25,43]</sup> that contributes to stabilizing the head and neck during movement, particularly rotation and flexion.<sup>[45,46]</sup> The elastic fibers provide flexibility, allowing the ligament to stretch and return to its normal length.<sup>[16]</sup> Johnson et al.<sup>[42]</sup> suggest the architecture of the nuchal ligament indicates that it directs forces from the associated muscles to the lower cervical spine to prevent unnecessary loading on the upper neck.

**Sexual dimorphism:** No sex differences of the nuchal ligament were discussed in any of the publications reviewed.

### Mastoid Process

Three muscles that attach to the mastoid process have been included in this review: sternocleidomastoid, splenius capitis, and longissimus capitis. These muscles lie from superficial (sternocleidomastoid<sup>[8]</sup>) to deep (longissimus capitis<sup>[8,14]</sup>) in the neck.<sup>[14,15,37]</sup> Fifteen publications (six dissection, nine imaging) provide architectural data for sternocleidomastoid, alongside an additional 13 publications specifically related to observations of anatomical variation. For splenius capitis, multiple studies discussed this muscle, with architectural data available in four dissection and five imaging studies. Less research has focused on longissimus capitis, with architectural data reported in five (four dissection, one imaging) studies.

**Sternocleidomastoid:** Sternocleidomastoid is a long, flat, oblique, superficial muscle enclosed in deep fascia.<sup>[8,13,21]</sup> It has a thick centre and broad ends<sup>[12,13,21]</sup> and can generally be divided into four segments, variable in size,<sup>[50]</sup> based on attachment sites: sternomastoid, sternooccipital, cleidooccipital, and cleidomastoid.<sup>[17,38,50]</sup> Kamibayashi and Richmond<sup>[17]</sup> describe the first three of these segments as superficial and parallel to one another, while the fourth lies deeper at a different orientation. The sternocleidomastoid

separates the neck into the anterior and posterior triangles, and is covered by platysma<sup>[12,21,22,24]</sup> and the superficial layer of deep cervical fascia.<sup>[51]</sup> Anatomical variation is common in this muscle<sup>[12,21,52,53]</sup> and is described below.

**Attachment sites:** Sternocleidomastoid attaches distally to the sternum (manubrium) and clavicle, and proximally to the mastoid process and superior nuchal line.<sup>[8,13,16–19,22,24,29,30,38,50,51,54]</sup> It separates inferiorly at its distal attachment and has a thick proximal attachment.<sup>[51]</sup> Houseman et al.<sup>[8]</sup> and Rea<sup>[24]</sup> give more detail to this description with distal attachments at the anterior surface of the manubrium and superior medial third of the clavicle and proximal attachments at the outer mastoid process and lateral superior nuchal line. The clavicular attachment is detailed in Phadnis and Bain<sup>[29]</sup> as arising from the medial curve of the posterior surface, opposite to the pectoralis major clavicular head and lateral to the sternohyoid clavicular attachment. Taken together, these studies largely agree that the sternocleidomastoid attaches distally to the medial half of the clavicle and anterior manubrium and proximally to the mastoid process and lateral superior nuchal line.

Some publications provide enthesis information for sternocleidomastoid. The manubrium attachment is round and tendinous and the clavicular attachment as flat, wide, and variable in size,<sup>[13,16]</sup> while the proximal attachment is described as thick.<sup>[51]</sup> Lee et al.<sup>[54]</sup> report data for the manubrial attachment with an enthesis area of 8.3 (range: 6.8–9.9) cm<sup>2</sup>. No data are available for the clavicular or cranial entheses.

**Muscle architecture:** Muscle architecture data are presented in **Table 3**. Fascicle length ranged between 11–14.1 cm, with the males from the study by Kennedy et al.<sup>[50]</sup> exhibiting the highest mean values. The range for pennation angle from these studies was 0–20° and is consistent with the variable angles seen across the four different sections of this muscle. Of the five studies that provided values for mass/volume, data from three were obtained from dissection, one from both dissection and imaging (MRI), and one from imaging (MRI). Mass obtained from cadaveric specimens had a small range (38.8–40.4 g), showing consistency across these studies.<sup>[17–19]</sup> Volume from dissection, however, was smaller at 24.8 cm<sup>3</sup> for males and 15.2 cm<sup>3</sup> for females.<sup>[50]</sup> Compared with dissection, the volume obtained via imaging was larger,<sup>[39,50]</sup> although the volume for females from Kennedy et al.<sup>[50]</sup> fell within range of the reported masses from the above dissection studies.

The PCSA ranged between 1.3–4.9 cm<sup>2</sup> across all dissection studies, with the reported mean PCSA from an

**Table 3**  
Muscle architecture data for sternocleidomastoid.

Study	Sample/sex/age	Fascicle <sup>1</sup>		Muscle <sup>1</sup>			
		Length (cm)	Pennation angle (°)	Volume (cm <sup>3</sup> ) or mass (g)	PCSA (cm <sup>2</sup> )	CSA (cm <sup>2</sup> )	
Dissection studies	Bayoglu et al. (2017)	n=1 Male 79 years	11	0	38.8 (g)	3.8	-
	Borst et al. (2011) <sup>2</sup>	n=1 Male 86 years	13.9	0	39.2 (g)	2.9	-
	Kamibayashi and Richmond (1998)	n=9 <sup>2</sup> 7 M / 3 F 66–92 years	11.8 (0.9)	0–20	40.4 (9.0) (g)	3.7 (0.9)	-
	Van Ee et al. (2000)	n=6 4 M / 2 F 70–83 years	-	>3	-	4.9	-
Dissection and imaging (MRI) study	<i>Dissection</i> Kennedy et al. (2017)	n=6 3 M / 3 F 63–93 years	M: 14.1 (0.8) F: 12.3 (1.6)	-	24.8 (3.9) (cm <sup>3</sup> ) 15.2 (4.8) (cm <sup>3</sup> )	1.8 (0.3) 1.3 (0.3)	-
	<i>Imaging</i>		-	-	M: 72 (8.0) (cm <sup>3</sup> ) F: 39.4 (12) (cm <sup>3</sup> )	-	-
Imaging studies – MRI	Dawson et al. (2013)	n=10 10 M 26–54 years	-	-	-	-	5.3 (0.8)
	De Loose et al. (2009) <sup>3</sup>	n=25 25 M 20–40 years	-	-	-	-	6.3 (1.1)
	Elliot et al. (2014) <sup>4</sup>	n=34 Female 26.9 (5.6) years	-	-	-	-	2.3 (2.2–2.4)
	Li et al. (2014)	n=16 11 M / 5 F 23–33 years	-	-	-	-	5.0
	Reddy et al. (2021)	n=13 Male 30.5 (1.7) years	-	-	M: 107.9 (6.4) (cm <sup>3</sup> )	5.6 (0.3) <sup>5</sup>	9.9 (0.6) <sup>6</sup>
		n=17 Female 30.8 (1.7) years	-	-	F: 72.7 (3.5) (cm <sup>3</sup> )	4.1 (0.2) <sup>5</sup>	7.1 (0.4) <sup>6</sup>
	Uthaikhup et al. (2017) <sup>7</sup>	n=14 Female 64.2 (4) years	-	-	-	-	10.1 (0.7)
Imaging studies - Ultrasound	Alsalaheen et al. (2019)	n=34 20 M / 14 F 18–30 years	-	-	-	M: 4.1 (0.8) F: 2.8 (0.5)	-
	Botticchio et al. (2021)	n=17 12 M / 5 F 22.2 (1.9) years	-	-	-	-	3.9 (0.6)
	Kim et al. (2021)	n=18 11 M / 7 F 79.2 (10.7) years	-	-	-	-	1.4 (0.6) <sup>8</sup>

CSA: cross-sectional area; F: female; M: male; MRI: magnetic resonance imaging; PCSA: physiological cross-sectional area. <sup>1</sup>Mean values presented where relevant (standard deviation) given where available. <sup>2</sup>Ten cadavers were included (seven males, three females) with nine used for the analysis of sternocleidomastoid; however, the representation of each sex is not clear. <sup>3</sup>Data given for right side only. Fighter pilot neck pain study. Data here show control group with no neck pain. <sup>4</sup>Study looks at whiplash associated disorders measuring CSA at both C2–C3 and C5–C6. Data here given for healthy control group measured at the level of C5–C6. <sup>5</sup>Study estimated PCSA by dividing reconstructed muscle length by muscle volume and reporting reconstruction-based cross-sectional area (RCSA) as equivalent of PCSA. <sup>6</sup>Study reported anatomical cross-sectional area (ACSA), which was the maximum CSA of each muscle and may account for the large numbers. <sup>7</sup>Cervicogenic headache study of older female sample. Data show control group with no neck pain. <sup>8</sup>Ultrasound measurements taken on cadaveric material at upper, middle, and lower sections of the muscle. The CSA reported here is for the middle measurement.

ultrasound study<sup>[55]</sup> also falling within this range. Estimated PCSA from another imaging (MRI) study<sup>[39]</sup> showed larger values for males (5.6 cm<sup>2</sup>), with only females falling in the range of the other studies (4.1 cm<sup>2</sup>). As seen above, the Kennedy et al.<sup>[50]</sup> study had the lowest values, but it is unclear why, as the age ranges are similar for all publications. Additionally, a large range is evident for CSA obtained via imaging (1.4 cm<sup>2</sup> to 10.1 cm<sup>2</sup>), which is higher than the dissection data, although with some overlap.

**Function:** Sternocleidomastoid, when contracting bilaterally is primarily a cervical flexor,<sup>[41]</sup> producing flexion of the lower cervical spine, and concomitant extension of the upper cervical levels.<sup>[12,13,16,21,22]</sup> It contributes to other movements such as contralateral rotation and lateral bending,<sup>[20,21,51]</sup> with unilateral activation resulting in ipsilateral lateral flexion coupled with contralateral rotation.<sup>[24]</sup> Both sides also work together to elevate the clavicle and sternum during inspiration,<sup>[13,16]</sup> and the sternal head supports the sternoclavicular joint anteriorly.<sup>[30]</sup>

**Anatomical variation:** Anatomical variation has been regularly observed with case reports published on single cases,<sup>[56–66]</sup> although a few studies have looked at variation in multiple subjects.<sup>[52,53]</sup> Most of the case studies report bilateral supernumerary heads of the sternocleidomastoid,<sup>[58,61–64,66]</sup> while some observed additional heads on either the left<sup>[56,57,59,60]</sup> or right<sup>[65]</sup> side.

In these studies, populations represented included American-European,<sup>[58]</sup> Brazilian,<sup>[56]</sup> European,<sup>[64]</sup> Greek,<sup>[62]</sup> Indian,<sup>[52,57,65]</sup> Korean,<sup>[60,61,63]</sup> Spanish<sup>[53]</sup> and Turkish.<sup>[59,66]</sup> Additionally, males are over-represented in case studies on single individuals,<sup>[56–62,65,66]</sup> with only two studies discussing females.<sup>[63,64]</sup> This may suggest that females are not commonly studied, or that males exhibit variation in this muscle more regularly than females. Two cadaveric studies<sup>[52,53]</sup> that examined multiple individuals from both sexes reported variation only in males, in five<sup>[52]</sup> and three<sup>[53]</sup> of 18 cadavers, in each study.

**Sexual dimorphism:** Kennedy et al.<sup>[50]</sup> reported significantly larger sternocleidomastoid volume in males compared with females, from both dissection and MRI data. Similarly, Alsalaheen et al.<sup>[55]</sup> found significant differences in a number of architectural parameters, including PCSA, with larger values in males. Additionally, Reddy et al.<sup>[39]</sup> reported that males had significantly larger and stronger neck muscles than females, including sternocleidomastoid.

**Splenius capitis:** Splenius capitis is in the second layer of the posterior neck<sup>[14,15,37]</sup> deep to trapezius and sternocleidomastoid,<sup>[8,13,16]</sup> although the fibers do not cross the

midline like the trapezius.<sup>[25]</sup> Splenius capitis and cervicis form a layer over semispinalis capitis, and in cross-section splenius capitis can be seen as a distinct layer between trapezius and semispinalis capitis.<sup>[38]</sup> It should be noted that some authors consider splenius capitis and cervicis as a single muscle due to their continuity<sup>[17,67]</sup> and Vasavada et al.<sup>[20]</sup> reported that splenius cervicis is contiguous distally from splenius capitis and may, therefore, not be distinguishable at times. All other studies analyzed these two muscles separately.

**Attachment sites:** Splenius capitis attaches proximally to the mastoid process, lateral third of the superior nuchal line, and occiput and distally to the inferior half of the ligamentum nuchae and adjacent spinous processes.<sup>[8,11–13,16–18,21,22,25,30,38,67]</sup> Some variation exists mainly with respect to the distal attachment. However, most studies agree that splenius capitis attaches distally at the nuchal ligament (C3 to C7) and spinous processes, from C7 to T4.<sup>[8,11,17–20,25,38]</sup> No data were provided for either proximal or distal attachment site morphology for this muscle, such as the size of the tendinous enthesis.

**Muscle architecture:** Muscle architecture data are shown in **Table 4**. Mean fascicle length ranges between 8–10.5 cm, with the individual from Borst et al.<sup>[18]</sup> again exhibiting the largest values. However, the range for fascicle length reported by Kamibayashi and Richmond<sup>[17]</sup> does encompass the entirety of the reported values (7–10.7 cm). Pennation angle was consistent throughout studies with a range of 0–5°.

For mass, three dissection studies provided data, two of which included one individual, and one of which dissected splenius capitis and splenius cervicis together.<sup>[17–19]</sup> The combination of these muscles is reflected in the larger value for mass (42.9 g) from Kamibayashi and Richmond<sup>[17]</sup> compared with the other studies (14.6–27.1 g). Additionally, three dissection studies provided PCSA for splenius capitis with a range of 2.0–3.1 cm<sup>2</sup>,<sup>[18,19,32]</sup> with the outlier value of 4.3 cm<sup>2</sup> for both splenius capitis and cervicis.<sup>[17]</sup> Values for CSA from imaging (1.5–3.8 cm<sup>2</sup>) were consistent with PCSA obtained from dissection, although the large value from Li et al.<sup>[33]</sup> may be related to them reporting a maximum CSA.

In addition to the data presented in **Table 4**, Mayoux-Benhamou et al.<sup>[15]</sup> provided CT data for thickness and depth. They describe splenius capitis as a very thin muscle, with a mean thickness of 0.7 cm in males and 0.5 cm in females. The mean depth from the inner muscle border to skin was 1.9 cm for males and 1.7 cm for females, while the outer muscle border to skin depth was reported as a 1.3 cm for males and 1.2 cm for females.

**Table 4**  
Muscle architecture data for splenius capitis.

Study	Sample/sex/age	Fascicle <sup>1</sup>		Muscle <sup>1</sup>			
		Length (cm)	Pennation angle (°)	Mass (g)	PCSA (cm <sup>2</sup> )	CSA (cm <sup>2</sup> )	
Dissection studies	Bayoglu et al. (2017)	n=1 Male 79 years	8.0	0	14.6	2.0	-
	Borst et al. (2011)	n=1 Male 86 years	10.5	0	27.1	2.5	-
	Kamibayashi and Richmond (1998)	n=9 <sup>2</sup> 7 M / 3 F 66–92 years	8.6 (1.1)	0–5	42.9 (13.8) <sup>3</sup>	4.3 (1.0) <sup>3</sup>	-
	Van Ee et al. (2000)	n=6 4 M / 2 F 70–83 years	-	>3	-	3.1	-
Imaging studies - MRI	Dawson et al. (2013)	n=10 Male 26–54 years	-	-	-	-	2.5 (0.3)
	De Loose et al. (2009) <sup>4</sup>	n=25 Male 20–40 years	-	-	-	-	2.9 (0.7)
	Elliot et al. (2014) <sup>5</sup>	n=34 Female 26.9±5.6 years	-	-	-	-	1.9 (1.8–2)
	Li et al. (2014)	n=16 11 M / 5 F 23–33 years	-	-	-	-	3.8 <sup>6</sup>
	Uthaikhup et al. (2017) <sup>7</sup>	n=14 Female 64.2±4 years	-	-	-	-	1.5 (2.1)

CSA: cross-sectional area; F: female, M: male; MRI: magnetic resonance imaging; PCSA: physiological cross-sectional area. <sup>1</sup>Mean values presented where relevant (standard deviation) given where available. <sup>2</sup>Ten cadavers were included (seven males, three females) with nine used for the analysis of splenius capitis; however, the representation of each sex is not clear. <sup>3</sup>This study considered splenius capitis and cervicis together, hence the larger mass and PCSA values. <sup>4</sup>Data given for right side only. Fighter pilot neck pain study. Data here show control group with no neck pain. <sup>5</sup>Study examines whiplash associated disorders measuring CSA at both C2–C3 and C5–C6. Data here given for healthy control group measured at the level of C5–C6. <sup>6</sup>Study provided maximum CSA of splenius capitis at C2–C3 and C6–C7, which may account for the large number. <sup>7</sup>Cervicogenic headache study of older female sample. Data are for the control group with no neck pain.

**Function:** Splenius capitis acts as a cervical extensor when activated bilaterally<sup>[12,13,21,22,41,67]</sup> and produces ipsilateral axial rotation and lateral flexion of the head.<sup>[12,13,16,20–22,67]</sup> Additionally, it reinforces the nuchal ligament and provides stability to the upright head and neck.<sup>[12,25]</sup>

**Sexual dimorphism:** A CT study by Mayoux-Benhamou et al.<sup>[15]</sup> found that mean muscle thickness and depth were significantly larger ( $p < 0.05$ ) in males than females. Keidan et al.<sup>[67]</sup> found significant sex differences in splenius capitis and cervicis attachment sites in 35 cadavers (19 females, 16 males), with muscles covering more of the posterior neck in males than females.

**Longissimus capitis:** The longissimus capitis, also called trachelo-mastoideus in historical texts,<sup>[12,13,21,30]</sup> is a

long, thin muscle located in the third layer of the neck.<sup>[8,13,14,16]</sup> Longissimus is made up of three muscles – capitis, cervicis, thoracis – which extend from the mastoid process of the cranium to the lumbar vertebrae and form part of the erector spinae group.<sup>[13,20]</sup> Longissimus capitis is a continuation of longissimus cervicis.<sup>[17]</sup> Kamibayashi and Richmond<sup>[17]</sup> also describe it as a fleshy muscle that is difficult to dissect, due to its close adherence to the bone in several places. This is further complicated by the presence of intermediate tendons.<sup>[12,19]</sup>

**Attachment sites:** Longissimus capitis attaches proximally to the posterior aspect of the mastoid process<sup>[12,13,16,19,20,30]</sup> with a flat tendinous attachment.<sup>[21]</sup> Distally, it attaches at the transverse processes of the lower cervical and upper thoracic vertebrae.<sup>[8,13,16–21,38]</sup> The distal

**Table 5**  
Muscle architecture data for longissimus capitis.

Study	Sample/sex/age	Fascicle <sup>1</sup>		Muscle <sup>1</sup>			
		Length (cm)	Pennation angle (°)	Mass (g)	PSCA (cm <sup>2</sup> )	CSA (cm <sup>2</sup> )	
Dissection studies	Bayoglu et al. (2017)	n=1 Male 79 years	7.2	0	3.9	0.6	-
	Borst et al. (2011)	n=1 Male 86 years	6.5	0	5.5	0.8	-
	Kamibayashi and Richmond (1998)	n=9 <sup>2</sup> 7 M / 3 F 66–92 years	13–18 (muscle-tendon length)	-	16–24	-	-
	Van Ee et al. (2000)	n=6 4 M / 2 F 70–83 years	-	>3	-	1.0	-
Imaging study - MRI	Li et al. (2014)	n= 16 11 M / 5 F 23–33 years	-	-	-	-	1.2

CSA: cross-sectional area; F: female, M: male; MRI: magnetic resonance imaging; PSCA: physiological cross-sectional area. <sup>1</sup>Mean values presented where relevant (standard deviation) given where available. <sup>2</sup>Data are estimated from two individuals, PSCA value not provided.

attachments may vary, although are consistently in the same region: C2–C6,<sup>[17]</sup> C3–T5,<sup>[19]</sup> C4T2,<sup>[18]</sup> C4–T4,<sup>[38]</sup> and T1–T4.<sup>[8]</sup> Enthesis morphological data for longissimus attachment sites were not provided.

**Muscle architecture:** There were fewer studies on the longissimus capitis than on the other muscles covered in this review, which resulted in limited architectural data (Table 5). Two studies provided mean fascicle length (6.5 and 7.2 cm), and despite having data from only two individuals, both lengths are similar.<sup>[18,19]</sup> These studies also reported muscle mass with similar consistency between individuals (3.9 and 5.5 g). A third study provided estimations of length and mass from two individuals in their study, which appears to include the entirety of the muscle and tendon.<sup>[17]</sup> Pennation angle is consistent at less than 3°. PSCA ranged between 0.6–1.0 cm<sup>2</sup>, with a slightly larger reported CSA value of 1.2 cm<sup>2</sup>. No studies reviewed observed variation between males and females for the longissimus capitis muscle.

**Function:** The longissimus capitis stabilizes the vertebral column and cranium.<sup>[8]</sup> It contributes to extension of the head and neck<sup>[67]</sup> and unilaterally, produces ipsilateral axial rotation of the head<sup>[20]</sup> and lateral flexion of the cervical vertebrae.<sup>[21,67]</sup>

## Discussion

The soft tissues associated with the nuchal crest and mastoid process contribute to the musculature of the

head and neck, with their proximal attachments directly associated with the skeletal landmarks and their distal attachments covering broad areas of the cervical vertebrae, clavicle, and sternum/manubrium. Collectively, the associated muscles range from small to large, with the smallest dissection PSCA reported for longissimus capitis (0.6 cm<sup>2</sup>)<sup>[19]</sup> and the largest for sternocleidomastoid (4.9 cm<sup>2</sup>).<sup>[32]</sup> Imaging CSA values showed a large range from 1.2 cm<sup>2</sup> for longissimus capitis<sup>[33]</sup> to 36 cm<sup>2</sup> for upper trapezius,<sup>[33]</sup> although this large measurement was based on a single maximum CSA measurement at the level of C6 and C7. These soft tissues also contribute to the stability and movement of the head, neck, and shoulders. Specifically, upper trapezius, semispinalis capitis, splenius capitis, and longissimus capitis act as extensors of the neck when contracting bilaterally,<sup>[8,12,13,16,21,22,35,40,41,67]</sup> while sternocleidomastoid acts as a flexor<sup>[12,13,16,21,22,41]</sup> and the nuchal ligament provides stabilization.<sup>[45,46]</sup> They also contribute to cervical rotation and lateral flexion. The reviewed literature that discussed function focused mostly on the muscles' concentric actions, with limited discussion of eccentric muscle contraction. The emphasis on concentric functions in the existing literature suggests that research in this area should aim to explore more distinct muscular functions.

Although descriptions of the cervical muscles and nuchal ligament are numerous, there are limited architectural data presented in dissection and imaging studies.

Additionally, very few provide complete or uniform data. Some dissection studies reviewed here do report on several architectural parameters,<sup>[17-19]</sup> although two only included one individual.<sup>[18,19]</sup> Conversely, imaging studies often provide CSA measurements, with limited information on other architectural parameters.

The most widely studied muscles were upper trapezius and sternocleidomastoid. Five dissection studies provided architectural data for these muscles with four overlapping publications<sup>[17-19,32]</sup> and one study each, which explored trapezius<sup>[10]</sup> and sternocleidomastoid<sup>[50]</sup> individually. The architectural data for all other muscles were derived from the same four dissection studies that examined multiple muscles in the head, neck, and shoulders.<sup>[17-19,32]</sup> This illustrates that further studies are required to provide architectural data for these groups and segments of muscles. The imaging studies were more variable in representation of muscles, and one encompassed all the muscles in this review.<sup>[33]</sup> However, the measurements were often not as comparable due to the reporting of a maximum CSA value. Sternocleidomastoid was the most widely analyzed muscle with data from seven imaging studies,<sup>[33,34,41,50,55,68,69]</sup> although the study by Kennedy et al.<sup>[50]</sup> focused mostly on dissection, providing volume data from MRI. Longissimus capitis had the least amount of data, with architectural measurements limited to one imaging study,<sup>[33]</sup> which reflects the few studies that discussed this small muscle. Also, as described above, no architectural data was provided for the nuchal ligament, with the exception of the size of its entheses on the cranium.<sup>[9]</sup>

With the exception of two studies that provided entheses morphology of the nuchal ligament and sternocleidomastoid,<sup>[9,54]</sup> no other data were available for the size or shape of tendinous attachments or ligament entheses. Additionally, the existing literature does not provide detailed information for attachment sites, such as the location of attachment on the mastoid process. Further exploration in this area would assist in informing research into sexual dimorphism in the skeleton as it relates to muscular and skeletal robusticity. It may also improve our understanding of how soft tissues interact with the skeleton in other contexts. For example, some research in bioarchaeology examines entheses to study activity markers on the bone,<sup>[70,71]</sup> and data from anatomical studies could inform future research in this area.

Another area with limited discussion was the variation between dissection and imaging studies. One study compared data from both,<sup>[50]</sup> while another completed an imaging study on a cadaveric population.<sup>[72]</sup> As seen in the

ranges of measurements, imaging values were higher than those obtained from dissection, specifically for sternocleidomastoid.<sup>[50]</sup> This is to be expected given the older age of cadaveric specimens, compared with living individuals, and possible tissue shrinkage related to preservation processes.<sup>[50,72]</sup> Additionally, there may be a higher incidence of error in imaging studies, particularly when assessing single slice CSA measurements.<sup>[38,68]</sup> Finally, few publications addressed sex or population differences. Although sexual dimorphism was observed in four muscles – upper trapezius, semispinalis capitis, sternocleidomastoid, and splenius capitis – this was discussed in only six of the 19 studies<sup>[14,15,36,50,55,67]</sup> that provided architectural data. Of the other 13 studies, two included one individual,<sup>[18,19]</sup> four studied one sex,<sup>[34,41,68,69]</sup> one did not provide a breakdown of sex,<sup>[10]</sup> and six provided data for both sexes, but did not assess sexual dimorphism.<sup>[17,32,33,37,72,73]</sup> With the knowledge that sex differences do exist in humans, it seems relevant that potential variation in anatomical parameters between sexes should be consistently addressed. The field of anatomy would benefit by including both males and females in research to understand the role that sexual dimorphism plays not only for anthropological research, but also in terms of clinical and functional applications. Similarly, understanding of population variation in these muscles is limited. Although the studies reviewed were from diverse regions of the world – which was especially apparent in case reports of anatomical variation in sternocleidomastoid – only one discussed the possibility that population differences may influence their findings.<sup>[72]</sup>

Despite the amount of information available on the soft tissues associated with the nuchal crest and mastoid process, there are still some gaps in the literature that need to be addressed. Based on this review, it is clear that further research is warranted to provide comprehensive and uniform data on posterior cervical muscle architecture and entheses morphology, incorporating diverse populations and age groups. Moreover, although sexual dimorphism and population differences has been considered in some studies, these areas of require exploration in future studies.

### Conflict of Interest

The authors declare that there are no conflicts of interest.

### Author Contributions

JSDLP: study design, systematic search and screening of literature, drafting the manuscript, edits; HRB: supervising work, commenting on drafts and the final version of the manuscript; SEH: supervising work, commenting on drafts and the final version of the manuscript; SJW:

senior author, supervising work, commenting on drafts and final version of the manuscript.

## Funding

No funding was received for this research.

## References

- Buikstra JE, Ubelaker DH. Standards for data collection from human skeletal remains. Fayetteville: Arkansas Archeological Survey Research Series No. 44; 1994. p. 272
- Klales AR, Ousley SD, Vollner JM. A revised method of sexing the human innominate using Phenice's nonmetric traits and statistical methods. *Am J Phys Anthropol* 2012;149:104–14.
- Phenice TW. A newly developed visual method of sexing the os pubis. *Am J Phys Anthropol* 1969;30:297–301.
- Walker PL. Sexing skulls using discriminant function analysis of visually assessed traits. *Am J Phys Anthropol* 2008;136:39–50.
- White TD, Black MT, Folkens PA. Human osteology. 3rd ed. San Diego (CA): Elsevier Science & Technology; 2011. p. 688.
- Page MJ, McKenzie JE, Bossuyt PM, Boutron I, Hoffmann TC, Mulrow CD, Shamseer L, Tetzlaff JM, Akl EA, Brennan SE, Chou R, Glanville J, Grimshaw JM, Hrobjartsson A, Lalu MM, Li T, Loder EW, Mayo-Wilson E, McDonald S, McGuinness LA, Stewart LA, Thomas J, Tricco AC, Welch VA, Whiting P, Moher D. The PRISMA 2020 statement: an updated guideline for reporting systematic reviews. *BMJ* 2021;10372:n71.
- Flack NA, Nicholson HD, Woodley SJ. A review of the anatomy of the hip abductor muscles, gluteus medius, gluteus minimus, and tensor fascia lata. *Clin Anat* 2012;25:697–708.
- Houseman ND, Taylor GI, Pan WR. The angiosomes of the head and neck: anatomic study and clinical applications. *Plast Reconstr Surg* 2000;105:2287–313.
- Humphreys BK, Kenin S, Hubbard BB, Cramer GD. Investigation of connective tissue attachments to the cervical spinal dura mater. *Clin Anat* 2003;16:152–9.
- Johnson G, Bogduk N, Nowitzke A, House D. Anatomy and actions of the trapezius muscle. *Clin Biomech (Bristol, Avon)* 1994;9:44–50.
- Mercer SR, Bogduk N. Clinical anatomy of ligamentum nuchae. *Clin Anat* 2003;16:484–93.
- Gray H. Anatomy, descriptive and surgical. London: John W. Parker and Son, West Strand; 1858.
- Standring S. Gray's anatomy: the anatomical basis of clinical practice. 42nd ed. New York: Elsevier Limited; 2021. p. 1606.
- Rankin G, Stokes M, Newham DJ. Size and shape of the posterior neck muscles measured by ultrasound imaging: normal values in males and females of different ages. *Man Ther* 2005;10:108–15.
- Mayoux-Benhamou MA, Revel M, Wybier M, Barbet JP. Computerized tomographical study of dorsal neck muscles for insertion of EMG wire electrodes. *J Electromyogr Kinesiol* 1995;5:101–7.
- Sinnatamby CS, Last RJ. Last's anatomy: regional and applied. 12th ed. Edinburgh/New York: Churchill Livingstone/Elsevier; 2011. p. 560.
- Kamibayashi LK, Richmond FJ. Morphometry of human neck muscles. *Spine (Phila Pa 1976)* 1998;23:1314–23.
- Borst J, Forbes PA, Happee R, Veeger DH. Muscle parameters for musculoskeletal modelling of the human neck. *Clin Biomech (Bristol, Avon)* 2011;26:343–51.
- Bayoglu R, Geeraedts L, Groenen KHJ, Verdonschot N, Koopman B, Homminga J. Twente spine model: a complete and coherent dataset for musculo-skeletal modeling of the thoracic and cervical regions of the human spine. *J Biomech* 2017;58:52–63.
- Vasavada A, Ward S, Delp S, Lieber R. Architectural design and function of human back muscles. In: Herkowitz HN GS, Eismont FJ, Bell JR, Balderston RA, editors. The spine. 6th ed. Philadelphia (PA): Elsevier; 2011. p. 59–68.
- Knox R. A System of human anatomy on the basis of the "Traité D'Anatomie Descriptive" of M.H. Cloquet. 2nd ed. Edinburgh: Maclachlan and Stewart; 1831.
- Hansen JT, Netter FH, Machado CAG. Netter's clinical anatomy. 4th ed. Philadelphia (PA): Elsevier; 2019. p. 588.
- Fielding JW, Burstein AH, Frankel VH. The nuchal ligament. *Spine (Phila Pa 1976)* 1976;1:3–14.
- Rea P. Neck. In: Rea P, editor. Essential clinically applied anatomy of the peripheral nervous system in the head and neck. Amsterdam: Academic Press; 2016. p. 131–83.
- Allia P, Gorniak G. Human ligamentum nuchae in the elderly: its function in the cervical spine. *Journal of Manual and Manipulative Therapy* 2013;14:11–21.
- Abbott LC, Lucas DB. The function of the clavicle: its surgical significance. *Ann Surg* 1954;140:583–99.
- Giacomo GD, Pouliart N, Costantini A, Vita AD. Atlas of functional shoulder anatomy. Milano: Springer; 2008. p. 231.
- Kawtharani FI, Hasan SS. Anatomy of the clavicle and its articulations. In: Groh GI, editor. Clavicle injuries. A case based guide to diagnosis and treatment. Cham, Switzerland: Springer International Publishing; 2018. Chapter 1; p. 1–17.
- Phadnis J, Bain GI. Clavicle anatomy. In: Bain GI, Itoi E, Di Giacomo G, Sugaya H, editors. Normal and pathological anatomy of the shoulder. Berlin, Heidelberg: Springer; 2015. Chapter 8; p. 71–80.
- Frazer JE. The anatomy of the human skeleton. 2nd ed. London: J & A Churchill; 1920. p. 284.
- Klein Breteler MD, Spoor CW, Van der Helm FC. Measuring muscle and joint geometry parameters of a shoulder for modeling purposes. *J Biomech* 1999;32:1191–7.
- Van Ee CA, Nightingale RW, Camacho DL, Chancey VC, Knaub KE, Sun EA, Myers BS. Tensile properties of the human muscular and ligamentous cervical spine. *Stapp Car Crash J* 2000;44:85–102.
- Li F, Laville A, Bonneau D, Laporte S, Skalli W. Study on cervical muscle volume by means of three-dimensional reconstruction. *J Magn Reson Imaging* 2014;39:1411–6.
- Dawson RM, Latif Z, Haacke EM, Cavanaugh JM. Magnetic resonance imaging-based relationships between neck muscle cross-sectional area and neck circumference for adults and children. *Eur Spine J* 2013;22:446–52.
- Franklin D, Freedman L, Milne N, Oxnard CE. A geometric morphometric study of sexual dimorphism in the crania of indigenous southern Africans. *South African Journal of Science* 2006;102:229–38.

36. Valera-Calero JA, Gallego-Sendarrubias G, Fernandez-de-Las-Penas C, Cleland JA, Ortega-Santiago R, Arias-Buria JL. Cross-sectional area of the cervical extensors assessed with panoramic ultrasound imaging: preliminary data in healthy people. *Musculoskeletal Sci Pract* 2020;50:102257.
37. Rezasoltani A, Kallinen M, Malkia E, Vihko V. Neck semispinalis capitis muscle size in sitting and prone positions measured by real-time ultrasonography. *Clin Rehabil* 1998;12:36–44.
38. Elliott JM, Cornwall J, Kennedy E, Abbott R, Crawford RJ. Towards defining muscular regions of interest from axial magnetic resonance imaging with anatomical cross-reference: part II - cervical spine musculature. *BMC Musculoskelet Disord* 2018;19:171.
39. Reddy C, Zhou Y, Wan B, Zhang X. Sex and posture dependence of neck muscle size-strength relationships. *J Biomech* 2021;127:110660.
40. Rezasoltani A, Nasiri R, Faizei AM, Zaafari G, Mirshahvelayati AS, Bakhshidarabad L. The variation of the strength of neck extensor muscles and semispinalis capitis muscle size with head and neck position. *J Bodyw Mov Ther* 2013;17:200–3.
41. Uthaihpur S, Assapun J, Kothan S, Watcharasakul P, Elliott JM. Structural changes of the cervical muscles in elder women with cervicogenic headache. *Musculoskelet Sci Pract* 2017;29:1–6.
42. Johnson GM, Zhang M, Jones DG. The fine connective tissue architecture of the human ligamentum nuchae. *Spine (Phila Pa 1976)* 2000;25:5–9.
43. Kadri PAS, Al-Mefty O. Anatomy of the nuchal ligament and its surgical applications. *Neurosurgery* 2007;61:301–4.
44. Ono A, Tonosaki Y, Numasawa T, Wada K, Yamasaki Y, Tanaka T, Kumagai G, Aburakawa S, Takeuchi K, Yokoyama T, Ueyama K, Ishibashi Y, Toh S. The relationship between the anatomy of the nuchal ligament and postoperative axial pain after cervical laminoplasty: cadaver and clinical study. *Spine (Phila Pa 1976)* 2012;37:E1607–13.
45. Mitchell BS, Humphreys BK, O'Sullivan E. Attachments of the ligamentum nuchae to cervical posterior spinal dura and the lateral part of the occipital bone. *J Manipulative Physiol Ther* 1998;21:145–8.
46. Takeshita K, Peterson ET, Bylski-Austrow D, Crawford AH, Nakamura K. The nuchal ligament restrains cervical spine flexion. *Spine (Phila Pa 1976)* 2004;29:E388–93.
47. Dean NA, Mitchell BS. Anatomic relation between the nuchal ligament (ligamentum nuchae) and the spinal dura mater in the cranio-cervical region. *Clin Anat* 2002;15:182–5.
48. Nash L, Nicholson H, Lee AS, Johnson GM, Zhang M. Configuration of the connective tissue in the posterior atlanto-occipital interspace: a sheet plastination and confocal microscopy study. *Spine (Phila Pa 1976)* 2005;30:1359–66.
49. Zheng N, Yuan XY, Li YF, Chi YY, Gao HB, Zhao X, Yu SB, Sui HJ, Sharkey J. Definition of the to be named ligament and vertebral ligament and their possible effects on the circulation of CSF. *PLOS One* 2014;9:e103451.
50. Kennedy E, Albert M, Nicholson H. The fascicular anatomy and peak force capabilities of the sternocleidomastoid muscle. *Surg Radiol Anat* 2017;39:629–45.
51. Clark BS, Shah S, Chambers T. The sternocleidomastoid flap. *Operative Techniques in Otolaryngology-Head and Neck Surgery* 2019;30:138–44.
52. Saha A, Mandal S, Chakraborty S, Bandyopadhyay M. Morphological study of the attachment of sternocleidomastoid muscle. *Singapore Med J* 2014;55:45–7.
53. Ferreira-Arquez H. Multi headed sternocleidomastoid muscle: an anatomical study. *International Journal of Pharma and Bio Sciences* 2018;9:b249–56.
54. Lee JT, Campbell KJ, Michalski MP, Wilson KJ, Spiegl UJ, Wijdicks CA, Millett PJ. Surgical anatomy of the sternoclavicular joint: a qualitative and quantitative anatomical study. *J Bone Joint Surg Am* 2014;96:e166.
55. Alsalaheen B, Johns K, Bean R, Almeida A, Eckner J, Lorincz M. Women and men use different strategies to stabilize the head in response to impulsive loads: implications for concussion injury risk. *J Orthop Sports Phys Ther* 2019;49:779–86.
56. de Amorim AA, Lins CCDA, Cardoso APD, Damascena CG. Variation in clavicular origin of sternocleidomastoid muscle. A case report. *Int J Morphol* 2010;28:97–8.
57. Cherian SB, Nayak S. A rare case of unilateral third head of sternocleidomastoid muscle. *Int J Morphol* 2008;26:99–101.
58. Dupont G, Iwanaga J, Altafulla JJ, Lachkar S, Oskouian RJ, Tubbs RS. Bilateral sternocleidomastoid variant with six distinct insertions along the superior nuchal line. *Anat Cell Biol* 2018;51:305–8.
59. Fazliogullari Z, Cicekcibasi AE, Unver Dogan N, Yilmaz MT, Buyukmumcu M, Ziyilan T. The levator claviculae muscle and unilateral third head of the sternocleidomastoid muscle: case report. *Int J Morphol* 2010;28:929–32.
60. Heo YR, Kim JW, Lee JH. Variation of the sternocleidomastoid muscle: a case report of three heads and an accessory head. *Surg Radiol Anat* 2020;42:711–3.
61. Kim SY, Jang HB, Kim J, Yoon SP. Bilateral four heads of the sternocleidomastoid muscle. *Surg Radiol Anat* 2015;37:871–3.
62. Natsis K, Asouchidou I, Vasileiou M, Papathanasiou E, Noutsos G, Paraskevas G. A rare case of bilateral supernumerary heads of sternocleidomastoid muscle and its clinical impact. *Folia Morphol (Warsz)* 2009;68:52–4.
63. Oh JS, Kim CE, Kim J, Yoon SP. Bilateral supernumerary clavicular heads of sternocleidomastoid muscle in a Korean female cadaver. *Surg Radiol Anat* 2019;41:699–702.
64. Raikos A, Paraskevas GK, Triaridis S, Kordali P, Psillas G, Brand-Saberi B. Bilateral supernumerary sternocleidomastoid heads with critical narrowing of the minor and major supraclavicular fossae: Clinical and surgical implications. *Int J Morphol* 2012;30:927–933.
65. Sirasanagandla SR, Bhat KMR, Pamidi N, Somayaji SN. Unusual third head of the sternocleidomastoid muscle from the investing layer of cervical fascia. *Int J Morphol* 2012;30:783–5.
66. Anil A, Yasar YK, Anil F, Coskun ZK, Peker T. Variation of bilateral multiheaded sternocleidomastoid muscle. *Gazi Medical Journal* 2017;28:56–7.
67. Keidan L, Barash A, Lenzer Z, Pick CG, Been E. Sexual dimorphism of the posterior cervical spine muscle attachments. *J Anat* 2021;239:589–601.
68. De Loose V, Van den Oord M, Keser I, Burnotte F, Van Tiggelen D, Dumarey A, Cagnie B, Witvrouw E, Danneels L. MRI study of the morphometry of the cervical musculature in F-16 pilots. *Aviat Space Environ Med* 2009;80:727–31.
69. Elliott JM, Pedler AR, Jull GA, Van Wyk L, Galloway GG, O'Leary SP. Differential changes in muscle composition exist in

- traumatic and nontraumatic neck pain. *Spine (Phila Pa 1976)* 2014;39:39–47.
70. Benjamin M, Toumi H, Ralphs JR, Bydder G, Best TM, Milz S. Where tendons and ligaments meet bone: attachment sites ('entheses') in relation to exercise and/or mechanical load. *J Anat* 2006; 208:471–90.
71. Villotte S, Knusel CJ. Understanding enthesal changes: definition and life course changes. *International Journal of Osteoarchaeology* 2013;23:135–46.
72. Kim BS, Kim DS, Kang S, Kim JY, Kang B, Rhyu IJ, Yoon JS. Ultrasound-guided injection of the sternocleidomastoid muscle: a cadaveric study with implications for chemodenervation. *PM R* 2021;13:503–9.
73. Botticchio A, Mourad F, Fernandez-Carnero S, Arias-Buria JL, Santodomingo Bueno A, Mesa Jimenez J, Gobbo M. Short-term morphological changes in asymptomatic perimandibular muscles after dry needling assessed with rehabilitative ultrasound imaging: a proof-of-concept study. *J Clin Med* 2021;10:209–19.

**ORCID ID:**

J. S. De La Paz 0000-0002-4190-7835;  
 H. R. Buckley 0000-0003-1047-4288;  
 S. E. Halcrow 0000-0001-6038-7997;  
 S. J. Woodley 0000-0002-7288-0209

**Correspondence to:** Jade S. De La Paz, PhD

Department of Anatomy, School of Biomedical Sciences,  
 University of Otago, Dunedin, 9016, New Zealand  
 Phone: +64 0274341417  
 e-mail: jade.delapaz@otago.ac.nz

*Conflict of interest statement:* No conflicts declared.

This is an open access article distributed under the terms of the Creative Commons Attribution-NonCommercial-NoDerivs 4.0 Unported (CC BY-NC-ND4.0) Licence (<http://creativecommons.org/licenses/by-nc-nd/4.0/>) which permits unrestricted noncommercial use, distribution, and reproduction in any medium, provided the original work is properly cited. *How to cite this article:* De La Paz JS, Buckley HR, Halcrow SE, Woodley SJ. A systematic review of the anatomy of soft tissues associated with sexually dimorphic landmarks on the cranium. *Anatomy* 2022;16(2):93–107.

# Notes on the techniques of body restoration after autopsy and the possibility of embalming

Jan Frišhons<sup>1</sup> , Maksim A. Kislov<sup>2</sup> , Marcela Bezdickova<sup>3</sup> , Veronika Dzetkucicová<sup>1</sup> 

<sup>1</sup>Department of Anatomy, Faculty of Medicine, Masaryk University, Brno, Czech Republic

<sup>2</sup>Department of Forensic Medicine, Sechenov Moscow State Medical University, Moscow, Russia

<sup>3</sup>Department of Anatomy, Swansea University Medical School, Swansea, United Kingdom

## Abstract

Knowledge of the technique of body restoration, recovery and embalming of corpses is important both from an ethical point of view and from an identification point of view. Conventional autopsy remains one of the main methods of forensic medicine. Different techniques are described within the article starting with basic restoration techniques and describing more advanced and difficult procedures in body reconstructions. Many European and other countries have the necessity of body modification imposed in recommendations or legislation. There are many tried and tested dissection techniques of different body parts that guarantee maximum yield of findings and at the same time an excellent level of reconstruction of the body back to its original state. With high-quality embalming procedures and with the accurate solution choice, only small changes show up as very slow mild dehydration over many months.

**Keywords:** autopsy; body restoration; embalming; preservation; reconstruction

Anatomy 2022;16(2):108–113 ©2022 Turkish Society of Anatomy and Clinical Anatomy (TSACA)

## Introduction

Knowledge of the technique of body restoration, recovery and embalming of corpses is important both from an ethical point of view and from an identification point of view. Despite the development of virtual approaches, conventional autopsy remains one of the main methods of forensic medicine. Knowing appropriate body restoration procedures is essential to treat the body in a dignified and ethical manner. Ideal treatment depends on accurate skin incisions. National laws of each country regulate the body handling after the death. In Europe e.g., Recommendation no. R (99) 3 of Cabinet Ministers' Committee on the coordination of medical-legal autopsy rules; Council of Europe from 2000 and European rule of funeral services EN 15017:2005. Another example, in the Russian Federation, this matter is regulated by the Federal law from 1996 N 8-FZ "Burial and funeral services" and regional laws, e.g., the Law of the City of Moscow from 1997 no. N 11 and Federal Law of 2011 N 323-FZ "Basis on protecting the health of citizens in the Russian Federation".

By volume and purpose, the methods of handling corpses can be divided into several groups. The aim of

this review is to suggest the techniques of body restoration after autopsy and the possibility of embalming documenting the experience of our Institutions.

## Basic Body Restoration After Autopsy

It is performed after each autopsy. The fluids are removed from the open cavities by inserting absorbent material into the cranial cavity, neck and pelvis. Dissected organs are inserted back into the open chest and abdominal cavity. Cavities are covered with absorbent material, sternum placed in a position and the skin is sewed up using the main autopsy suture (**Figure 1**) with a needle puncture at a distance of 0.5–1 cm from the skin incision is sewed up and the body is washed. The stomata and additional openings are closed with a tobacco or Z-shaped stitch (**Figures 2 and 3**).

## Body Restoration After Special Autopsy Techniques

An enucleated eyeball replacement can be shaped from a self-hardening mixture (selfpolymerizing resins, modeling materials, etc.) of an appropriate shape and size and

fixed in a suitable position. Finally, an artificial eye cap is placed under the eyelids. In organs where enucleation is carried out in short postmortem intervals, “hematoma” and edema of the paraplasmic tissues are possible. This artefact can be repaired by dehydration with concentrated ethanol followed by cosmetic adjustment. It is possible to replenish the volume of the destroyed eyeball by injecting a fixation fluid. Reconstruction of the damaged part of the orbit with the eyeball consists of replacing the removed part of the bone with a suitable material and treatment of soft tissues.<sup>[1]</sup> Modification after skull base block removal is possible using a carotid siphon for fixation of the lower jaw and repair of soft tissues with a suitable epoxy adhesive.<sup>[2]</sup> Adjustment after opening the mouth; the removed bone is replaced with a 3D print or with a suitable casting from a different material such as wood.<sup>[3]</sup>

**Reconstruction after block evisceration of the spinal cord by dorsal approach:** the spinal canal is filled with an absorbent material with a retainer, or when fixing the cervical segment of the spine, e.g., with a wire strip wrapped around by a dressing. Removing spinous processes, drilling opposite holes in the occipital bone both at the distal part and at the base and wiring them provide support. Next step is sealing the base with absorbent material, and also the subcutaneous tissue of the back and neck. If the part of the skull’s base is removed, a suitably sized prosthesis is inserted and secured with screws and tiles.

**Reconstruction after dissection of the subcutaneous tissue, vessels, etc.:** The soft subcutaneous tissue is treated with a denaturing agent, a fixative and introduced by an absorbent material. The application of a glove or intradermal suture depends on the location; it is also possible to use cyanoacrylate or tissue adhesive subcutaneously.<sup>[4]</sup> In Russian Federation, the removed part of the skull is usually replaced with a casting from Polyvik polymer (Russian Federation Company) which hardens in 10–15 minutes.

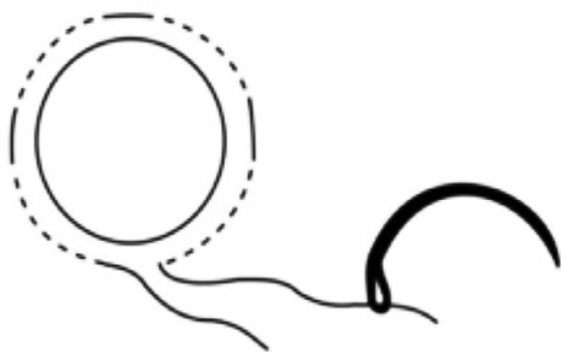


Figure 2. Tobacco stitch. Graphics by Jiri Tauš.

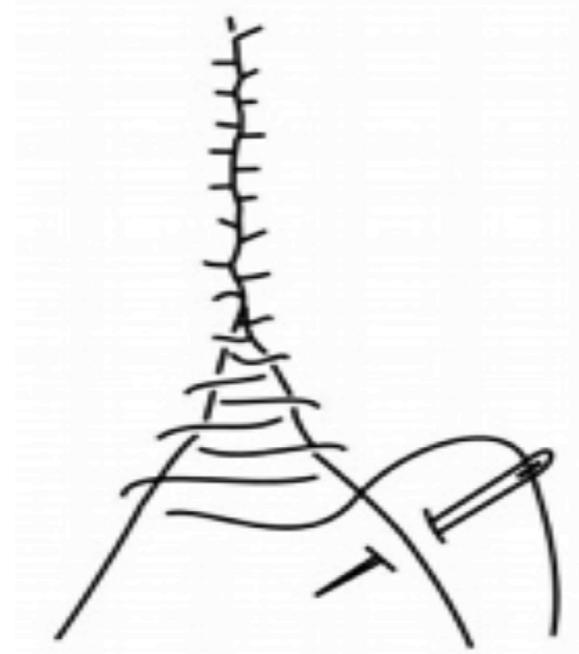


Figure 1. Basic autopsy suture. Graphics by Jiri Tauš.

The base of the skull is covered with long strips of rag soaked in a creamy gypsum mixture. Two strips 50 cm long are casted into the casting for subsequent fixation of the position in the temporoparietal and occipital regions and fixed on the skull and spine. The fixation of the occipital region to the spine is performed in the cervical spine or to the clavicle and from the temporoparietal regions towards the mandibular rami. Subsequently, soft tissue correction is performed.<sup>[5]</sup> Reconstruction after opening the face consists of replacing the removed part of the bones with a suitable material, for example, a 3D print.<sup>[6]</sup> Lobes of soft tissue are fixed with epoxy resin or internal sutures through small holes drilled into the bone. Processing of soft tissues

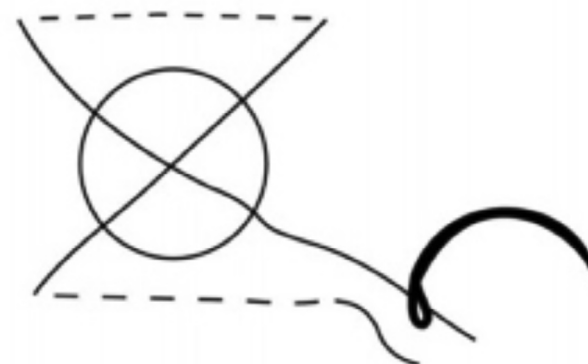


Figure 3. Z suture. Graphics by Jiri Tauš.

is difficult at the root of the nose, zygomatic arches and inner corners of the eyes.<sup>[7]</sup> A piece of cotton wool soaked in 10% formalin is introduced into the external auditory canal. The removed bones are replaced with a 3D print or wooden prosthesis, and their position is fixed with a cable tie or wire. The volume of soft tissues is regulated, for example, with a cloth. Finally, the soft tissues are processed as described above.

### Extended Body Restoration (Health and Safety Protocol)

It consists of adjusting the eyelids, closing the mouth, adjusting the hair, and closing the openings/holes in the body. These adjustments are made at the request of the relatives or according to the requirements. The cranial cavity is filled with absorbent material. The base and vault of the skull are limited from movement by holes in the temporal and occipital regions through which the wires pass, then the absorbent material is inserted under the soft integument of the skull and sutured. The eyelids are closed in a 2:3 ratio of the lower and upper eyelids with a plastic eyelid. An absorbent material is injected into the oral cavity and nasal cavity. The mouth is closed with an internal suture running from the base of the mandible through the vestibule of the mouth through the nasal septum back into the oral cavity where the knot is tied (Figure 4). Hairs are washed dry or damp. After dissection, the clavicles can be brought together using a cable tie through the drilled holes. The skin of the skin incision in the thoracic and abdominal cavities can be perforated before suturing, for example, with a Malco HP18 sheet metal punch.<sup>[8]</sup> The sharp edges of the ribs

are covered with a suitable material. The penis is closed by a ligament in a condom. An absorbent material soaked in a preservative solution is inserted into the rectum and vagina. The whole body is washed with aromatic disinfectant soap. Nail care products and cosmetics can be applied with makeup brush or with an airbrush.

**Reconstruction of body parts** damaged mechanically or otherwise is performed to reduce the psychological trauma of person providing identification. When carrying out reconstruction it is important to observe the anatomical structures using correct proportions. Part of the destroyed skeleton is replaced, for example, with a 3D print, a polyurethane prosthetics,<sup>[9]</sup> plasticine blocks<sup>[10]</sup> and other materials. Lobes of soft tissues are collected by stitching them with intradermal (Figure 5) and other sutures or cyanoacrylate glue and attached to the substrate, e.g., using epoxy resin. The missing parts of soft tissues can be replaced with an autocutaneous graft or reconstructive wax, followed by surface cosmetic adjustments. The restoration can be made from pulp, plaster, bone paste, cotton, paraffin-impregnated cellulose, wool and other materials. When the frame is complete or there are most of the fragments of the frame, they are cleaned, drilled, and wired or connected with small plates. After assembly, the skeleton of the skull is wrapped with foil and a light plaster of paris is poured through a small hole in the temporal bone to strengthen it.<sup>[11-15]</sup> In some cases, it is possible to perform computed tomography of the damaged head with a virtual reconstruction of the skull for subsequent printing missing elements using a 3D printer. If most of the frame is missing, it is necessary to replace this part, for example, with a modified 3D casting. If it is

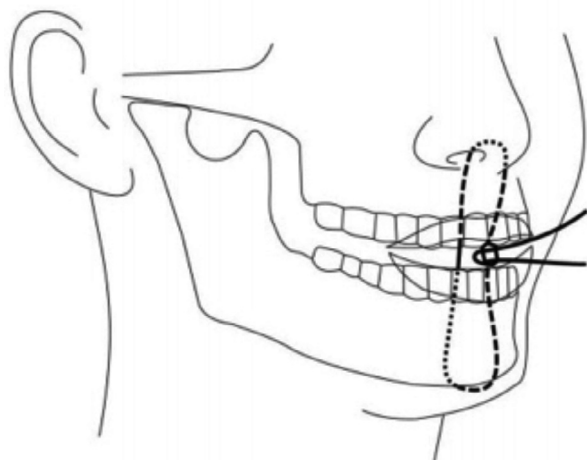


Figure 4. Internal suture to close the lips. Graphics by Jiri Tauš.

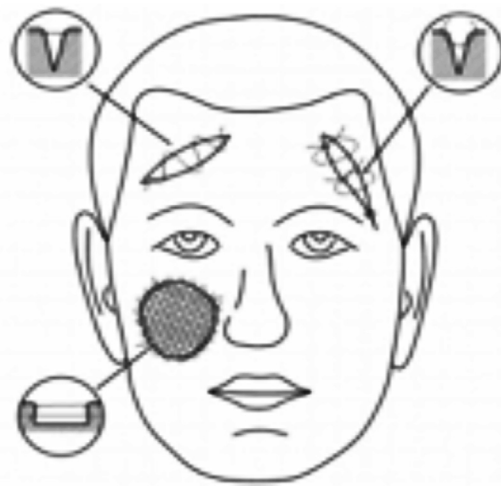


Figure 5. Possibilities of correcting soft tissue defects with various sutures and wax. Graphics by Jiri Tauš.

necessary to correct the surface of the subcutaneous tissue, it can be used by injecting a mixture of 8 parts of paraffin and 2 parts of white petroleum jelly, heated to 44 °C, followed by cooling or Celladamm 16–20%, white beeswax 55–70%, paraffin 6–19% and petroleum jelly 6–12%.<sup>[16]</sup> Bruises on the skin can be removed by wiping with special soap with a shaving brush for about one hour. Removal of swelling of facial tissues has been accomplished with anhydrous embalming with compresses. Partial drying of small skin areas, parchment-like, can be eliminated, in particular, with a solution of water, acetic acid and hydrogen peroxide. For example, to reduce the results of putrefactive processes, the head tissues could be impregnated with preservative solution via blood vessels and impregnation takes 24 hours with a solution of 750 ml of formalin, 2250 ml of deodorant, 750 ml of isopropyl alcohol, 750 ml of alaminol and up to 9000 ml of water. Then the tissues are fixed in a solution of 125 ml of formaldehyde, 1000 ml of hydrogen peroxide, 1000 ml of acetic acid, 500 ml of isopropyl alcohol, 500 ml of deodorant, 250 ml of alaminol and 10,000 ml of water.<sup>[17]</sup> This preservation procedure is performed to reduce the psychological trauma of individuals providing identification, should such procedure be required.

**Preservation of the corpse or part of it** is usually performed before reconstruction of soft tissues, before using some complex autopsy methods, at the request of relatives, for shortterm storage or for shipping to temporarily prevent the development of post-mortem changes. This can be done arterially or by injecting a preservative solution into the subcutaneous tissue (**Figure 6**). For temporary preservation, a 5–10% aque-



**Figure 6.** Points of injection of the fixing solution into the subcutaneous tissue of the face. Graphics by Jiri Tauš.

ous solution of formalin with other substances is the most preferable to use.<sup>[18]</sup> Solution options: 5–10% formaldehyde solution, 50–96% alcohol, 5–10% phenol solution or 0.2–0.7% anolyte solution.<sup>[19]</sup>

**Body embalming** has been performed at the request of relatives for a funeral ceremony or in relation to the international transport to suspend decomposition processes. Either commercially produced, for example, Dodge Company, Arthyl 26 Hygeco France and others, or experimentally mixed solutions of formaldehyde, ethanol, phenol, glycerin, water and other components are used. Other solutions suggestions include:

- sublimate 10 g, formalin 100 ml, alcohol 200, water 700;
- formalin solution 150 ml, alcohol 200 ml, water 650 ml, potassium acetate 50 g;
- zinc chloride solution 50 g, formalin 100 ml, alcohol 200 ml, water 650 ml;
- solution for Vyvodtsev;
- glycerin 1700 ml, water 1000 ml, thymol 5 g (previously dissolved in alcohol);
- glycerin solution 600 ml, alcohol 200, formalin 200 ml, potassium acetate 30 g;
- solution of Melnikov-Razvedenkov;
- glycerin 200–600 ml, potassium acetate 200–800 g, water 1000 ml.<sup>[20]</sup>

Perfusion is carried out manually with a syringe, hand pump, gravity flow from a height of 2.5 m, peristaltic or embalming pump. The volume of the embalming solution is usually 7 to 14 liters. The choice of the volume and composition of the solution depends on the size of the body, the degree of postmortem changes, the cause of death and other aspects. The most used perfusion site is through the femoral artery or the common carotid artery. It is also possible to use the ulnar, radial, brachial, or tibial arteries, etc. After arterial embalming, the openings of perfusion sites are closed with absorbent material, tissue glue and skin suture.

### Body Embalming Without Autopsy

It is performed through an intact arterial bed with venous drainage, fan-shaped aspiration of the contents of the body cavities followed by the introduction of an embalming solution or subcutaneous injection into the limbs, face or chest and abdominal cavities.

### Embalming the Body After Autopsy

Residual fluid is removed from open body cavities, limbs and head are sprayed onto the severed ends of the femoral, brachial, and common carotid arteries. The dis-

sected organs are placed in a plastic bag with a solution for embalming, sealed and inserted into the cavity. After the completion of the injection of the vessels of the limb, an additional injection of the subcutaneous tissue of the chest cavity is performed. The holes and incisions on the body are sealed and closed as described above.<sup>[21–23]</sup>

The main body restoration should be carried out properly after each autopsy to a state that most closely resembles a pre-autopsy state. A special type of restoration is performed in cases of a special opening or treatment technique, when it is necessary to fix dissected tissues or replace removed structures. In some cases, the reparation of devastating injuries is a notable success.<sup>[24]</sup> With high-quality embalming, there is no development of post-mortem changes for more than 10 days.<sup>[25]</sup> In case the embalming solution has been selected correctly, only small changes show up as very slow mild dehydration over many months.

## Conclusion and Recommendations

Although extensive body restoration is not a standard part of the forensic field, it is pertinent to know these techniques and thus improve the quality of cadaver care in order to maximise respect shown to these bodies. Most of the substances contained in embalming solutions, i.e., formaldehyde, ethanol, phenol, potassium acetate, acetic acid and others, have a sanitary effect and destroy most infectious agents. Histoacrylic adhesive can also be used to close and repair skin incisions in young children.<sup>[26–28]</sup> Knowledge about treatment and simple rules of body fixation can be easily used in forensic practice.<sup>[29,30]</sup>

## Conflict of Interest

The authors declare that there are no conflicts of interest.

## Author Contributions

JF: project development/manuscript writing, MAK: project development/data collection, MB: manuscript writing and editing, VD: data collection.

## Funding

No funding was received for this research.

## References

- Parsons MA, Start RD. ACP best practice no 164: necropsy techniques in ophthalmic pathology. *J Clin Pathol* 2001;54:417–27.
- Langlois NEL, Little D. A method for exposing the intraosseous portion of the carotid arteries and its application to forensic case work. *Am J Forensic Med Pathol* 2003;24:35–40.
- de Jonge HK, van Merkesteyn JP, Bras J. Reconstruction of the lower half of the facial skeleton after removal of the mandible at autopsy. *Int J Oral Maxillofac Surg* 1990;19:155–7.
- Frišhons J. Pitevná a preparační techniky v tělních krajinách [Autopsy and preparation techniques in body landscapes]. *Gnosis Medica* 2017;4:5–44.
- Avdeev AI. Metod kosmetičeskogo iz'jatija kostej mozgovogo cherepa. Izbrannye voprosy sudebno-medicinskoj jekspertizy [The method of cosmetic from the “bones of the cerebral skull”. Selected questions of forensic medical examination]. *Habarovsk* 2018;17:9–10.
- Frišhons J, Kislov MA, Leonov SV. Ispol'zovanie 3D-pechati v sudebnoj medicene [The use of 3D printing in forensic medicine]. *Forensic Medicine* 2018;2:10–2.
- Kopija P, Frišhons J, Joukal M. Modifikace pitvy obličeje [Facial autopsy modification]. *Gnosis Medica* 2013;1:24–7.
- Duflou J, McNamara B, Cluney R. A safer method for body restoration following autopsy. *J Forensic Sci* 2013;59:224–5.
- Joukal M, Frišhons J. A facial reconstruction and identification technique for seriously devastating head wounds. *Forensic Sci Int* 2015;252:82–6.
- Leonov SV, Vlasjuk IV. Restavracija vneshnej trubny. Habarovsk, Izdatel'stvo DvGMU, editors. In: Body surface restoration (practical guide). Khabarovsk; Dvgtu Publishing. 2008.
- Frišhons J, Hejna P, Leonov SV, Vojtišek T, Krajsa J, Stoklásková K, Rambousek P, Zeman M. Přehled postmortálních technik pro případy rekonstrukce mutilujících poranění obličeje [An overview of postmortem techniques for the reconstruction of mutilating facial injuries]. *Criminal Proceedings* 2018;62:49–59.
- Kladov SJu. Posmertnaja restavracija lica. Pohoronnyj dom: rossijskij informacion noanaliticheskij [Postmortem face restoration. Funeral Home: Russian information]. *Journal of Novosibirsk* 2006; 11:44–7.
- Namestnikova JuG. Restavracija lica trupa dlja celi ego opoznanija [Restoration of the face of the body for the whole ego acquaintance]. *The Doctor* 1948;1:63–6.
- Cin'kovskij BP. K vopros o tualeta i restavracija trupov [To the question of the toilet and the restoration of corpses] Collection of Scientific State Vinnik 1956;2:187–94.
- Sal'kov AA. Iskusstvennoe ozhivlenie trupa neizvestnoj lichnosti s cel'ju ee opoznanija [Artificial revival of the corpse of an unknown person in order to identify it] *Forensic Medical Examination* 1928;7: 54–61.
- Abramov I. Restavracionnaja plasticheskaja massa [Restorative plastic mass]. 2006; Patent RF No: 2576820 C1.
- Buromskij IV, et. al. Sposob ustanovlenija prochnogo karkasa V sostojanii gnilostnogo razlozhenija. Patent RF # 2390997. Obshhestvo s ogranichennoj otvetstvennost'ju “KB-Centr” [Method of establishing a strong frame in a state of putrefactive decomposition. RF patent # 2390997. KB-Center limited liability company]. 2010.
- Kuznecov LE. Bal'zamirovanie i restavracija trupov [Embalming and restoration of corpses] *Medicine* 1999; 496 p.
- Didenko AS, Smirenin SA, Vorob'ev AA. Bal'zamirovanie trupov v uslovijah sovremennyh lokal'nyh vooruzhennyh konfliktov [Embalming of corpses in the conditions of modern local armed conflicts]. *Epic Class Fighter Journal* 2004;14:16–9.
- Medvedev II. Osnovy patologoanatomicheskoi tehniki. [Fundamentals of pathological and anatomical technique. A guide for hospital prospectors and medical students.] 3rd ed. Moscow: M. Medicine; 1969. 288p.
- Ikeda K. Preparation of the autopsied body for embalming. *American Journal of Clinical Pathology* 1938;2-4:127–34.

22. Williams HW, Henderson DG. Restoration of autopsied bodies. *N Engl J Med* 1934;211:371.
23. Peasley ED. A method for restoring the body after autopsy. *JAMA* 1936;107:1378-9.
24. Krupin KN, Frishons Y, Kislov MA. Method of determining the corpse face's appearance to the life form. *Russian Journal of Forensic Medicine* 2018;4:28-31.
25. Golushko VP, Mazevskej VI, Anin JA. Osobnosti metodicheskogo podhoda k bal'zamirovaniju tel umersih na dlitel'nyj srok [Features of the methodological approach to embalming the bodies of the deceased for a long time]. *Journal of the GrSMU* 2008;4:133-5.
26. Harris MD. Reconstruction of fetuses after dissection. *J Clin Pathol* 1992;45:90.
27. Mott C, Chambers HM. Repair of fetal bodies after dissection. *J Clin Pathol* 1992;45:183.
28. Gau GS, Napier K, Bhundia J. Use of a tissue adhesive to repair fetal bodies after dissection. *J Clin Pathol* 1991;44:759-60.
29. Donlon S, Ruddy GN. Reconstruction of the body. In: Burton JL, Ruddy GN, editors. *The hospital autopsy*. 3rd ed. London, UK: HodderArnold; 2010. p. 308-14.
30. Frishons J, Strnad A, Rambousek P. Zachovat těla zemřelých [Preserve the bodies of the dead]. *Universe* 2020;10:2-5.

**ORCID ID:**

J. Frišhons 0000-0003-2998-2602;  
 M. A. Kislov 0000-0002-9303-7640;  
 M. Bezdickova 0000-0002-5798-4528;  
 V. Dzetkucicová 0000-0001-8545-6864

**Correspondence to:** Marcela Bezdickova, MD

Department of Anatomy, Swansea University Medical School,  
 Swansea, SA2 8PP, Wales, UK  
 Phone: +44 798 5441983  
 e-mail: marcela.bezdickova@swansea.ac.uk

*Conflict of interest statement:* No conflicts declared.

This is an open access article distributed under the terms of the Creative Commons Attribution-NonCommercial-NoDerivs 4.0 Unported (CC BY-NC-ND4.0) Licence (<http://creativecommons.org/licenses/by-nc-nd/4.0/>) which permits unrestricted noncommercial use, distribution, and reproduction in any medium, provided the original work is properly cited. *How to cite this article:* Frišhons J, Kislov MA, Bezdickova M, Dzetkucicová V. Notes on the techniques of body restoration after autopsy and the possibility of embalming. *Anatomy* 2022;16(2):108-113.

# In vivo experimental models of schizophrenia: mechanisms, features, advantages, disadvantages

Zeynep Mine Altunay<sup>1</sup> , Aysel Alphan<sup>2</sup> , Esat Adıgüzel<sup>2,3</sup> 

<sup>1</sup>Department of Neuroscience, School of Medicine, University of Connecticut, Farmington, CT, USA

<sup>2</sup>Department of Neuroscience, Institute of Health Sciences, Pamukkale University, Denizli, Türkiye

<sup>3</sup>Department of Anatomy, Faculty of Medicine, Pamukkale University, Denizli, Türkiye

## Abstract

The experimental models of human diseases are indispensable research methods which are undesirable to be tested on humans. It is inevitable for researchers who continue their careers in the field of anatomy to be aware of these methods. Here, experimental schizophrenia models that can be used to reveal brain functions and also pathophysiology of schizophrenia are discussed. It is aimed to give general information about the features of the experimental schizophrenia models that can be used by researchers in morphological sciences; therein the references should be considered for the setup of the experimental schizophrenia models. In this review, *in vivo* model of schizophrenia used on etiopathogenesis, pathophysiology, drug discovery and behavioral analysis are represented. And also we briefly indicate the molecular mechanisms of the experimental models that mimic schizophrenia-like symptoms and its behavioral outputs.

**Keywords:** animal models; experimental models; mental disorders; schizophrenia

Anatomy 2022;16(2):114–123 ©2022 Turkish Society of Anatomy and Clinical Anatomy (TSACA)

## Introduction

Morphological sciences have been mostly concerned with describing the structural features of organisms. As research techniques have been developed today, the scope of research in anatomy, which is one of the main branches of morphology, has also expanded. The experimental animal models developed based on evolutionary relationship of the human and other species have begun to be used in research to understand function of organism and pathology of illness. *In vivo* and *in vitro* experimental models are indispensable way for applying methods that are undesirable to be tested on humans. To be aware of these methods is inevitable for researchers who continue their careers in the field of anatomy. Here, experimental schizophrenia models that can be used to reveal brain functions and pathophysiology of the illness are discussed. It is aimed to give general information about the features of the experimental models; therein the references should be considered for the setup of the experimental schizophrenia models.

In this review, we represent the *in vivo* model of schizophrenia for researches on etiopathogenesis, pathophysiology, drug discovery and behavioral analysis. In addition, we briefly indicate the molecular mechanisms of the experimental models that mimic schizophrenia-like symptoms and its behavioral outputs.

## In Vivo Models of Schizophrenia (General Characteristics of Schizophrenia)

Schizophrenia is a serious and complex mental illness that has neurodevelopmental origin. It affects approximately 1% of the general population and is thought to result from interplay between genetic and environmental factors. It is unclear that how these risk factors collectively contribute to pathology. As multiple etiological factors contribute to the schizophrenia spectrum, altered symptomatology can be observed as the condition progresses. Symptoms of schizophrenia is classified primarily into three: positive, negative, and cognitive symptoms.<sup>[1–3]</sup> Positive symptoms (hallucinations, delusions, disorganized thought processes, disorganized or catatonic behavior, etc.) have an acute

onset, respond to antipsychotics and are composed of biochemical dysregulations.<sup>[4]</sup> Negative symptoms (affective flattening, alogia, apathy, anhedonia and asociality, attention disorders, etc.) respond to antipsychotics weakly, can be seen in combination with cognitive and behavioral disorders which also contain abnormal involuntary movements.<sup>[1,4]</sup> Cognitive symptoms (attention disorders, memory deficits, executive functioning, etc.) respond poorly to drugs and have negative effects on illness processes, quality of daily life.<sup>[1,5]</sup>

Although the pathophysiology of schizophrenia is not identified completely, it is well recognized that it has a complex structure. As a result, rather than relying on a single approach to explain schizophrenia, a combination of different approaches such as chemical, environmental, genetic, and structural components may be more helpful in understanding schizophrenia's pathogenesis.<sup>[3,6]</sup>

Alterations in neurotransmitters are one of the most important aspects of schizophrenia pathophysiology.<sup>[7,8]</sup> Reduced plasma dopamine metabolites are a sign of dopaminergic dysregulation in patients with a poor prognosis and social impairments. Higher dopamine metabolites, on the other hand, are detected mostly in patients with positive symptoms.<sup>[9]</sup> Glutamatergic hypofunction,<sup>[10]</sup> serotonergic dysregulation (as 5-HT1A receptor overexpression),<sup>[11]</sup> and changes in prefrontal cortex gamma-aminobutyric acid (GABA) neurotransmission (such as GABA-A receptor upregulation) have all been reported in the neurotransmitter researches.<sup>[12]</sup>

The researches on the brains of schizophrenic subjects are focused mainly on temporal cortex, frontal cortex, striatum, thalamus, hippocampus.<sup>[13-15]</sup> In these researches, decrease in temporal cortex, hippocampus, amygdala and parietal cortex volume are reported.

Genetic predisposition, because of the strong link with schizophrenia etiogenesis, is a crucial issue for most of the researches.<sup>[16]</sup> DISC1,<sup>[17]</sup> and dystrobrevin binding protein 1 (DTNBP1), dysbindin,<sup>[18]</sup> NRG1, ErbB4,<sup>[19]</sup> GAD, BDNF<sup>[20,21]</sup> are some of the mostly studied genes in the schizophrenia researches. Furthermore, environmental factors that include physiological, pharmacologic and psychological events have an influence on schizophrenia etiopathogenesis.<sup>[22]</sup>

In present review, we provide a brief overview of five animal models of schizophrenia. Also, we summarized common pathways involved in schizophrenia-like brain and behavioral abnormalities, which are specific to the animal model of interest.

At least twenty animal models of schizophrenia have been using in researches, and new ones are created in line

with purposes of the researches. In this review, we focused on prevalently used animal models:

- pharmacologic animal models,
- lesion animal models,
- neurodevelopmental animal models,
- genetic-epigenetic animal models,
- combinations of animal models

## Pharmacologic Animal Models

In 1950's first animal model of schizophrenia was developed in the basis of amphetamine. Psychosis that stimulated with amphetamine is used to mimic positive symptoms.<sup>[23]</sup> Pharmacologic animal models are based on the dysregulations in neurotransmitters. However, these models have constructive validity, they maintain limited information about cognition and thought processes.<sup>[24-38]</sup>

**Serotonergic approach:** Serotonergic (5-HT) neurotransmission is reported as an important issue for schizophrenia: Indolamines' (LSD: lyseric acid diethylamide) and phenethylamines' (mescaline), two main hallucinogenic drugs, effect mechanisms are mentioned to be mediated by 5-HT2A receptors.<sup>[38]</sup> On the other hand decrease in 5-HT2A receptor and increase in 5-HT1A receptor in the prefrontal cortex<sup>[39]</sup> are reported, and also the neuroendocrine respond to 5-HT2A receptor agonists is found to be weaker in schizophrenic individuals than healthy subjects.<sup>[40]</sup> In dopaminergic and glutamatergic animal models and also in human subjects, LSD mechanism on startle habituation and pre-pulse inhibition (PPI) are shown to act directly via 5-HT2A receptor stimulation.<sup>[41]</sup> Similarly phencyclidine (PCP) acts via indirect activation of 5-HT2A receptors and impairs PPI.<sup>[42]</sup> 5-HT5A receptor antagonist ASP5736's (N-(diaminomethylene)-1-(3,5-difluoropyridin-4-yl)-4-fluoroi-soquinoline-7-carboxamide (2E)-but-2-enedioate) therapeutic effects on positive and cognitive symptoms of schizophrenic individuals are mentioned as a validity for serotonergic approach.<sup>[11]</sup>

**Dopaminergic approach:** In dopaminergic approach, it is assumed that dysregulation in dopamine (DA) neurotransmission leads to the manifestation of the disorder. Positive symptoms are proposed to be thrived as a consequence of hyperactivity in mesolimbic dopaminergic neurons.<sup>[25]</sup> On the other hand, hypo-dopaminergic processes in fronto-cortical areas are proposed to lead negative symptoms.<sup>[26]</sup>

Locomotor hyperactivity and stereotypic behaviors can be induced after a single amphetamine administration in the animal models. Repeated amphetamine administration may cause impairment in locomotor activity and hyperac-

tivation in striatum dopaminergic neurotransmission, however alterations in social interaction may not observed in this animal model of schizophrenia. As a conclusion it is claimed that DA based animal models have limited constructive validity.<sup>[23,27]</sup>

**Glutamatergic approach:** Despite the amphetamine model, through the glutamatergic approach cognitive deficits, negative and positive symptoms, can be mimicked in the same animal model.<sup>[28-30]</sup> N-methyl-D-aspartate receptor (NMDAR) inhibitors like PCP, dizocilpine and kethamine are reported to induce schizophrenia like symptoms (hallucination, delusion, etc.) in healthy subjects.<sup>[28,29,31,32]</sup> Especially PCP is mentioned as an effective inducer of positive symptoms together with its influence on negative and cognitive symptoms.<sup>[28,33]</sup> PCP treatment to animals can mimic several behavioral and neurochemical abnormalities reported in schizophrenic patients, including hyperlocomotion, impairments in pre-pulse inhibition,<sup>[41]</sup> social interaction, working memory, and cognition.<sup>[35,36]</sup> Chronic PCP administration has been linked to a decrease in social contact. The acute treatment of haloperidol and clozapine are reported to reverse social interaction in the same study. As a result of those findings researchers concluded that this model mimics social withdrawal which is a negative symptom of schizophrenia.<sup>[33,39]</sup> The effects of PCP on gene expression in the brain are explored, and the expression levels of 146 genes (associated with apoptosis, neurological disorders, and schizophrenia-related genes) are found to be altered. Analyzing the signalization pathways reveal an increase in calcium signaling and long-term synaptic potentiation. These findings also support the use of PCP injection as a schizophrenia animal model.<sup>[37]</sup>

**GABAergic approach:** In prefrontal cortex  $\gamma$ -aminobutyric acid (GABA) neurons receive synaptic inputs from dopaminergic terminals, on the other hand they have inhibitory control over excitatory outputs of the pyramidal neurons, and also they have regulatory effects on developmental alterations that are seen in late adolescence. This mechanism makes GABAergic, dopaminergic and glutamatergic interactions a considerable issue in schizophrenia researches.<sup>[43,44]</sup>

Increase in GABA-A receptor expression<sup>[45]</sup> and decrease in glutamic acid decarboxylase 67 (GAD67) expression in prefrontal cortex<sup>[46]</sup> reflect GABAergic alterations that consist in pathophysiology of schizophrenia. After a decrease in calcium flux as a result of NMDAR hypofunction, GAD67 downregulation has been reported as a result of interneurons' response to NMDAR antagonism.<sup>[47]</sup> The decrease in PPI after injection of the GABA-A receptor antagonist picrotoxin to the rat medial pre-

frontal cortex<sup>[48]</sup> and the decrease in parvalbumin-containing GABAergic interneurons after prenatal MAM injection<sup>[49]</sup> have both been demonstrated in animal studies.

Risk factors like early life stress and trauma are shown to increase psychosis risk and accomplish subjects more vulnerable to hippocampal hyperactivity in their late life by impairing developing GABAergic neurons.<sup>[50]</sup> Hippocampal hyperactivity is associated with cognitive dysfunction<sup>[51]</sup> and impairment in perceived reality.<sup>[52]</sup> In schizophrenic individuals hippocampal hyperactivity level<sup>[52]</sup> or glutamatergic dysregulation leads to decrease in hippocampal volume which is used to mimic hippocampal dysfunction in developmental animal models of schizophrenia.<sup>[51]</sup>

## Lesion Animal Models

Because of the prefrontal cortex's executive functions in attention, working memory, social interaction and emotional processes, prefrontal cortical lesions are widely used in schizophrenia researches.<sup>[53]</sup> Behavioral experiments support the prefrontal cortex's regulatory role on subcortical DA activity.<sup>[54]</sup> Increase in amphetamine induced stereotypic behavior and continuous hyperexcitability with stress exposure are reported after prefrontal cortex lesion in adult rats.<sup>[55]</sup>

Hippocampal formation plays a key function in prefrontal cortex modulation and has direct control over the dopaminergic system.<sup>[56]</sup> Because of these features, lesions of hippocampal formation are used in researches: Excitotoxic lesions of dorsal and ventral hippocampus are found to stimulate different behavioral profiles. Lesions of dorsal hippocampus are not found to be effective in amphetamine induced locomotor activity.<sup>[57]</sup> However by kainic acid administration, neural loss is reported in dorsal hippocampus, and this model is proposed as a neurodegenerative animal model of schizophrenia.<sup>[58]</sup> On the other hand, lesions of ventral hippocampus by DA agonists are found to stimulate locomotor activity.<sup>[57]</sup>

Because of its importance in filtering sensory information, the thalamus is being addressed in researches. Abnormalities in corticothalamic limbic system are proposed as a useful target for studying sensorimotor deficits.<sup>[57]</sup> To sum up, although lesion models have face and predictive validity, dimensions of lesions and adult nature have limiting impacts on construct validity.

Lesions of ventral hippocampus are developed to mimic pathological conditions including ventricular enlargement and hippocampal atrophy. Abnormal behaviors after adolescence are reported to be induced by excitatory toxin ibotenic acid microinjection as a neonatal

lesion of ventral hippocampus. This model is shown to be resulted in behavioral alterations in different developmental stages: Spatial and working memory deficits are reported on postnatal day 25, however increase in social withdrawal and aggression are seen on postnatal day 35. Increase in sensitivity to dopaminergic and glutamatergic agonists, impairments in PPI and reward mechanisms and increase in drug sensitivity are reported around postnatal day 56.<sup>[13]</sup>

## Neurodevelopmental Animal Models

Weinberger (1986) was the first to propose the neurodevelopmental hypothesis, stating that brain developmental defects that occur early in life increase the chance of clinical symptoms later in life.<sup>[13]</sup> Neurodevelopmental animal models consist of prenatal exposure to environmental risk factors or toxic compounds. Based on schizophrenia epidemiology neurodevelopmental animal models of schizophrenia have construct and face validity.<sup>[59,60]</sup>

There are several methods that are used to induce inflammation: polyriboinosinic-polyricocytidylic acid [poly(I:C)],<sup>[61]</sup> methylazoxymethanol acetate (MAM)<sup>[62]</sup> and bacterial endotoxin lipopolysaccharide (LPS).<sup>[63,64]</sup> On the other hand multiple environmental stressors can be used alone or together to induce molecular processes related with schizophrenia: Social isolation,<sup>[65]</sup> maternal separation,<sup>[66]</sup> water stress.<sup>[55]</sup>

Usage of two different stress factors in different developmental stages are proposed to be more effective to mimic schizophrenia spectrum, which is also called two-hit animal model of schizophrenia.<sup>[67]</sup> Prenatal LPS administration with juvenile stress or prenatal polyI:C with neonatal LPS.

**Polyriboinosinic-polyricocytidylic acids [poly(I:C)]:** Multiple proinflammatory cytokines are released through the binding of poly(I:C) to its receptor, toll-like receptor (TLR) 3.<sup>[68]</sup> This viral compound has several influences on rodents: After its prenatal administration pups are reported to have increased locomotor sensitivity to psychostimulants, impaired pre-pulse inhibition and new object recognition, social withdrawal in their late life (in their adolescence or young adulthood). However, spatial memory impairments are not reported in researches.<sup>[61,69,70]</sup> Together with those behavioral abnormalities neurochemical alterations like decrease in DA and glutamate levels in prefrontal cortex and hippocampus are shown.<sup>[70]</sup> Increase in striatal and accumbal D1 and D2 receptors' function, increase in D2 receptor function in frontal cortex, decrease in DA and increase in tyrosine hydroxylase in striatum are demonstrated.<sup>[71]</sup>

**Bacterial endotoxin lipopolysaccharide (LPS):** Bacterial endotoxin LPS has its action through TLR4 receptors on macrophages and other immune cells. After binding to its receptor, it triggers several signal transduction cascades like release of proinflammatory cytokines, activation of transcription factors (like kappaB) and anti-inflammatory modulators (cytokines, proteins, etc.).<sup>[72]</sup>

Multiple behavioral deficits are also reported as a consequence of LPS administration: increase in locomotor activity, decrease in sociality, impairment in PPI and memory, anxiety like behaviors.<sup>[69]</sup>

It is demonstrated that LPS administration leads to dysregulation of dopaminergic signalization: Increase in accumbal and striatal DA, decrease in striatal and frontal DA, decrease in frontal 3,4-dihydroxyphenylacetic acid (DOPAC), increase in frontal and decrease in striatal homovallinic acid levels.<sup>[71,73]</sup>

**Methylazoxymethanol acetate (MAM):** Prenatal MAM administration leads to developmental damage in fetal brain because of DNA synthesis inhibition during mitosis. This abnormal brain development results in multiple behavioral deficits like impairment in sociality, PPI, spatial cognition.<sup>[62]</sup> In another study increase in accumbal DA levels is reported. Increase in ventral tegmental DA activity and locomotor sensitivity to amphetamine are reversed by the injection of tetrodotoxin to ventral hippocampus.<sup>[74]</sup>

**Environmental stress:** Multiple environmental stress factors can be applied in different developmental stages acutely or chronically, alone or in combination: Social isolation, restraint, noise, light, water. Sociality is reported to be critical for normal developmental processes of rats; they have socially active nature which also has hierarchical rules.<sup>[59]</sup> For this reason any kind of social deprivation can result in abnormal brain development which also leads to locomotor hyperactivity, impaired cognition, increased anxiety, depressive like behaviors and aggression which are also reported as schizophrenia symptoms.<sup>[59,65]</sup>

Stress exposure stimulates the release of stress hormones that resulted in dysregulation of several neurochemical compounds: decrease in DA, DOPAC and homovallinic acid levels,<sup>[75]</sup> increase in striatal and accumbal, decrease in frontal serotonin levels, increase in corticostriatal noradrenaline level which are related to anxiety and positive symptoms,<sup>[76]</sup> downregulation in cortical parvalbumin containing GABAergic neurotransmission.<sup>[65]</sup>

Schizophrenia-like behavioral and neurochemical abnormalities that are generated by using environmental stressors can be reversed by antipsychotics, and this condition is proposed to be sufficient for this model's validity.<sup>[77]</sup>

## Genetic Animal Models (Knockout & Transgenic)

Genetic studies are identified several specific genes that are associated with schizophrenia disorder.<sup>[78-90]</sup> Generally, twin studies are shown that schizophrenia is a predominant genetic disorder, with estimates of heritability risk ranging at 50–80%. In researches it is demonstrated that single effects of a major gene are unlikely to mimic schizophrenia's complexity; instead, polygenic models consists of multiple-risk genes can provide the best expression for schizophrenia.<sup>[91,92]</sup>

**There are several genetic animal models of schizophrenia:** neurodevelopmental candidate genes (reelin, BDNF, GAD37, N-CAM); hyperdopaminergic hypothesis related genes (Akt, PP2A, B-arrestin 2, DARPP-32); hypoglutamatergic approach related genes (NMDR receptor subunit 1, calciceurin knockout); susceptibility genes of schizophrenia (COMT, NRG1, Dysbindin, DISC1, RGS-4, CHRNA7, NPAS3, PRODH2 [22q11]).<sup>[2,78-80,93]</sup>

N-methyl-D-aspartat (NMDA) receptor subunits importance in schizophrenia neuropathology is reported in schizophrenic postmortem brain tissues: decrease in NR1 subunit expression,<sup>[78]</sup> deficits in associative learning processes are linked with NMDAR dependent plasticity.<sup>[79]</sup> Hyperlocomotion, stereotypic behavior, decrease in social interaction, deficits in cognition and abnormal brain development, impairment in working memory, anhedonia and anxiety,<sup>[2,80]</sup> impairment in spatial memory, hyperactivity in novel environment and depression<sup>[81]</sup> are reported in NR1 mutant animal models of schizophrenia. These behavioral anomalies are not seen if NR1 subunit deficiency is generated in adolescence.<sup>[2]</sup>

DISC1's influence on neuronal migration, synaptic plasticity, neurogenesis together with its effect on mechanisms in schizophrenia onset, is demonstrated in multiple researches.<sup>[82-84]</sup> Schizophrenia like behavioral deficits are reported in genetic models of DISC1: Hyperactivity in novel environment, immobility in forced swimming test, impairment in pre-pulse inhibition,<sup>[85]</sup> hyper or hypolocomotion, impairment in cognition and alterations in brain morphology which are also compatible with schizophrenic subjects' symptoms.<sup>[86,87]</sup>

In multiple studies, it is reported that “dysbindin1”, coded by DTNBP1, has an influence in regulation of exocytosis and vesicular genesis during neurotransmitter release. In addition, it has a role in dopaminergic and glutamatergic neurotransmissions. On the other hand it is shown that DTNBP1 associates with prefrontal and cortical functions of schizophrenic individuals, whereas episodic and working memory of healthy individuals. Decrease in

dysbindin1 mRNA and protein expressions are reported in postmortem brain tissues of schizophrenic subjects.<sup>[1,88]</sup> Sand (Sdy) mice have DTNBP1 homozygote mutations that lead to lack of dysbindin1 protein expression.<sup>[88]</sup>

Schizophrenia like behavioral alterations as increase in locomotor activity, cognitive deficits, decrease in social interaction, and impairment in PPI and response adaptation to sensory stimulus are demonstrated.<sup>[89]</sup> Sdy mice can be used to investigate dysbindin's potential pathways: decrease in mGluRI signalization and its association with synaptic plasticity are shown. Heterozygote mutants are also used in researches.<sup>[88]</sup>

## Combinations of Animal Models

To generate an animal model, combination of multiple animal models that includes several molecular mechanisms is suggested to mimic the complex mechanisms of schizophrenia. Animal models consist of multiple parameters can be more useful in understanding mechanisms of schizophrenia and generating more effective therapeutic strategies.<sup>[83,84,90,91]</sup> For instance, measuring the adult behavioral alterations in dominant-negative N-terminus human DISC1 (DN-DISC1) expressing transgenic mice is used with the combination of neonatal<sup>[83]</sup> and prenatal<sup>[84]</sup> poly(I:C) injection. Deficits in hippocampus dependent fear memory, working memory, object recognition memory, decrease in sociality, aggressive behavior are reported in neonatal poly(I:C) injected DN-DISC1 mice.<sup>[83]</sup> To determine the efficiency of animal models, behavioral alterations are investigated by using four different experimental groups: (1) control group, (2) standard genetic group (3), environmental group, (4) gene × environment group. Behavioral paradigms are found to be worsening in gene × environment group, and these kind of models are suggested to be critical for animal model's validity.<sup>[91]</sup>

## Behavioral Parameters and Their Testing Methods

Clinical symptoms and related behavioral parameters in animal models of schizophrenia:

**Positive symptoms:** In animal models hyperlocomotion in novel environment and as a response to stress are linked with psychomotor agitation, delusion, hallucination and psychosis which are seen in human subjects. Stereotypic behaviors, hyperlocomotion and vulnerability to stress can be investigated by open field test. In animal models hyperactivity can be measured and observed as postural disorders, climbing behavior, stereotypic movements (repeated sniffing, licking, etc.). Instead of catatonia, the term “catalepsy” is used for animals and can be measured by wire grids and bar test.

**Negative symptoms:** Anhedonia, lack of motivation are seen as an increased immobility in animal models and can be measured by forced swimming and sucrose preference tests. To identify mood disorders, elevated plus maze, light/dark box and open area tests can be used. Social withdrawal which is seen in schizophrenic individuals can be measured by social interaction tests in animal models. There are several protocols for social interaction tests: 3-Chamber social interaction and social novelty preference paradigm are commonly used.

**Cognitive disorders:** In animal models schizophrenia-like cognitive deficits can be evaluated by multiple parameters, that consist of working memory, long term memory, spatial learning memory, executive functions by using cognitive tests: Barnes maze, Radial arm maze, Morris water maze, T or Y maze, attentional set shifting task, 5-choice serial-reaction time test, radial arm maze.

### Conclusion

There are multiple animal models of schizophrenia (Table 1), targeting specific mechanisms of interest. Recent researches are focused on the animal models that consist of multiple mechanisms and researchers are mentioned the requirement for the combination of multiple models to mimic this spectrum.

Animal models can reflect one or more symptoms of schizophrenia, however this disorder has much more of that. For instance animal model of amphetamine can reflect hyperactivity as a response to striatal dopaminergic activity, however other symptoms like cognitive deficits can not be observed by this animal model.<sup>[27]</sup> On the other hand in the model of glutamatergic hypofunction, hyperactivity and worsening in positive symptoms are demonstrated.<sup>[30]</sup> It is shown that prefrontal glutamatergic hypofunction leads not only positive symptoms, but also negative symptoms together with cognitive deficits.<sup>[28,29]</sup>

In researches it is demonstrated that preference of animals' strain, developmental stages for any administration (like LPS, etc.) or any environmental stressors that will be applied, is critical for the studies' purpose and results.<sup>[62]</sup> For instance after single or repeated PCP administration, decrease in sociality is reported,<sup>[30]</sup> whereas social deficits as a response to amphetamine administration is contradictory. Prenatal administration of MAM and poly (I:C) are reported to lead decrease in sociality, however preadolescent administration of MAM also results with social deficits.<sup>[74]</sup> As a response to neonatal lesion of ventral hippocampus, decrease in social interaction together with the increase in aggression is shown.<sup>[14]</sup> Repeated administration of PCP is found to induce anhedonia like behavior,

**Table 1**  
Results of the measurements (n=55).

Animal model	Approaches	Clinical symptoms*	Schizophrenia like symptoms	Behavioral task
Pharmacological	Serotonergic Dopaminergic Glutamatergic GABAergic	Positive	Hiperlocomotion Climbing behavior Stereotypic movements Postural disorders	Open field test Wire grids Bar test PPI
Lesion	Hippocampal Thalamic			
Neurodevelopmental	Poly(I:C) LPS MAM Stress	Negative	Social interaction Novelty preference Explorative behavior	3-Chamber SI & NP Resident intruder Social play Self grooming
Genetic	Knock out Transgenic			
Combined models	Env × Env Env × Gene Gene × Gene Gene × Env × Env	Cognitive	Social cognition Memory Executive functioning Attention	Morris water maze Barnes maze Radial arm maze Latent inhibition 5-CSRTT Attentional set shifting T/Y maze

\*Type of clinical symptom of schizophrenia depends on the animal model that was chosen and developmental stage of the animal model that was formed. Animal model may include one, two or all of the symptoms. 5-CSRTT: five card sorting reaction time test; Env: environmental; Gene: genetic; LPS: lipopolysaccharide; MAM: methylazoxymethanol acetate; NP: novelty preference; Poly(I:C): polyriboinosinic-polyricotidylic acid; PPI: pre-pulse inhibition; SI: social interaction.

however single administration of PCP is reported to be insufficient.<sup>[28,39]</sup>

Requirement of generating novel animal models that mimic positive, negative and cognitive disorders together in one model are demonstrated. That kind of models can include multiple molecular mechanisms like the schizophrenia spectrum itself. Thus, by using combination of multiple animal models, all forms of validity can be maintained which can also leads to investigation of better therapeutic strategies and better understanding of schizophrenia's etiopathogenesis.<sup>[94]</sup> By this point of view, combining the interaction of two or more impact factors, as environment × gene, gene × gene, environment × environment, environment × gene × environment are proposed to be useful for modeling schizophrenia.<sup>[6,95,96]</sup>

As a result, according to their research hypothesis researchers need to decide which experimental animal model or models to choose. This review aimed to provide a perspective to researchers who will conduct research on the physiopathology or treatment of schizophrenia.

### Conflict of Interest

The authors declare that there are no conflicts of interest.

### Author Contributions

ZMA: study design, systematic search and screening of literature, drafting the manuscript, edits; AA: systematic search and screening of literature, commenting on drafts and the final version of the manuscript; EA: senior author, supervising work, commenting on drafts and final version of the manuscript.

### Funding

No funding was received for this research.

### References

- Andreasen NC. Symptoms, signs, and diagnosis of schizophrenia. *Lancet* 1995;346:477–81.
- Belforte JE, Zsiris V, Sklar ER, Jiang Z, Yu G, Li Y, Quinlan ME, Nakazawa K. Postnatal NMDA receptor ablation in corticolimbic interneurons confers schizophrenia like phenotypes. *Nat Neurosci* 2010;13:76–83.
- Andreassen OA, Thompson WK, Dale AM. Boosting the power of schizophrenia genetics by leveraging new statistical tools. *Schizophr Bull* 2014;40:13–17.
- Uzun Ö. Pozitif – negatif belirtiler. In: Ceylan E, Çetin M, editors. *Şizofreni*. Vol. 1. İstanbul: Yerküre Tanıtım ve Yayıncılık; 2005. p. 643–56.
- Foussias G, Remington G. Negative symptoms in schizophrenia: avolition and Occam's razor. *Schizophr Bull* 2010;36:359–69.
- Bayer TA, Falkai P, Maier W. Genetic and non-genetic vulnerability factors in schizophrenia: the basis of the "two hit hypothesis". *J Psychiatr Res* 1999;33:543–8.
- Kim DH, Stahl SM. Antipsychotic drug development. *Curr Top Behav Neurosci* 2010;4:123–39.
- Taly A. Novel approaches to drug design for the treatment of schizophrenia. *Exp Opin Drug Discov* 2013;8:1285–96.
- Murray RM, Lappin J, Di Forti M. Schizophrenia: from developmental deviance to dopamine dysregulation. *Eur Neuropsychopharmacol* 2008;18:S129–34.
- Inta D, Monyer H, Sprengel R, Meyer-Lindenberg A, Gass P. A comprehensive review: mice with genetically altered glutamate receptors as models of schizophrenia. *Neurosci Biobehav Rev* 2010;34:285–94.
- Yamazaki M, Harada K, Yamamoto N, Yarimizu J, Okabe M, Shimada T, Ni K, Matsuoka N. ASP5736, a novel 5-HT<sub>5A</sub> receptor antagonist, a meliorates positive symptoms and cognitive impairment in animal models of schizophrenia. *Eur Neuropsychopharmacol* 2014;24:1698–708.
- Penschuck S, Flagstad P, Didriksen M, Leist M, Michael-Titus AT. Decrease in parvalbumin-expressing neurons in the hippocampus and increased phencyclidine-induced locomotor activity in the rat methylazoxymethanol (MAM) model of schizophrenia. *Eur J Neurosci* 2006;23:279–84.
- Lipska BK, Jaskiw GE, Braun AR, Weinberger DR. Prefrontal cortical and hippocampal modulation of haloperidol-induced catalepsy and apomorphine-induced stereotypic behaviors in the rat. *Biol Psychiatry* 1995;38:255–62.
- Tseng KY, Chambers RA, Lipska BK. Neonatal ventral hippocampal lesion as a heuristic neurodevelopmental model of schizophrenia. *Behav Brain Res* 2009;204:295–305.
- Flagstad P, Mork A, Glenthøj BY, van Beek J, Michael-Titus AT, Didriksen M. Disruption of neurogenesis on gestational day 17 in the rat causes behavioral changes relevant to positive and negative schizophrenia symptoms and alters amphetamine-induced dopamine release in nucleus accumbens. *Neuropsychopharmacology* 2004;29:2052–64.
- Rodriguez-Murillo L, Gogos JA, Karayiorgou M. The genetic architecture of schizophrenia: new mutations and emerging paradigms. *Annu Rev Med* 2012;63:63–80.
- Niwa M, Kamiya A, Murai R, Kubo KI, Gruber AJ, Tomita K, Lu L, Tomisato S, Jaaro-Peled H, Seshadri S, Hiyama H, Huang B, Kohda K, Noda Y, O'Donnell P, Nakajima K, Sawa A, Nabeshima T. Knockdown of DISC1 by in utero gene transfer disturbs postnatal dopaminergic maturation in the frontal cortex and leads to adult behavioral deficits. *Neuron* 2010;65:480–9.
- Papaleo F, Yang F, Garcia S, Chen J, Lu B, Crawley JN, Weinberger DR. Dysbindin-1 modulates prefrontal cortical activity and schizophrenia-like behaviors via dopamine/D2 pathways. *Mol Psychiatry* 2012;17:85–98.
- Mei L, Xiong W. Neuregulin 1 in neural development, synaptic plasticity and schizophrenia. *Nat Rev Neurosci* 2008;9:437–52.
- Aberg KA, McClay JL, Nerella S, Clark S, Kumar G, Chen W, Khachane AN, Xie L, Hudson A, Gao G, Harada A, Hultman CM, Sullivan PF, Magnusson PKE, van den Oord EJ. Methylome-wide association study of schizophrenia: identifying blood biomarker signatures of environmental insults. *JAMA Psychiatry* 2014;71:255–64.
- Ikegame T, Bundo M, Murata Y, Kasai k, Kato T, Iwamoto K. DNA methylation of the BDNF gene and its relevance to psychiatric disorders. *J Hum Genet* 2013;58:434–8.

22. Van Os J, Kenis G, Rutten BPF. The environment and schizophrenia. *Nature* 2010;468:203–12.
23. Featherstone RE, Rizos Z, Kapur S, Fletcher PJ. A sensitizing regimen of amphetamine that disrupts attentional set-shifting does not disrupt working or long-term memory. *Behav Brain Res* 2008;189:170–9.
24. Marcotte ER, Pearson DM, Srivastava LK. Animal models of schizophrenia: a critical review. *J Psychiatry Neurosci* 2001;26:395–410.
25. Carlsson A. The dopamine theory revisited. In: Hirsch SR, Weinberger DR, editors. *Schizophrenia*. Oxford: Blackwell Science; 1995. p. 379–400.
26. Dworkin RH, Opler LA. Simple schizophrenia, negative symptoms, and prefrontal hypodopaminergia. *Am J Psychiatry* 1992;149:1284–5.
27. Papaleo F, Yang F, Garcia S, Chen J, Lu B, Crawley JN, Weinberger DR. Dysbindin-1 modulates prefrontal cortical activity and schizophrenia-like behaviors via dopamine/D2 pathways. *Mol Psychiatry* 2012;17:85–98.
28. Javitt DC, Zukin SR. Recent advances in the phencyclidine model of schizophrenia. *Am J Psychiatry* 1991;148:1301–8.
29. Krystal JH, Karper LP, Seibyl JP, Freeman GK, Delaney R, Bremner JD, Heninger GR, Bowers MB Jr, Charney DS. Subanesthetic effects of the noncompetitive NMDA antagonist, ketamine, in humans. *Arch Gen Psychiatry* 1994;51:199–214.
30. Jenkins TA, Harte MK, Reynolds GP. Effect of subchronic phencyclidine administration on sucrose preference and hippocampal parvalbumin immunoreactivity in the rat. *Neurosci Lett* 2010;471:144–7.
31. Cohen J, Struening EL. Opinions about mental illness in the personnel of two large mental hospitals. *J Abnorm Psychol* 1962;64:349–60.
32. Xia Y, Wang CZ, Liu J, Anastasio NC, Johnson KM. Brain-derived neurotrophic factor prevents phencyclidine induced apoptosis in developing brain by parallel activation of both the ERK and PI-3K/Akt pathways. *Neuropharmacology* 2010;58:330–6.
33. Seillier A, Giuffrida A. Evaluation of NMDA receptor models of schizophrenia: Divergences in the behavioral effects of sub-chronic PCP and MK-801. *Behav Brain Res* 2009;204:410–5.
34. Geyer MA, Krebs-Thomson K, Braff DL, Swerdlow NR. Pharmacological studies of prepulse inhibition models of sensorimotor gating deficits in schizophrenia: a decade in review. *Psychopharmacology (Berl)* 2001;156:117–54.
35. Noda A, Noda Y, Kamei H, Ichihara K, Mamiya T, Nagai T, Sugiura S, Furukawa H, Nabeshima T. Phencyclidine impairs latent learning in mice: interaction between glutamatergic systems and sigma(1) receptors. *Neuropsychopharmacology* 2001;24:451–60.
36. Jentsch JD, Roth RH. The neuropsychopharmacology of phencyclidine: from NMDA receptor hypofunction to the dopamine hypothesis of schizophrenia. *Neuropsychopharmacology* 1999;20:201–25.
37. Martin MV, Mirnics K, Nisenbaum LK, Vawter MP. Olanzapine reversed brain gene expression changes induced by phencyclidine treatment in non-human primates. *Mol Neuropsychiatry* 2015;1:82–93.
38. Harrison PJ, Burnet PW. The 5-HT<sub>2A</sub> (serotonin<sub>2A</sub>) receptor gene in the aetiology, pathophysiology and pharmacotherapy of schizophrenia. *J Psychopharmacol* 1997;11:18–20.
39. Burnet PW, Eastwood SL, Harrison PJ. [<sup>3</sup>H]WAY-100635 for 5-HT<sub>1A</sub> receptor autoradiography in human brain: a comparison with [<sup>3</sup>H]8-OH-DPAT and demonstration of increased binding in the frontal cortex in schizophrenia. *Neurochem Int* 1997;30:565–74.
40. Abi-Dargham A, Laruelle M, Aghajanian GK, Charney D, Krystal J. The role of serotonin in the pathophysiology and treatment of schizophrenia. *J Neuropsychiatry Clin Neurosci* 1997;9:1–17.
41. Geyer MA. Behavioral studies of hallucinogenic drugs in animals: implications for schizophrenia research. *Pharmacopsychiatry* 1998;31:S73–9.
42. Yamada S, Harano M, Annoh N, Nakamura K, Tanaka M. Involvement of serotonin 2A receptors in phencyclidine-induced disruption of prepulse inhibition of the acoustic startle in rats. *Biol Psychiatry* 1999;46:832–8.
43. Lewis DA, Pierri JN, Volk DW, Melchitzky DS, Woo TU. Altered GABA neurotransmission and prefrontal cortical dysfunction in schizophrenia. *Biol Psychiatry* 1999;46:616–26.
44. Homayoun H, Moghaddam B. NMDA receptor hypofunction produces opposite effects on prefrontal cortex interneurons and pyramidal neurons. *J Neurosci* 2007;27:11496–500.
45. Benes FM, Vincent S, Alsterberg G, Bird ED, SanGiovanni JP. Increased GABA<sub>A</sub> receptor binding in superficial layers of cingulate cortex in schizophrenics. *J Neurosci* 1992;12:924–9.
46. Akbarian S, Kim JJ, Potkin SG, Hagman JO, Tafazzoli A, Bunney WE, Bunney WE Jr, Jones EG. Gene expression for glutamic acid decarboxylase is reduced without loss of neurons in prefrontal cortex of schizophrenics. *Arch Gen Psychiatry* 1995;52:258–66.
47. Zhang Y, Behrens MM, Lisman JE. Prolonged exposure to NMDAR antagonist suppresses inhibitory synaptic transmission in prefrontal cortex. *J Neurophysiol* 2008;100:959–65.
48. Japha K, Koch M. Picrotoxin in the medial prefrontal cortex impairs sensorimotor gating in rats: reversal by haloperidol. *Psychopharmacology (Berl)* 1999;144:347–54.
49. Guidotti A, Auta J, Davis JM, Dong E, Grayson DR, Veldic M, Zhang X, Costa E. GABAergic dysfunction in schizophrenia: new treatment strategies on the horizon. *Psychopharmacology (Berl)* 2005;180:191–205.
50. Tricoire L, Pelkey KA, Erkkila BE, Jeffries BW, Yuan X, McBain CJ. A blueprint for the spatiotemporal origins of mouse hippocampal interneuron diversity. *J Neurosci* 2011;31:10948–70.
51. Tregellas JR, Smucny J, Harris JG, Olincy A, Maharajh K, Kronberg E, Eichman LC, Lyons E, Freedman RE. Intrinsic hippocampal activity as a biomarker for cognition and symptoms in schizophrenia. *Am J Psychiatry* 2014;171:549–56.
52. Schobel SA, Chaudhury NH, Khan UA, Paniagua B, Styner MA, Asllani I, Inbar BP, Corcoran CM, Lieberman JA, Moore H, Small SA. Imaging patients with psychosis and a mouse model establishes a spatiotemporal pattern of hippocampal dysfunction and implicates glutamate elevation as a pathogenic driver. *Neuron* 2013;78:81–93.
53. Levin HS, Eisenberg HM, Benton AL. *Frontal lobe and dysfunction*. Oxford: Oxford University Press; 1991. 448 p.
54. Le Moal M, Simon H. Mesocorticolimbic dopaminergic network: functional and regulatory roles. *Physiol Rev* 1991;71:155–234.
55. Jaskiw GE, Weinberger DR. Ibotenic acid lesions of medial prefrontal cortex augment swim-stress-induced locomotion. *Pharmacol Biochem Behav* 1992;41:607–9.

56. Grace AA. Gating of information flow within the limbic system and the pathophysiology of schizophrenia. *Brain Res Brain Res Rev* 2000;31:330–41.
57. Mittleman G, Bratt AM, Chase R. Heterogeneity of the hippocampus: effects of subfield lesions on locomotion elicited by dopaminergic agonists. *Behav Brain Res* 1998;92:31–45.
58. Csernansky JG, Csernansky CA, Kogelman L, Montgomery EM, Bardgett ME. Progressive neurodegeneration after intracerebroventricular kainic acid administration in rats: implications for schizophrenia? *Biol Psychiatry* 1998;44:1143–50.
59. Lewis DA, Levitt P. Schizophrenia as a disorder of neurodevelopment. *Annu Rev Neurosci* 2002;25:409–32.
60. Koenig JJ, Elmer GI, Shepard PD, Lee PR, Mayo C, Joy B, Hercher E, Brady DL. Prenatal exposure to a repeated variable stress paradigm elicits behavioral and neuroendocrinological changes in the adult offspring: potential relevance to schizophrenia. *Behav Brain Res* 2005;156:251–61.
61. Meyer U. Prenatal poly(i:C) exposure and other developmental immune activation models in rodent systems. *Biol Psychiatry* 2014;75:307–15.
62. Moore H, Jentsch JD, Ghajarnia M, Geyer MA, Grace AA. A neurobehavioral systems analysis of adult rats exposed to methylazoxymethanol acetate on E17: implications for the neuropathology of schizophrenia. *Biol Psychiatry* 2006;60:253–64.
63. Kirsten TB, Taricano M, Flório JC, Palermo-Neto J, Bernardi MM. Prenatal lipopolysaccharide reduces motor activity after an immune challenge in adult male offspring. *Behav Brain Res* 2010;211:77–82.
64. Lin YL, Wang S. Prenatal lipopolysaccharide exposure increases depression-like behaviors and reduces hippocampal neurogenesis in adult rats. *Behav Brain Res* 2014;259:24–34.
65. Powell SB, Sejnowski TJ, Behrens MM. Behavioral and neurochemical consequences of cortical oxidative stress on parvalbumin-interneuron maturation in rodent models of schizophrenia. *Neuropharmacology* 2012;62:1322–31.
66. Van Vugt RWM, Meyer F, van Hulten JA, Vernooij J, Cools AR, Verheij MMM, Martens GJM. Maternal care affects the phenotype of a rat model for schizophrenia. *Front Behav Neurosci* 2014;8:1–9.
67. Davis J, Moylan S, Harvey BH, Maes M, Berk M. Neuroprogression in schizophrenia: pathways underpinning clinical staging and therapeutic corollaries. *Aust N Z J Psychiatry* 2014;48:512–29.
68. Forrest CM, Khalil OS, Pizar M, Smith RA, Darlington LG, Stone TW. Prenatal activation of toll-like receptors-3 by administration of the viral mimetic poly(I:C) changes synaptic proteins, N-methyl-D-aspartate receptors and neurogenesis markers in offspring. *Mol Brain* 2012;5:22.
69. Arseneault D, St-Amour I, Cisbani G, Rousseau LS, Cicchetti F. The different effects of LPS and poly I:C prenatal immune challenges on the behavior, development and inflammatory responses in pregnant mice and their offspring. *Brain Behav Immun* 2014;38:77–90.
70. Bitanirhive BKY, Peleg-Raibstein D, Mouttet F, Feldon J, Meyer U. Late prenatal immune activation in mice leads to behavioral and neurochemical abnormalities relevant to the negative symptoms of schizophrenia. *Neuropsychopharmacology* 2010;35:2462–78.
71. Vuillermot S, Weber L, Feldon J, Meyer U. A longitudinal examination of the neurodevelopmental impact of prenatal immune activation in mice reveals primary defects in dopaminergic development relevant to schizophrenia. *J Neurosci* 2010;30:1270–87.
72. Aderem A, Ulevitch RJ. Toll-like receptors in the induction of the innate immune response. *Nature* 2000;406:782–7.
73. Ozawa K, Hashimoto K, Kishimoto T, Shimizu E, Ishikura H, Iyo M. Immune activation during pregnancy in mice leads to dopaminergic hyperfunction and cognitive impairment in the offspring: a neurodevelopmental animal model of schizophrenia. *Biol Psychiatry* 2006;59:546–54.
74. Lodge DJ, Behrens MM, Grace AA. A loss of parvalbumin containing interneurons is associated with diminished oscillatory activity in an animal of schizophrenia. *J Neurosci* 2009;29:2344–54.
75. Möller M, Du Preez JL, Viljoen FP, Berk M, Emsley R, Harvey BH. Social isolation rearing induces mitochondrial, immunological, neurochemical and behavioural deficits in rats, and is reversed by clozapine or N-acetyl cysteine. *Brain Behav Immun* 2013;30:156–67.
76. Möller M, Du Preez JL, Viljoen FP, Berk M, Harvey BH. N-acetyl cysteine reverses social isolation rearing induced changes in corticostriatal monoamines in rats. *Metab Brain Dis* 2013;28:687–96.
77. Fone KCF, Porkess MV. Behavioural and neurochemical effects of post-weaning social isolation in rodents—relevance to developmental neuropsychiatric disorders. *Neurosci Biobehav Rev* 2008;32:1087–102.
78. Ibrahim HM, Healy DJ, Hogg AJ Jr, Meador-Woodruff JH. Nucleus-specific expression of ionotropic glutamate receptor subunit mRNAs and binding sites in primate thalamus. *Brain Res Mol Brain Res* 2000;79:1–17.
79. Stephan KE, Baldeweg T, Friston KJ. Synaptic plasticity and dysconnection in schizophrenia. *Biol Psychiatry* 2006;59:929–39.
80. Fradley RL, O'Meara GF, Newman RJ, Andrieux A, Job D, Reynolds DS. STOP knockout and NMDA NR1 hypomorphic mice exhibit deficits in sensorimotor gating. *Behav Brain Res* 2005;163:257–64.
81. Miyamoto Y, Yamada K, Noda Y, Mori H, Mishina M, Nabeshima T. Hyperfunction of dopaminergic and serotonergic neuronal systems in mice lacking the NMDA receptor 1 subunit. *J Neurosci* 2001;21:750–7.
82. Ming GL, Song H. DISC1 partners with GSK3beta in neurogenesis. *Cell* 2009;136:990–2.
83. Ibi D, Nagai T, Koike H, Kitahara Y, Mizoguchi H, Niwa M, Jaaro-Peled H, Nitta A, Yoneda Y, Nabeshima T, Sawa A, Yamada K. Combined effect of neonatal immune activation and mutant DISC1 on phenotypic changes in adulthood. *Behav Brain Res* 2010;206:32–7.
84. Abazyan B, Nomura J, Kannan G, Ishizuka K, Tamashiro KL, Nucifora F, Pogorelov V, Ladenheim B, Yang C, Krasnova IN, Cadet JL, Pardo C, Mori S, Kamiya A, Vogel MW, Sawa A, Ross CA, Pletnikov MV. Prenatal interaction of mutant DISC1 and immune activation produces adult psychopathology. *Biol Psychiatry* 2010;68:1172–81.
85. Harrison PJ, Weinberger DR. Schizophrenia genes, gene expression and neuropathology: on the matter of their convergence. *Mol Psychiatry* 2005;10:40–68.
86. Schurov IL, Handford EJ, Brandon NJ, Whiting PJ. Expression of disrupted in schizophrenia 1 (DISC1) protein in the adult and developing mouse brain indicates its role in neurodevelopment. *Mol Psychiatry* 2004;9:1100–10.
87. Shen S, Lang B, Nakamoto C, Zhang F, Pu J, Kuan SL, Chatzi C, He S, Mackie I, Brandon NJ, Marquis KL, Day M, Hurko O, McCaig CD, Riedel G, St Clair D. Schizophrenia-related neural and

- behavioral phenotypes in transgenic mice expressing truncated Disc1. *J Neurosci* 2008;28:10893–904.
88. Bhardwaj SK, Ryan RT, Wong TP, Srivastava LK. Loss of dysbindin-1, a risk gene for schizophrenia, leads to impaired group I metabotropic glutamate receptor function in mice. *Front Behav Neurosci* 2015;9:72.
  89. Xu Y, Sun Y, Ye H, Zhu L, Liu J, Wu X, Wang L, He T, Shen Y, Wu JY, Xu Q. Increased dysbindin-1B isoform expression in schizophrenia and its propensity in aggregates formation. *Cell Discov* 2015;1:15032.
  90. Neeley EW, Berger R, Koenig JI, Leonard S. Strain dependent effects of prenatal stress on gene expression in the rat hippocampus. *Physiol Behav* 2011;104:334–9.
  91. Petrowski Z, Adam G, Tuboly G, Kekesi G, Benedek G, Keri S, Horvath G. Characterization of gene-environment interactions by behavioral profiling of selectively bred rats: the effect of NMDA receptor inhibition and social isolation. *Behav Brain Res* 2013;240:134–45.
  92. Nestler EJ, Hyman SE. Animal models of neuropsychiatric disorders. *Nat Neurosci* 2010;13:1161–9.
  93. Weinberger DR, Egan MF, Bertolino A, Callicott JH, Mattay VS, Lipska BK, Berman KF, Goldberg TE. Prefrontal neurons and the genetics of schizophrenia. *Biol Psychiatry* 2001;50:825–44.
  94. Maric NP, Svrakic DM. Why schizophrenia genetics needs epigenetics: a review. *Psychiatr Danub* 2012;24:2–18.
  95. Muraki K, Tanigaki K. Neuronal migration abnormalities and its possible implications for schizophrenia. *Front Neurosci* 2015;9:74.
  96. Ram E, Raphaeli S, Avital A. Prepubertal chronic stress and ketamine administration to rats as a neurodevelopmental model of schizophrenia symptomatology. *Int J Neuropsychopharmacol* 2013;16:2307–14.

**ORCID ID:**

Z. M. Altunay 0000-0002-7663-7417;  
 A. Alphan 0000-0001-9624-2036;  
 E. Adigüzel 0000-0002-1110-5786



**Correspondence to:** Esat Adigüzel, MD

Department of Anatomy, Faculty of Medicine,  
 Pamukkale University, Denizli, Türkiye  
 Phone: +90 542 711 80 31  
 e-mail: adiguzel@pau.edu.tr

*Conflict of interest statement:* No conflicts declared.

This is an open access article distributed under the terms of the Creative Commons Attribution-NonCommercial-NoDerivs 4.0 Unported (CC BY-NC-ND4.0) Licence (<http://creativecommons.org/licenses/by-nc-nd/4.0/>) which permits unrestricted noncommercial use, distribution, and reproduction in any medium, provided the original work is properly cited. *How to cite this article:* Altunay ZM, Alphan A, Adigüzel E. *In vivo* experimental models of schizophrenia: mechanisms, features, advantages, disadvantages. *Anatomy* 2022;16(2):114–123.

# Bilateral agenesis of the long head of the biceps tendon

Semra Duran<sup>1</sup> , Muhammet Batuhan Gökhan<sup>2</sup> 

<sup>1</sup>Department of Radiology, Ankara Bilkent City Hospital, University of Health Sciences, Ankara, Türkiye

<sup>2</sup>Department of Radiology, Ankara Bilkent City Hospital, Faculty of Medicine, Ankara Yıldırım Beyazıt University, Ankara, Türkiye

## Abstract

The congenital variations of the biceps brachii muscle are seen quite frequently, however, the agenesis of the long head, is extremely rare. Diagnosis can be difficult, especially in cases with traumatic shoulder pain. In this paper, a 25-year-old female patient with bilateral biceps tendon agenesis is presented. Shoulder examination was negative for any signs of a traumatic biceps injury. Magnetic resonance imaging revealed congenital absence of the long head of biceps tendon and bilateral shallowness of the intertubercular groove.

**Keywords:** congenital absence; long head of biceps tendon; magnetic resonance imaging; shoulder

Anatomy 2022;16(2):124–126 ©2022 Turkish Society of Anatomy and Clinical Anatomy (TSACA)

## Introduction

The biceps brachii is a two-headed (short and long heads) muscle spanning two joints. It originates from the scapula and attaches distally to the bicipital or radial tuberosity of the radius. It acts as a strong supinator and flexor of the elbow and as an important stabilizer of the shoulder, especially in abduction and internal rotation.<sup>[1]</sup>

Congenital absence of the long head of the biceps (LHB) tendon is a rare variation and its prevalence is unknown. The publications reporting congenital absence of bilateral LHB tendon are limited.<sup>[2]</sup>

Due to the infrequency of this condition, clinical diagnosis is very difficult, and in cases with trauma, it is nearly impossible to distinguish it from tendon rupture.<sup>[3]</sup> Ultrasound and magnetic resonance imaging (MRI) shows an excellent diagnostic accuracy in detecting pathologies of the LHB tendon.<sup>[4]</sup>

In this case report, we present a patient with congenital absence of the bilateral LHB tendon who admitted to hospital with the complaint of shoulder pain.

## Case Report

A 25-year-old female patient presented with a complaint of bilateral shoulder pain. The patient had no history of major trauma. Physical examination of both shoulders

revealed symmetric range of motion in all planes. There was no “Popeye” sign to indicate a torn, retracted LHB tendon. She did not demonstrate signs of laxity or hypermobility in her upper extremities.

Shoulder MRI was performed with the patient in the supine position and the arm adducted in mild external rotation. MRI of both shoulders revealed bilateral absence of the LHB tendon and shallow intertubercular groove (**Figure 1**). There was no evidence of rotator cuff tears or labral tears bilaterally.

## Discussion

The biceps muscle has two heads, the short and the long head, distinguished according to their origin at the coracoid process and supraglenoid tubercle of the scapula, respectively. From its origin on the glenoid, the long head remains tendinous as it passes through the shoulder joint and through the intertubercular groove of the humerus.<sup>[5,6]</sup>

The function of the tendon of LHB at the shoulder remains controversial and uncertain. Biceps brachii primarily acts as a flexor and supinator at the elbow. Many electromyographic studies have shown that it only plays an active role in elbow movements but not shoulder.<sup>[7]</sup> Some studies suggest that it plays an active role in the collapse of the humeral head during shoulder abduction.<sup>[8,9]</sup>

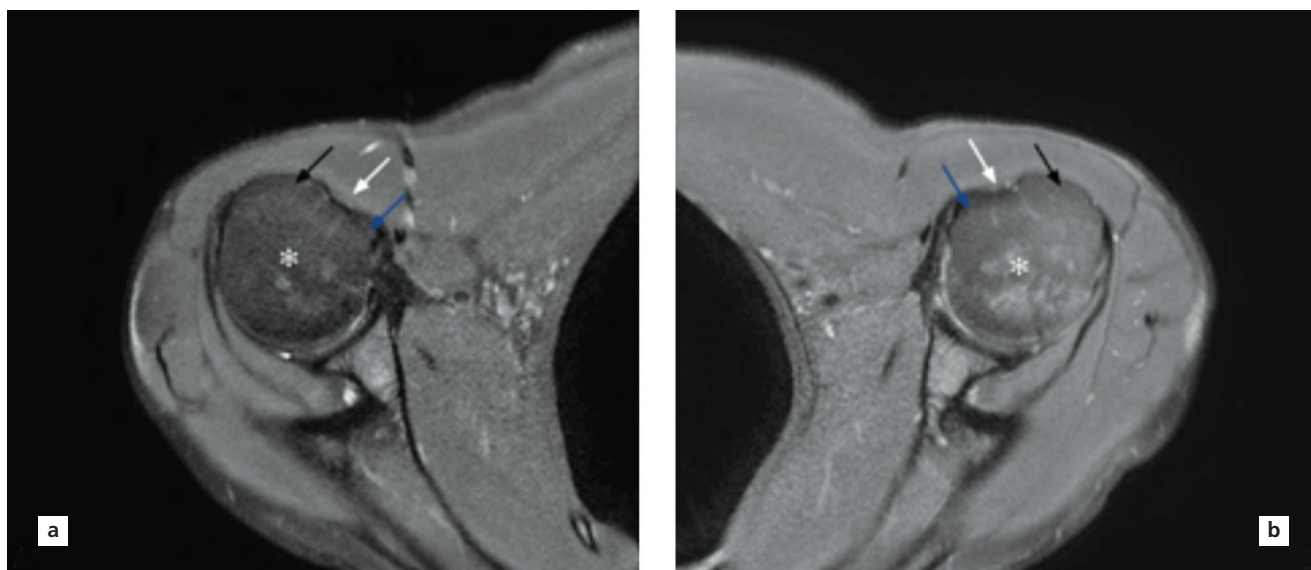


**Figure 1.** Axial fat suppressed proton-density weighted MR images. (a) right; (b) left shoulders. Biceps long head tendon is not observed, intertubercular sulcus is shallow (white arrow). Asterisk: head of humerus; black arrow: greater tubercle of humerus; blue arrow: lesser tubercle of humerus.

LHB tendon has quite wide range of variations. In cadaver studies, the presence of multiple heads is the most commonly reported variation, with a prevalence of 8–20%.<sup>[9–11]</sup> In addition to the number of tendons, the origin of LHB differs between individuals, and it is stated in the literature that approximately 50% originates from the supraglenoid tubercle, and the remaining 50% is variable from different regions of the superior glenoid labrum.<sup>[5,12]</sup> Besides all these variations, congenital absence of LHB tendon is an exceedingly rare anomaly. It is often accompanied by findings such as hypoplastic intertubercular groove and shoulder instability.<sup>[13]</sup>

The unilateral absence of LHB has been reported in the literature to be associated with some skeletal and non-skeletal congenital anomalies (57%) such as spina bifida, VATER syndrome, and congenital limb abnormalities.<sup>[14,15]</sup> Bilateral absence is extremely rare, with only nine previous reports in the literature to the best of our knowledge.<sup>[2,3,10,13,14,16–19]</sup> Diagnosing the pathologies related to LHB could be challenging both on clinical examination and radiologically.<sup>[20]</sup> Although arthroscopy is considered as the gold standard method; MRI is the most preferred one. The shallowness of the intertubercular groove is the most important finding in differentiating it from traumatic injuries and biceps tears.<sup>[3,4,13,20]</sup> In our case, bilateral shallow intertubercular grooves were observed as stated in the literature.

In most cases described in the literature, patients might have shoulder pain like our case, and one of the

cases published by Kwapitz et al.<sup>[17]</sup> was asymptomatic. Although it was stated that the absence of LHB might cause shoulder instability in some cases,<sup>[19]</sup> this was valid for our case. In our case, there was no other accompanying pathology detected by physical examination and MRI.

Surgical intervention is not performed in most of the cases with absent tendons, and arthroscopic interventions are applied for other accompanying shoulder pathologies. Although there is no consensus yet, non-steroidal anti-inflammatory drugs and physical therapy are used for patients with isolated long head absence.<sup>[1,2]</sup> Since there was no other accompanying pathology, our patient was treated symptomatically with nonsteroidal anti-inflammatory drugs. Symptoms improved with physical therapy and medical treatment.

## Conclusion

LHB agenesis should be kept in mind in the absence of major trauma and other accompanying findings in patients with shoulder pain.

## Conflict of Interest

The authors declare that there is no conflict of interests regarding the publication of this paper.

## Author Contributions

SD: data collection, data analysis, manuscript writing and editing; MBG: data collection, data analysis, manuscript writing and editing.

## Ethics Approval

This report has been prepared in accordance with the Helsinki Declaration and does not require any kind of approval of the Ethical Committee.

## Funding

This research received no funding.

## References

- Landin D, Myers J, Thompson M, Castle R, Porter J. The role of the biceps brachii in shoulder elevation. *J Electromyogr Kinesiol* 2008; 18:270–5.
- Kumar CD, Rakesh J, Tungish B, Singh DM. Congenital absence of the long head of biceps tendon & its clinical implications: a systematic review of the literature. *Muscles Ligaments Tendons J* 2018;7: 562–9.
- Koplas MC, Winalski CS, Ulmer WH Jr, Recht M. Bilateral congenital absence of the long head of the biceps tendon. *Skeletal Radiol* 2009;38:715–9.
- Zappia M, Chianca V, Di Pietto F, Reginelli A, Natella R, Maggialetti N, Albano D, Russo R, Sconfienza LM, Brunese L, Faletti C. Imaging of long head biceps tendon. A multimodality pictorial essay. *Acta Biomed* 2019;90:84–94.
- Vangsness CT Jr, Jorgenson SS, Watson T, Johnson DL. The origin of the long head of the biceps from the scapula and glenoid labrum. An anatomical study of 100 shoulders. *J Bone Joint Surg Br* 1994;76:951–4.
- Beltran J, Jbara M, Maimon R. Shoulder: labrum and bicipital tendon. *Top Magn Reson Imaging* 2003;14:35–49.
- Yamaguchi K, Riew KD, Galatz LM, Syme JA, Neviaser RJ. Biceps activity during shoulder motion: an electromyographic analysis. *Clin Orthop Relat Res* 1997;(336):122–9.
- Warner JJ, McMahon PJ. The role of the long head of the biceps brachii in superior stability of the glenohumeral joint. *J Bone Joint Surg Am* 1995;77:366–72.
- Buck FM, Dietrich TJ, Resnick D, Jost B, Pfirrmann CW. Long biceps tendon: normal position, shape, and orientation in its groove in neutral position and external and internal rotation. *Radiology* 2011;261:872–81.
- El Abiad JM, Faddoul DG, Baydoun H. Case report: broad insertion of a large subscapularis tendon in association with congenital absence of the long head of the biceps tendon. *Skeletal Radiol* 2019;48:159–62.
- Rodríguez-Niedenführ M, Vázquez T, Choi D, Parkin I, Sañudo JR. Supernumerary humeral heads of the biceps brachii muscle revisited. *Clin Anat* 2003;16:197–203.
- Pal GP, Bhatt RH, Patel VS. Relationship between the tendon of the long head of biceps brachii and the glenoidal labrum in humans. *Anat Rec* 1991;229:278–80.
- Rego Costa F, Esteves C, Melão L. Bilateral congenital agenesis of the long head of the biceps tendon: the beginning. *Case Rep Radiol* 2016;2016:4309213.
- Maldjian C, Borrero C, Adam R, Vyas D. Nature abhors a vacuum: bilateral prominent rotator cable in bilateral congenital absence of the long head of the biceps tendon. *Skeletal Radiol* 2014;43:75–8.
- Smith EL, Matzkin EG, Kim DH, Harpstrite JK, Kan DM. Congenital absence of the long head of the biceps brachii tendon as a VATER association. *Am J Orthop (Belle Mead NJ)* 2002;31:452–4.
- Winston BA, Robinson K, Crawford D. “Monocept” a brief report of congenital absence of the long head of the biceps tendon and literature review. *Case Rep Orthop* 2017;2017:1090245.
- Kwapisz A, Xu M, Koenig J, MacDonald P, McRae S, Marsh J. Uncommon bilateral absence of long heads of the biceps tendons in twin sisters: a report of 2 cases. *JBJS Case Connect* 2021;11:e20.00878.
- Kuhn KM, Carney J, Solomon D, Provencher M. Bilateral absence of the long head of the biceps tendon. *Mil Med* 2009;174:548–50.
- Yoon SH, Heo K, Yoo JS, Kim SJ, Seo JB. Posterior shoulder instability in the patients with bilateral congenital absence of long head of biceps tendon: a case report. *Clin Shoulder Elb* 2018;21:240–5.
- Traverso A, Piasecki K, Gallusser N, Farron A. Agenesis of the long head of the biceps brachii tendon: ignored variations of the anatomy and the next tendon to disappear? *BMJ Case Rep* 2020;13:e234962.

### ORCID ID:

S. Duran 0000-0003-0863-2443;  
M. B. Gökhan 0000-0002-3579-7887



### Correspondence to:

Muhammet Batuhan Gökhan, MD  
Department of Radiology, Faculty of Medicine,  
Ankara Yıldırım Beyazıt University, Ankara, Türkiye  
Phone: +90 0505 547 64 37  
e-mail: mbgokhan@gmail.com

*Conflict of interest statement:* No conflicts declared.

This is an open access article distributed under the terms of the Creative Commons Attribution-NonCommercial-NoDerivs 4.0 Unported (CC BY-NC-ND4.0) Licence (<http://creativecommons.org/licenses/by-nc-nd/4.0/>) which permits unrestricted noncommercial use, distribution, and reproduction in any medium, provided the original work is properly cited. *How to cite this article:* Duran S, Gökhan MB. Bilateral agenesis of the long head of the biceps tendon. *Anatomy* 2022;16(2):124–126.

# A large unilateral persistent sciatic vein: a case report

Vincent Kipkorir , Dennis Ochieng , Fiona Nyaanga , Isaac Cheruiyot , Wanjiku Ndung'u ,  
Musa Misiani , Jeremiah Munguti , Beda Olabu 

Department of Human Anatomy, School of Medicine, College of Health Sciences, University of Nairobi, Nairobi, Kenya

## Abstract

Persistent sciatic vein is considered a relatively rare anatomical finding, commonly associated with the Klippel-Trenaunay-Weber syndrome. We report a case of a large unilateral persistent sciatic vein in the right lower limb of an adult male cadaver, identified during routine dissection. The size of the vein was comparable to the sciatic nerve and it was originated from the union of posterior tibial veins at the distal end of the popliteal fossa. It was ascending in the posterior part of the thigh, medial to the sciatic nerve, before coursing through the infrapiriform foramen of the greater sciatic foramen and terminating by draining into the internal iliac vein. Further dissection revealed conventional anatomy of the femoral venous system. The epidemiology, anatomy, diagnosis and management a persistent sciatic vein are also discussed.

**Keywords:** lower limb venous variation; persistent sciatic vein

Anatomy 2022;16(2):127–130 ©2022 Turkish Society of Anatomy and Clinical Anatomy (TSACA)

## Introduction

The sciatic vein is an embryological vessel that forms the main stem of the primordium of the deep venous system of the lower limb. It is usually located on the dorsal aspect, following the course of the sciatic nerve.<sup>[1,2]</sup> With the establishment of the definitive deep venous system, the vein usually involutes, with its remnants forming the inferior gluteal vein, satellite vein of the sciatic nerve, and perforating veins of the lower limb.<sup>[3,4]</sup> It may however fail to degenerate, and remains as the persistent sciatic vein (PSV) (*vena comitans nervi ischiadici persistens*).<sup>[2]</sup>

First described by Servell in 1978, PSV is a rare anatomical finding that may occur as an isolated entity, or in association with the Klippel-Trenaunay-Weber syndrome (KTWS).<sup>[5]</sup> KTWS is a rare congenital vascular anomaly characterized by a triad of capillary malformation, varicose veins and soft tissue/ bone hypertrophy.<sup>[2,5,6]</sup> When present, the PSV can assume any of the three forms as described by Cherry et al.<sup>[5]</sup> as; complete type (arises from the popliteal vein or its tributaries, ascends along the sciatic nerve, and terminates in the internal iliac vein), upper type (arises from the muscular veins of the upper thigh, runs along the sciatic nerve and terminates in the internal iliac vein) or the lower type

(limited to the distal thigh, arises from the popliteal fossa, and terminates in the deep femoral vein).<sup>[5,7,8]</sup>

We present here a case of a unilateral large complete PSV and discuss the epidemiology, anatomy, diagnosis and management of PSV.

## Case Report

During routine cadaveric dissection, we observed a case of a large PSV in the right lower limb of an adult male cadaver. The PSV, comparable in size to the sciatic nerve, originated from the posterior tibial veins at the distal region of the popliteal fossa, without connection to the popliteal vein. Instead, anterior tibial veins joined to form the popliteal vein, which received all the genicular veins (**Figure 1**). From the popliteal fossa, the PSV ascended in the posterior part of the thigh, medial the sciatic nerve (**Figure 2a**). Within the proximal thigh and gluteal region, it was located between the sciatic nerve and the posterior femoral cutaneous nerve of the thigh (**Figure 2b**). It then passed through the infrapiriform foramen to enter the pelvis, where it terminated by draining into the internal iliac vein (**Figure 2c**). Further investigation revealed conventional anatomy of the femoral venous system (**Figure 2d**).

## Discussion

PSV is a relatively rare congenital vascular variation caused by failure of degeneration of the principal trunk of the primitive deep venous system of the lower limb.<sup>[2]</sup> It was classified by the International Society of the Study of Vascular Anomalies (ISSVA) in 2014 as a “channel-type” or “truncal” vascular malformation.<sup>[9]</sup> In 1978, Servell hypothesized that the vessel developed as a collateral channel for lower limb venous return in cases where the femoral vein was obstructed.<sup>[5]</sup> Cherry et al.,<sup>[5]</sup> and Baskerville et al.,<sup>[10]</sup> in their large case series of patients with PSV reported that the FV is almost always patent in these individuals, disproving this hypothesis. Nonetheless, there are several cases of hypoplastic femoral vein in patients with PSV.<sup>[4,6]</sup>

The prevalence of PSV in the general population is unknown. Literature suggests that the PSV may be more common in certain individuals, such as those with recurrent varicose veins of the lower limb. In a retrospective analysis of ascending phlebographies and varicographies of 1200 patients with varicose veins, Trigaux et al.,<sup>[4]</sup> identified a PSV in 7 (0.5%) patients. The prevalence of PSV is even higher in individuals with the KTWS.<sup>[4,11,12]</sup> For instance, Cherry et al.,<sup>[5]</sup> found a PSV in 20 (48%) out of 41 KTWS patients who were diagnosed through magnetic resonance imaging (MRI). A similar study on KTWS by Noel et al.,<sup>[12]</sup> found a PSV prevalence of 20%. It is noteworthy that in both studies, MRI was performed only on a subgroup of KTWS patients with symptomatic presentation (41 out of 279 in the study by Cherry et al.,<sup>[5]</sup> and 20 out of 290 in the study by Noel et al.<sup>[12]</sup> As such, the prevalence reported in these studies should be interpreted with caution due to possible selection bias.

PSV can be present unilaterally<sup>[5,13–15]</sup> or bilaterally,<sup>[5,7,11,12]</sup> and can occur as a single large vein<sup>[4,12]</sup> or a network of veins.<sup>[4,5]</sup> It can also present concurrently with a persistent sciatic artery.<sup>[12,15]</sup> When present, the PSV can assume any of the three forms as described by Cherry et al.<sup>[5]</sup> The PSV displays typical features of a medium-size vein, with a thin tunica intima, thin muscular tunica media, and a thick well-developed tunica adventitia.<sup>[11]</sup> There are conflicting reports on the presence of valves within the PSV. Koç et al.,<sup>[11]</sup> in their case report of bilateral PSV found 3 valves in each of the veins. However, 2 large studies on KTWS patients failed to demonstrate any valves within the PSV.<sup>[5,12]</sup>

PSV is asymptomatic in the majority of individuals and is diagnosed incidentally during routine investigations. It may be symptomatic in a small subset of individuals and

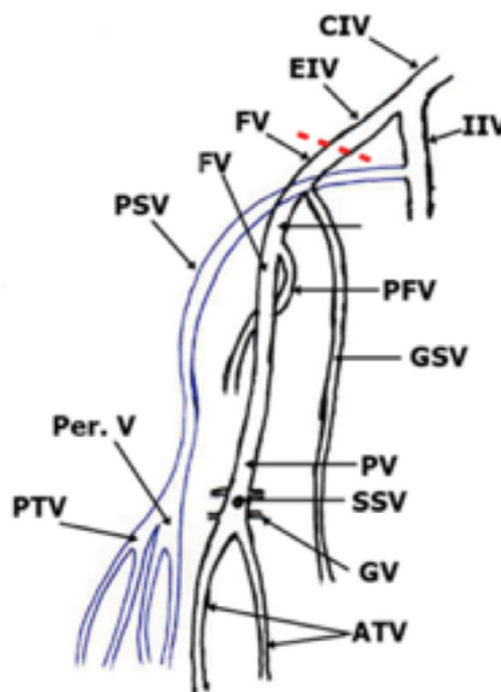


**Figure 1.** Illustration showing the origin, course and tributaries of the persistent sciatic vein drawn in blue. ATV: anterior tibial veins; CIV: common iliac vein; EIV: external iliac vein; FV: femoral vein; GSV: great saphenous vein; GV: genicular veins; IIV: internal iliac vein; Per. V: persistent vein; PFV: deep femoral vein; PSV: persistent sciatic vein; PTV: posterior tibial veins; PV: popliteal vein; SSV: small saphenous vein.

has been cited in the literature as an unusual cause of recurrent lower limb varicose veins and chronic venous reflux.<sup>[4,5,12,13,15]</sup> For instance, Trigaux et al.<sup>[4]</sup> reported that posterior leg varices in 6 out of 7 patients were drained by a PSV and not the short saphenous vein, suggesting a possible causal role. PSV should therefore be ruled out in all patients with recurrent varicose veins of the calf or posterior thigh. The PSV has also been reported as a site of deep venous thrombosis and subsequent pulmonary thromboembolism.<sup>[4,5,16]</sup>

Definitive diagnosis of PSV is usually made through imaging studies. Initial studies mainly relied on varicography and ascending phlebography.<sup>[4,5,10]</sup> These modalities are however invasive and have a low sensitivity,<sup>[5,13]</sup> and have therefore been largely replaced by newer imaging modalities such as Doppler ultrasonography and MRI. Doppler sonography is non-invasive, fast, and relatively cheap, but is limited as its diagnostic accuracy is operator-dependent. Magnetic resonance imaging venography is considered a reliable modality in the assessment of the anatomy of the deep venous system of the limb and the



**Figure 2.** Dissection of (a) posterior thigh; (b) gluteal region; (c) hemi-pelvis displaying the sciatic vein (yellow stars) and its relations, and (d) anterior thigh displaying the conventional anatomy of the femoral triangle. Note the sciatic vein coursing through the posterior thigh with the tibial nerve and common peroneal nerve forming its most immediate and distal lateral relations respectively in (a). The sciatic vein crossing inferior to the piriformis muscle with the sciatic nerve and the posterior femoral cutaneous nerve of the thigh forming its lateral and medial relations respectively in (b). The sciatic vein coursing through the infrapiriform compartment to drain into the internal iliac vein in (c). The great saphenous vein draining into the femoral vein in (d). AL: adductor longus; CPN: common peroneal nerve; FA: femoral artery; FN: femoral nerve; GM: gluteus minimus; GSV: great saphenous vein; IIV: internal iliac vein; L5: fifth lumbar vertebra; LBF: long head of biceps femoris; SBF: short head of biceps femoris; PFCN: posterior femoral cutaneous nerve of the thigh; PM: piriformis; SM: semimembranosus; SN: sciatic nerve; ST: semitendinosus; SV: sciatic vein; TN: tibial nerve.

pelvic area,<sup>[16]</sup> and is therefore appropriate modality for investigating presence of a PSV.

Due to the rarity of the PSV, its management has yet to be standardized. The majority of the PSV are asymptomatic, and may not require any treatment. Treatment is however indicated in patients with recurrent varicose veins within the PSV territory.<sup>[13]</sup> Patients with mild symptoms may require simple stab avulsion, stripping, or excision of the varicosities.<sup>[5,13]</sup> Severe cases of claudication may require surgical excision of the PSV.<sup>[6,12]</sup> This however requires the presence of a patent superficial and deep femoral venous system. In patients with hypoplasia of the femoral venous system, the great saphenous vein from the

unaffected side may be used to reconstruct the continuity of the deep venous system of the lower limb via a popliteal vein-great saphenous vein anastomosis.<sup>[12]</sup> The role of endovascular therapies for a PSV is still not yet established.

## Conclusion

Although relatively rare in the general population, PSV is more common in individuals with varicose veins and KTWS syndrome. It should be considered as a differential in cases of recurrent varicose veins and/or chronic venous insufficiency of the lower limb.

## Acknowledgement

We appreciate the role that the donors of the cadaver used herein in contributing to the furtherment of the study of Anatomy both as a science and as a field of medicine.

## Conflict of Interest

The authors declare that there is no conflict of interests regarding the publication of this paper.

## Author Contributions

VK: protocol/project development; manuscript writing/editing, review and approval of the manuscript; DO: data collection and analysis, review and approval of the manuscript; FN: data collection and analysis, review and approval of the manuscript; IC: protocol/project development; manuscript writing/editing, review and approval of the manuscript; WN: data collection and analysis, review and approval of the manuscript; MM: data collection and analysis, review and approval of the manuscript; JM: protocol/project development; manuscript writing/editing, review and approval of the manuscript; BO: protocol/project development; manuscript writing/editing, review and approval of the manuscript.

## Ethics Approval

This study was conducted in accordance with the ethical guidelines of the Helsinki Declaration and its later amendments. Ethical provision for this cadaveric study is as provided in the constitution under CAP 249 of the Human Anatomy act.

## Funding

None.

## References

- Caggiati A, Bergan JJ, Glocviczki P, Jantet G, Wendell-Smith CP, Partsch H. Nomenclature of the veins of the lower limbs: an international interdisciplinary consensus statement. *J Vasc Surg* 2002;36:416–22.
- Kachlik D, Pechacek V, Musil V, Baca V. The deep venous system of the lower extremity: new nomenclature. *Phlebology* 2012;27:48–58.
- Hamilton HE, Darke SG. Persistent sciatic vein—unusual cause of reflux from the popliteal fossa and sural nerve damage. *Eur J Vasc Endovasc Surg* 1999;17:539–41.
- Trigaux JP, Vanbeers BE, Delchambre FE, de Fays FM, Schoevaerdt JC. Sciatic venous drainage demonstrated by varicography in patients with a patent deep venous system. *Cardiovasc Intervent Radiol* 1989;12:103–6.
- Cherry KJ, Glocviczki P, Stanson AW. Persistent sciatic vein: diagnosis and treatment of a rare condition. *J Vasc Surg* 1996;23:490–7.
- Srisuwan T, Arworn S, Rerkasem K. Case series of isolated primary persistent sciatic vein. *Int J Low Extrem Wounds* 2013;12:219–22.
- Cardoso BB, Alvarenga CO, Miyahara MD, Burihan MC, Lima MR, Kuwahara MC, Silva RC. Persistent sciatic vein [Persistência da veia ciática]. *Journal Vascular Brasileiro* 2010;9:137–40.
- Latarjet M, Liard AR. Anatomía humana. 4th ed. Buenos Aires: Editorial Médica Panamericana; 2004. p. 928.
- Ahlawat S, Fayad LM, Durand DJ, Puttgen K, Tekes A. International society for the study of vascular anomalies classification of soft tissue vascular anomalies: survey-based assessment of musculoskeletal radiologists' use in clinical practice. *Curr Probl Diagn Radiol* 2019;48:10–6.
- Baskerville PA, Ackroyd JS, Browse NL. The etiology of the Klippel-Trenaunay syndrome. *Ann Surg* 1985;202:624–7.
- Koç T, Gilan İY, Külekçi GD, Kurtoğlu Z. Bilateral persistent sciatic vein: report of a case with developmental, histological and clinical aspects. *Surg Radiol Anat* 2014;36:189–94.
- Noel AA, Glocviczki P, Cherry Jr KJ, Rooke TW, Stanson AW, Driscoll DJ. Surgical treatment of venous malformations in Klippel-Trenaunay syndrome. *J Vasc Surg* 2000;32:840–7.
- Hamilton HE, Darke SG. Persistent sciatic vein—unusual cause of reflux from the popliteal fossa and sural nerve damage. *Eur J Vasc Endovasc Surg* 1999;17:539–41.
- Labropoulos N, Tassiopoulos AK, Gasparis AP, Phillips B, Pappas PJ. Veins along the course of the sciatic nerve. *J Vasc Surg* 2009;49:690–6.
- Parry DJ, Aldoori MI, Hammond RJ, Kessel DO, Weston M, Scott DJ. Persistent sciatic vessels, varicose veins, and lower limb hypertrophy: an unusual case or discrete clinical syndrome? *J Vasc Surg* 2002;36:396–400.
- Trihan JE, Perez-Martin A, Thollet C, Belhadj-Chaidi R, Escure E, Guillaumat J, Lanéelle D. Thrombosis of previously silent persistent sciatic vein in non Klippel-Trenaunay syndrome patient. *J Med Vasc* 2020;45:13–7.

### ORCID ID:

V. Kipkorir 0000-0001-6946-8857; D. Ochieng 0000-0002-9403-5831; F. Nyaanga 0000-0001-9880-1436; I. Cheruiyot 0000-0002-1211-8247; W. Ndung'u 0009-0003-8307-4020; M. Misiani 0000-0001-9735-5702; J. Munguti 0000-0003-4259-2385; B. Olabu 0000-0003-0782-8006

deomed®

### Correspondence to:

Vincent Kipkorir, BSc. Anat (Hons)  
Department of Human Anatomy, School of Medicine, College of Health Sciences, University of Nairobi, 30197-00100, Nairobi, Kenya  
Phone: +0720576705  
e-mail: vincentkipkorir42357@gmail.com

Conflict of interest statement: No conflicts declared.

This is an open access article distributed under the terms of the Creative Commons Attribution-NonCommercial-NoDerivs 4.0 Unported (CC BY-NC-ND4.0) Licence (<http://creativecommons.org/licenses/by-nc-nd/4.0/>) which permits unrestricted noncommercial use, distribution, and reproduction in any medium, provided the original work is properly cited. *How to cite this article:* Kipkorir V, Ochieng D, Nyaanga F, Cheruiyot I, Ndung'u W, Misiani M, Munguti J, Olabu B. A large unilateral persistent sciatic vein: a case report. *Anatomy* 2022;16(2):127–130.

## Obituary

<http://dergipark.org.tr/en/pub/anatomy>  
Received: March 22, 2022; Accepted: April 7, 2022  
doi:10.2399/ana.22.Ob01

# In dedication to Mustafa Fevzi Sargon (1965–2022)

**Deniz Demiryürek** 

*Department of Anatomy, Hacettepe University Faculty of Medicine, Ankara, Türkiye*

Anatomy 2022;16(2):131–132 ©2022 Turkish Society of Anatomy and Clinical Anatomy (TSACA)

## Through the Memories of his Friend by Prof. Deniz Demiryürek

Writing about a close friend after his death is the first time for me. I realised it is so hard.

Prof. Dr. Mustafa Fevzi Sargon, among us, Sargon was a very special mentor, teacher, role model and a real friend. I met him at December 1995, at the New Year reception of Anatomy Department; Hacettepe University Faculty of Medicine. Those days he was doing his military service and was wearing his army costume when I met him.

Although I knew him from the years we studied at Ankara University Faculty of Medicine, we could not have the chance to meet.

After I started my PhD of Anatomy, he was one my mentors and we studied together with great productivity. My first international publication was done with his great supports. Not only being a great anatomist, Sargon was a real friend. He was always together with me during my whole academic life till his retirement. His sudden decision about retiring was a great shock for me. What would I do after him? It was so hard to adapt the position but I could manage.

We were in close touch with him in his new academic life, first at Atılım University and after Lokman Hekim University. We were gathering for academic studies, social events. But one day, the saddest news from him, the second shock for me about him happened. He left us suddenly.

It is not easy to bare his non-presence. When you lost your real friend, academic role model, it is not easy. I am missing him so much and will always remember him (**Figure 1**).



**Figure 1.** Mustafa Fevzi Sargon (1965–2022).

## Through the Eyes of his Family by Mert Sargon; Son of Prof. Mustafa Sargon

If I have to introduce you Mustafa Sargon with a few words, ever since I could remember, besides being a thoughtful, responsible and devoted family man who had always been supporting us; he was an ethical scientist with full of passion for studying, learning, teaching and research.

The world of Medicine was an inseparable part of him. As he had taken his first step into this world as an anatomist in Hacettepe University, he regarded Hacettepe as his home and was holding the university in very high esteem.

That world which we can call as “a second home” was not only a home for him individually, but also a home for all of us, as his nuclear family.

His enthusiasm to the science, his colleagues and his students, and his dedication to his profession made our family an integral part of his career, our daily subjects generally based on them. Hence, we were accompanying him in his profession which he has devoted his life.

After his passing, we realized that there was not a “second home” in his “world”. In the world of Mustafa Sargon, there was one and only one world. Hacettepe (& world of medicine) and we were a single family that settled in the same heart, same world. His colleagues, friends and students – whom we have known since early years – are always with us. We feel him mostly in the laboratories and classrooms where he devoted his life mostly. After his retirement, he continued his career in different universities with the same passion. Nevertheless, Hacettepe is enshrined in our (and his) heart as the place he started his career and also the place where his children grew up.

As an exemplary professor who had touched countless students’ life, conducted research and published many articles, he was also regarding his family as his students, teaching us many subjects and sharing issues about his profession. We would often find ourselves reading the books he had written and examining his anatomy models, try to understand him from his eyes. When we regard him as an academician, we were realizing many new things about him and his character which we had not noticed before by only regarding him as a father. Hence, in order to understand and feel him correctly, it is not enough for us to regard him only as a father.

Besides being a great father, due to his influence on his environment and contributions to Anatomy, we feel lucky, proud of being his family and being educated by him. After we lost him, we felt the support and sincerity of all his colleagues and students in such a way that, his efforts to his profession were not in vain. We will stay together, always remember you with respect and proud of you.

**ORCID ID:**

D. Demiryürek 0000-0001-8781-1719

**Correspondence to:** Deniz Demiryürek, MD, PhDDepartment of Anatomy, Faculty of Medicine,  
Hacettepe University, 06100, Sıhhiye, Ankara, Turkey

Phone: +90 312 305 23 59

e-mail: mdeniz@hacettepe.edu.tr

*Conflict of interest statement:* No conflicts declared.

This is an open access article distributed under the terms of the Creative Commons Attribution-NonCommercial-NoDerivs 4.0 Unported (CC BY-NC-ND4.0) Licence (<http://creativecommons.org/licenses/by-nc-nd/4.0/>) which permits unrestricted noncommercial use, distribution, and reproduction in any medium, provided the original work is properly cited. *How to cite this article:* Demiryürek D. In dedication to Mustafa Fevzi Sargon (1965–2022). *Anatomy* 2022;16(2):131–132.

# In dedication to Professor Mustafa Sargon

Nihal Apaydın<sup>1-4</sup> 

<sup>1</sup>Department of Anatomy, School of Medicine, Ankara University, Ankara, Türkiye

<sup>2</sup>Department of Multidisciplinary Neuroscience, Institute of Health Sciences, Ankara University, Ankara, Türkiye

<sup>3</sup>Brain Research Center (AU-BAUM), Ankara University, Ankara, Türkiye

<sup>4</sup>Neuroscience and Neurotechnology Center of Excellence (NÖROM), Ankara, Türkiye

Anatomy 2022;16(2):133–136 ©2022 Turkish Society of Anatomy and Clinical Anatomy (TSACA)

It was 10th of February 2022; a cool winter day, before noon, around 10.00 am. We were in the middle of a proficiency exam of a PhD candidate with our colleagues from Hacettepe University; Mustafa Aldur and Ceren Güneç Beşer. Mustafa Aldur received a phone call and wanted to answer thinking that it may not be a missed one. While talking his face turned to white and could talk only with few words. The news he had was sad, very sad... The sadness I felt when we learned that Mustafa Sargon had a heart attack with that phone call, deepened even more in the evening with the news of his death at the age of 56.

Mustafa Sargon, was truly a great scientist and a dedicated teacher. He was such a good-humored, hard-working, nice and polite friend. He loved his profession and students with passion and such committed to his job that; his last words became “I am well, my lesson will start soon, please help me take to the lab.”

It was a great honor and a privilege for me to work with him in the Council of European Association of Anatomy and Clinical Anatomy (EACA) and in the “Anatomy” journal. He was one of the outstanding editors of our journal and was like my right arm. His contributions to the publication process of our journal is irretrievable. Just a month before his death, we were talking about plans for hosting a future EACA congress. As the General Secretary of EACA Congress held in Istanbul in 2009, he deserved to be the president in 2027 Congress, but unfortunately his life wasn’t enough to do it.

Mustafa Sargon’s contributions to the Anatomy and Medicine cannot be repayable, but we would like to dedicate this issue to his memory in order to express even a little bit of our loyalty towards him. On this occasion, I would like to thank Prof. Dr. Deniz Demiryürek for his contributions.

This was a big shock not only for his family, close friends and colleagues but also for all the anatomists

worldwide. After learning of his death, his friends and colleagues wanted to convey their condolences to the entire Anatomy family through me. I would also like to share these messages in this issue that we dedicate to his memory, of course with the permission of the authors. Rest in peace Sargon, you will be greatly missed here.

With my deepest regards.

## Condolence Messages to Mustafa Sargon in the Order of Arrival

So sad and so sudden –

Please send my deepest sympathies to his family – what a loss not only to them but to the anatomical world in general  
Life is so precious -we must all live it to the full.

Warmest Regards

Phantom of the fens

**Peter Abrahams**, MBBS FRCS(ED) FRCR DO(Hon) FHEA FRSA

*Prof. “Emeritus” of Clinical Anatomy, Warwick Medical School, National Teaching fellow & Life Fellow, Girton College, Cambridge Visiting Prof. LKC School of Medicine NTU Singapore; Consultant to Brunel Medical School, UK*

What terribly sad news, those that you never wish to hear.  
Mustafa was a great anatomist and a wonderful man.

I ask that you please present my heartfelt condolences to his family, his friends and to all my wonderful Turkish friends, who I am sure are deeply suffering with this terrible loss.

**Diogo Pais**, Secretary-General International Federation of Associations of Anatomists (IFAA); Secretary-General International Committee of Symposia on Morphological Sciences (ICSMS); Full Professor and Chairman Department of Anatomy; Chairman Ethics Research Committee

So sorry to hear such sad news. He leaves a lasting legacy. My thoughts are with his friends and family and with the Turkish anatomical community.

**Bernard Moxham**, B.Sc., B.D.S., PhD, FHEA, FRSB, Hon FAS, FSAE; Emeritus Professor of Anatomy; Immediate Past President of the International Federation of Associations of Anatomists (IFAA) and Past President of the Anatomical Society and the European Federation for Experimental Morphology (EFEM); Founder of the Trans-European Pedagogic Anatomical Research Group (TEPARG)

Mustafa was a fine anatomist, he has a profound intellect. We have attended numerous congresses together, always exchanging avant-garde ideas.

We'll miss him.

**Raffaele De Caro**, Professor of Human Anatomy; Past-President of European Association of Clinical Anatomists (EACA); Director, Department of Neuroscience, Institute of Human Anatomy, University of Padua, Italy; Director, Unit of Clinical Anatomy, Department of General Surgery, University-Hospital of Padua; Director, National Reference Center for the Conservation and Use of the Bodies of the Deceased, University of Padua

Very sad news, really. For sure, Mustafa was a great anatomist, and not only in Turkey but in the large field of clinical anatomy. He was a great support of our journal SRA, both through publications and clear analysis of submissions. I remember the great congress in Istanbul. Moreover, it was always a great pleasure to meet him, as a so nice person.

Kind regards,

**Fabrice Duparc**, MD, PhD; Editor in Chief; Surgical and Radiologic Anatomy; EACA Past President

I am really devastated by this tragic message. Not only was Mustapha a great anatomist, but it always was a huge pleasure to meet him in person in various meetings. I will forward your notice to the entire list of EACA members.

With my deepest sympathies,

**Bruno Grignon**, MD, PhD  
EACA Secretary General

This is a great loss and I am deeply saddened. Mustafa has always been a role model for me, we were negotiating Sobotta, he is my vintage, I can't believe it.

I bow down to his character.

**Friedrich Paulsen**, Prof. Dr. Padua, HonFAS I; Head Institute of Functional and Clinical Anatomy I FAU Erlangen;

Friedrich Alexander University Erlangen-Nürnberg; President European Federation of Experimental Morphology

What a tragedy. Mustafa was a giant in our world of anatomy so this is a huge loss.

Best wishes,

**R. Shane Tubbs**, PhD, MS, PA-C. Director of Surgical Anatomy, Tulane University School of Medicine; Editor in Chief of Clinical Anatomy; President Elect (2021-2023) of American Association of Clinical Anatomy (AACA)

Please convey to his family our deepest condolences.

Regards

**Marios Loukas**, MD, PhD. Dean of Basic Sciences SGU; Past President of American Association of Clinical Anatomy (AACA); Department of Anatomical Sciences, St. George's University, Grenada, West Indies

Very bad news, he was the smile and the joy of the Anatomical meetings. I miss him. Please, pass to his family and the Turkish Association of Anatomists my deepest condolences.

**Jose Sanudo**, Profesor Anatomía y Embriología, Facultad de Medicina, Universidad Complutense de Madrid; EACA Past President

Mustafa was a great anatomist.

My deepest condolences to you and your family, with all of our anatomy colleagues in Turkey and world-wide.

**Professor Konstantinos Natsis**, MD, PhD, BSc, FFIMS, FEBSM. Orthopaedic Surgeon; President of Committee on Health, AUTH; President of Sports Medicine Association of Greece; Vice President of EFSMA; EC member of FIMS; President Hellenic Anatomical Society Department of Anatomy & Surgical Anatomy School of Medicine, Faculty of Health Sciences, Aristotle University of Thessaloniki

I am in shock. Mustafa has always been so very kind and supportive – he was amongst the very first people I met on my first international trip, and has ever since been a wonderful friend, always quietly sharing a joke with his cheeky grin. At my first meetings he was, and has ever since, been such a great support, always enthusiastic for the work of others. I will be forever thankful for his friendship and guidance, and will miss him at the many varied meetings we attended. No one quite mastered the quiet, almost magical, appearance out of nowhere, followed by a quiet nod and smile, as much as Mustafa.

Please share my deepest condolences with his family, with all of our wonderful anatomy colleagues in Turkey and with his many friends world-wide.

**Quentin A. Fogg**, *Associate Professor in Clinical Anatomy; PhD, FRCPS (Glasg); President (2021-2022), Australian and New Zealand Association of Clinical Anatomists*

---

What a horrible and sad information! We lose a very sophisticated experienced anatomist, always modest and never insistent. His work was on a constant high level and therefore a shining example for young colleagues.

Personally, I will miss his wonderful smile and politeness as well as himself entirely.

**Georg Feigl**, *Prof. FA. Dr. med. univ., Institute of Anatomy and Clinical Morphology University of Witten/Herdecke, Germany*

---

So sad news. Too young!

A great anatomist, scientist and personality.

Everyone has a good word to say for Professor Mustafa Sargon.

No doubt, his loss is huge for his family first and our anatomical society as well.

Best regards to everyone,

**Trifon D. Totlis**, *MD, PhD, Assist. Professor in Surgical Anatomy, Medical School, Aristotle Univ. of Thessaloniki, Greece; Consultant Orthopaedic Surgeon, The-MIS Orthopaedic Center; European Knee Associates Board Member (a section of ESSKA); Vice-President of the Regenerative Medicine Association of Greece*

---

The announcement was received with great sadness. Please convey my deepest sympathy to Mustafa's family and colleagues at his university. Mustafa was well known in the larger academic community and he will be remembered for his academic achievements, professionalism and deep kindness.

**Cristian Stefan**, *MD, Clinical Professor, Department of Molecular Pathobiology, New York University College of Dentistry*

---

What a bad and a sad message. It is a really big loss for our anatomical community. Mustafa was the great anatomist, the great teacher and such a good person and friend. I will miss him a lot.

Please send my deepest sympathy to his family.

**Václav Báča**, *MD, PhD, EACA Honorary President; Rector, College of Polytechnics Jihlava, Check Republic*

---

What a very sad message!

What an amazing person!

I am very sorry for this loss.

Please send his family a lot of comfort and peace!

Greetings from Innsbruck,

**Marko Korschake**, *Prof. Dr. med. univ., Vice Head Institute of Clinical and Functional Anatomy; Medical University of Innsbruck (MUI); Institute of Clinical and Functional Anatomy*

---

Mustafa, great and the most modest anatomist I have ever met will remain and live in our thoughts and memories. I still remember the meeting in Bodrum where I met him first time and he cared for me greatly.

With deep sorrough,

**David Kachlík**, *PhD, Department of Anatomy, Second Faculty of Medicine, Charles University, Prague, Czech Republic*

---

My deep condolences.

**Antonio Gonçalves Ferreira**, *Director of the University Clinic of Neurosurgery at FMUL, Lisboa; President of the European Association of Stereotactic and Functional Neurosurgery (ESSFN); EACA Past President*

---

What terribly sad news!

It was truly a pleasure to have gotten to know Mustafa. He was a great anatomist.

I am deeply saddened by the news of his loss.

My most sincere condolences.

**Michał Polgaj**, *EACA Board Member*

---

I would like to express my deep sorrow for the sudden and untimely loss of this wonderful man. Mustafa Sargon had a lot to offer in the anatomy family. We will always remember his kindness and his smile. My heartfelt condolences to his family in this difficult time. Also a great thank to Nihal for the immediate notification of his death, as well as to Prof. Grignon for the extended notification to all members of the EACA.

**Mara Piagkou**, *Assoc. Professor, DDS, MD, MSc, PhD, Department of Anatomy, Medical School; National and Kapodistrian University of Athens Greece; Deputy Vice President of the Public Health of Greece*

---

Mustafa, a great anatomist. A great loss for EACA and for anatomical world.

We will miss his refinement.

With deepest condolences

**Veronica Macchi**, *Professor of Human Anatomy; Institute of Human Anatomy, Department of Neurosciences, University of Padua; Unit of Clinical Anatomy, Department of General Surgery, University-Hospital of Padua; National Reference Center for the Conservation and Use of the Bodies of the Deceased, University of Padua; Director of the Interdepartmental Research Center for Body Training “A. Vesalius”, University of Padua; Treasurer of European Association of Clinical Anatomist*

What terribly sad news! I never met Mustafa, but I know him for his work and as a great anatomist. I ask that you please present my condolences to his family, his friends and to all Turkish anatomists, who I am sure are deeply suffering with this terrible loss.

**Carla Stecco**, *Department of Neuroscience, Institute of Human Anatomy, University of Padua, Italy*

It's terrible to hear about this loss and I express my sincere sympathy.

Best regards,

**Mirela Eric**, *Full Professor, MD, PhD, Plastic Surgeon at University of Novi Sad, Faculty of Medicine University of Novi Sad, Faculty of Medicine; President of Serbian Anatomical Society*

It is hard to believe that Mustafa passed away. It is too sad. Anatomy is no more pleasant without him. I lost a very good friend with a good humour and a smiling face, and a hardworking colleague with whom I worked at TSACA and EACA for many years. I'm in deep sorrow.

**Salih Murat Akkın**, *MD, Professor of Anatomy & Dean of medical School, SANKO University, Gaziantep; Past President of TSACA (2005-2006), Past President of EACA (2009-2011), Founding Editor of the journal “Anatomy”.*

**ORCID ID:**

N. Apaydın 0000-0002-7680-1766

deomed®

**Correspondence to:** Nihal Apaydın, MD, PhD

Department of Anatomy, Ankara University,  
School of Medicine, Sıhhiye, Ankara, Türkiye  
Phone: +90 312 595 82 48  
e-mail: napaydin@gmail.com

*Conflict of interest statement:* No conflicts declared.

This is an open access article distributed under the terms of the Creative Commons Attribution-NonCommercial-NoDerivs 4.0 Unported (CC BY-NC-ND4.0) Licence (<http://creativecommons.org/licenses/by-nc-nd/4.0/>) which permits unrestricted noncommercial use, distribution, and reproduction in any medium, provided the original work is properly cited. *How to cite this article:* Apaydın N. In dedication to Professor Mustafa Sargon. *Anatomy* 2022;16(2):133–136.

# 17th Annual Congress of the European Association of Clinical Anatomy (EACA) and the 14th Annual Congress of the International Symposium of Clinical and Applied Anatomy (ISCAA)

Dear colleagues, dear anatomists, and friends of anatomy,

I would like to invite you to Prague for a joint meeting of the *17th Congress of the European Association of Clinical Anatomy (EACA)* and the *14th Annual Congress of the International Symposium of Clinical and Applied Anatomy (ISCAA)*. It will be a unique meeting that will follow the long-standing tradition of both organizations that brings together morphology scientists from across the generation spectrum, across the range of professional focus and across the world. I cordially invite you to meet in Prague, one of the most beautiful and historic European cities.

Prague is a historic royal city with unique monuments, and it is the home of Charles University, the oldest university east and north of the Alps. *Come to soak up the atmosphere and beauty of Prague, come to meet and talk face to face after a practically three-year hiatus due to COVID restrictions, come to personally meet with old friends and colleagues you have not seen in a long time, and personally meet colleagues you only know from online meetings in virtual space.* I invite you to take advantage of this

opportunity and *join us in the beautiful, warm, safe, and friendly heart of Europe.*

I am convinced that with the beautiful city of Prague as the backdrop, you will gain professional knowledge and establish new working collaborations. During the special social gatherings, you will have a chance to make new friendships and renew old ones.

Dear colleagues, friends, and anatomists at heart, I look forward to meeting you in person again in Prague from *September 14 to September 17, 2023. Face to face again!*

Early Bird Registration was open, Call for Paper is open till July 1st, 2023 at the Congress website <https://www.eaca-iscaa2023prague.com/>, where you can find all details about our congress.

We are looking forward to meeting you in person in Prague!

Prof. Vaclav Baca, Congress President  
Honorary President of EACA



**EACA & 20  
ISCAA 23**

**CLINICAL  
AND APPLIED  
ANATOMY**



Joint congress of  
**European  
Association  
of Clinical  
Anatomy  
(EACA)**  
and  
**International  
Symposium  
of Clinical  
and Applied  
Anatomy  
(ISCAA)**

*Face-to-face  
again!*

**SEPTEMBER  
14<sup>TH</sup>-17<sup>TH</sup>, 2023  
PRAGUE**

Developmental Anatomy and Histology,  
Applied Molecular Biology and Genetics  
Anatomy, Histology, Embryology,  
Variations, Malformations, Diseases

Locomotor System

Cardiovascular System

Respiratory System

Digestive System

Urogenital System

Endocrine System

Nervous System

Sense Organs

**Dental Investigations**

**Radiological Investigations**

**Anthropology**

**Comparative Anatomy**

**History of Anatomy, Histology  
and Embryology**

**Education in Morphological**

**Sciences**

**Translational research**

**in Anatomy**

**Varia**

***Early Bird Registration is open!  
Call for Paper is open!***

**<https://www.eaca-iscaa2023prague.com/>**



---

# Table of Contents

---

Volume 16 / Issue 2 / August 2022

(Continued from back cover)

## Reviews

**A review of the anatomy of soft tissues associated with sexually dimorphic landmarks on the cranium** 93

Jade S. De La Paz, Hallie R. Buckley, Siân E. Halcrow, Stephanie J. Woodley

**Notes on the techniques of body restoration after autopsy and the possibility of embalming** 108

Jan Frišhons, Maksim A. Kislov, Marcela Bezdicikova, Veronika Dzetkucicová

***In vivo* experimental models of schizophrenia: mechanisms, features, advantages, disadvantages** 114

Zeynep Mine Altunay, Aysel Alphan, Esat Adıgüzel

## Case Reports

**Bilateral agenesis of the long head of the biceps tendon** 124

Semra Duran, Muhammet Batuhan Gökhan

**A large unilateral persistent sciatic vein: a case report** 127

Vincent Kipkorir, Dennis Ochieng, Fiona Nyaanga, Isaac Cheruiyot, Wanjiku Ndung'u, Musa Misiani, Jeremiah Munguti, Beda Olabu

## Obituaries

**In dedication to Mustafa Fevzi Sargon (1965–2022)** 131

Deniz Demiryürek

**In dedication to Professor Mustafa Sargon** 133

Nihal Apaydın

## Announcement

**17th Annual Congress of the European Association of Clinical Anatomy (EACA) and the 14th Annual Congress of the International Symposium of Clinical and Applied Anatomy (ISCAA)** 137

Vaclav Baca

### On the Front Cover:

Mustafa Fevzi Sargon (1965–2022). From Demiryürek D. In dedication to Mustafa Fevzi Sargon (1965–2022). *Anatomy* 2022;16(2):131–132.

---

## Table of Contents

---

Volume 16 / Issue 2 / August 2022

### Original Articles

<b>The radiological anatomy of clivus for surgical approaches</b>	51
Tuğba Moralı Güler, Ömer Faruk Ünal, Gökmen Kahiloğulları	
<b>Relationship between the carrying angle and some other parameters related to muscle strength and endurance in healthy young adults</b>	56
Kübra Erdoğan, Mehmet Ali Malas, Deniz Bayraktar, Hilal Uzunlar, Derya Özer Kaya	
<b>Evaluation of trabecular structure of hamate using micro-computed tomography</b>	62
Hakan Ocak, Hakan Hamdi Çelik, Mert Ocak, Ferhat Geneci	
<b>Morphometric relationship of nasolacrimal duct with maxillary sinus and nasal septum</b>	69
Aycan Canlı, Alper Vatanserver, Emrah Akay	
<b>Total anomalous pulmonary venous connection: preoperative anatomy, physiology, preoperative evaluation, surgical considerations and single centre clinical experiences</b>	76
Başak Soran Türkcan, Mustafa Yılmaz, Atakan Atalay	
<b>Determination of knee joint line in relation to bony landmarks: a CT study in Turkish population</b>	81
Cem Özcan, Ali Şahin	
<b>Effects of the position of uncinat process on olfactory fossa depth and lateral lamella length</b>	88
Ömer Hızlı, Serkan Kayabaşı, Deniz Özkan	

*(Contents continued on inside back cover)*